Development of a functional model for tomato paste rheology

A thesis presented in partial fulfilment of the requirements for the degree of

Master of Food Technology

at Massey University,

Manawatu,

New Zealand.

Noorul Faridatul Akmal

2017

Abstract

Tomato paste is a seasonal product, processed for retail or packed aseptically in bulk to use as a raw ingredient for manufacturing many other tomato based products such as sauces, ketchup, and soups. Paste is added to formulated food products to provide flavour, tomato solids, and viscosity. Viscosity is mostly imparted by the insoluble solids but there is a contribution from the soluble solids in the tomato paste. Because the composition and physical nature of tomato solids varies with processing methods, tomato variety and maturity, the functional properties of tomato pastes can also be highly variable. The objective of this study was to develop methodologies that could be used to characterise tomato paste batches in such a way that the functionality of the paste is predictable. Ideally rheological functionality should be predictable from compositional information and characterisation should require a minimum of measurement effort.

This work explored how paste composition impacted on paste rheology and found that much of the variation in flow properties of tomato concentrates can be explained by appropriate characterisation of the water insoluble and soluble solids levels in the paste. Serum contributes to the flow behaviour of tomato paste due to the presence of soluble solids in the serum. In particular, it was found that it was primarily sugars that cause this effect, potentially by enhancing the pectin-pectin interactions in the WIS components of the paste. In this work it was found that there were measurable differences in serum viscosity between pastes, however good overall model predictions could be achieved without considering the serum phase beyond the soluble solids concentration.

The Herschel-Bulkley model was found to be the most appropriate model to describe the flow behaviour of tomato paste. Herschel Bulkley parameters could then be linked to the insoluble and soluble solids levels in the paste. For some pastes the model could be fitted with just one paste specific parameter plus four other generally fitted constants (which apply to any paste). When applied to other pastes however, at least one of the other parameters was also required to be paste specific. These parameters relate the yield stress and the flow behaviour index to the water insoluble solids content. Because these two parameters need to be fitted for individual pastes, it is thought that they are influenced by the particle size and shape and/or their composition of the WIS fraction. For example elongated particles will orientate within a flow field with varying shear rates, thereby influencing the flow behaviour index.

There is potential to fit the two key paste specific parameters for a paste from a single flow curve. This could provide an industry implementable method to characterise tomato paste batches. Such a characterisation method would be useful for predicting flow behaviour under different processing conditions and how dilution during product formulation will affect viscosity. Future work should be carried out to extend this work to those aims.

Acknowledgments

A very special gratitude goes to New Zealand Ministry of Foreign Affairs and Trade for giving me the opportunity to study at Massey University under New Zealand Aid Programme. It is like a dream come true. I still remember the day I got the phone call informing that I have been granted to the New Zealand Asian Scholarship Awards, that day is still one of the best days in my life.

I would also like to express my eternal gratitude to my supervisor, Professor John Bronlund for his unwavering support and encouragement, and for helping me with the mathematical modelling, it is an art of analysing result and I am so glad that I am able to learn it from the expert. I want to thank also to my second supervisor, Dr Michael Parker who provided me with rheological advice.

Appreciation also goes out to Michelle Tamehana who helped me with the rheometer and provided me with technical support.

Margaret Low and Jacinta Gould from New Zealand High Commission in Malaysia and Sylvia Hooker, Jamie Hooper, and Dave Broderick from International Student Support Massey University, thank you very much for being so approachable and for assisting me a lot with immigration policies as international student.

For those who contributed to this thesis indirectly. Thanks to Shu, Ava, and Sarie for a cup of coffee over the weekend for all these years. A special thanks goes to Anynda who always offered me a help and night ride home from the lab when I needed one. Thank you also to my social netball team for making my life more interesting and help me to release the tense by throwing ball every Saturday morning.

To my mother, thank you very much for your unconditional love, for teaching me so much about perseverance. Love you infinity.

Table of Contents

List of Tables

List of Figures

Chapter 1

Introduction

Tomato paste is a product resulting from the concentration of crushed tomatoes after the removal of skins and seeds, and contains not less than 24% natural tomato soluble solids (NTSS) (Hayes *et. al*, 1998). Tomato paste is produced during the tomato harvesting season which is a 12 to 14 week season per year. Due to this short harvest season, tomato paste is processed for retail or packed aseptically in pre-sterilized bag-in-drum or bag in crate systems of 4 or 1000 litre capacity that can be used up to 18 months later as raw ingredients for processing many other tomato based products such as sauce, ketchup, and soup.

Since tomato paste is a key ingredient in a wide range of different formulated food products (from pizza sauce to soups etc.), maintaining its quality is paramount for tomato processing industry. Paste is added to provide flavour, tomato solids, and viscosity in the formulated products. Among the different functional properties the tomato paste provides, viscosity is one of the most important quality characteristics of processed tomato products. Factors like seasonality (Garcia & Barrett, 2006), cultivars (Xu, Shoemaker, & Luh, 1986), fruit maturity (Garcia & Barrett, 2006), and processing conditions such as break temperature (Sherkat & Luh, 1977), finisher screen (Tanglertpaibul & Rao, 1987), and homogenization (Lopez-Sanchez, Nijsse, Blonk, Bialek, Schumm, & Langton, 2011) cause a great variation in the viscosity of tomato paste. Because of this variability, significant effort is made to reformulate products to achieve consistent viscosity with the variable paste ingredient.

Viscosity is mostly imparted by the insoluble solids (Marsh, Buhlert & Leonard, 1980) but there is a contribution from the soluble solids (Tanglertpaibul & Rao, 1987). Methodologies to characterize batches of tomato paste that allow the prediction of viscosity as a function of dilution with water and addition of sugars will be useful in tomato paste use. For use industrially, ideally rheological functionality should be predictable from compositional information about a paste and characterisation should require a minimum of measurement effort.

This project was aimed at development of a universal functional model that allows prediction of tomato paste viscosity from its compositional information.

CHAPTER 2

Literature review

2.1 Introduction

To develop a model to describe the flow behaviour of tomato paste, it is important to review existing literature on the composition and variation in tomato fruit. The structure of pectin and other cell wall components are important to the characteristic of resulting products. It is known that changes to these structures occur during ripening and processing and that these changes also contribute to variations in tomato paste. Because tomato paste is a very important food ingredient, its rheology has been previously characterised and may form the basis for an overall model development. These topics are reviewed in this chapter.

2.2 Tomato fruit anatomy

Tomato is a member of the genus *Lycopersicon,* belonging to the plant family *Solanaceae.* Botanically, the fruit of the tomato is regarded as a berry as the seeds are formed within a fleshy mesocarp (Davies, Hobson, & McGlasson, 1981). The tomato fruit anatomy is described in Figure 2.1.

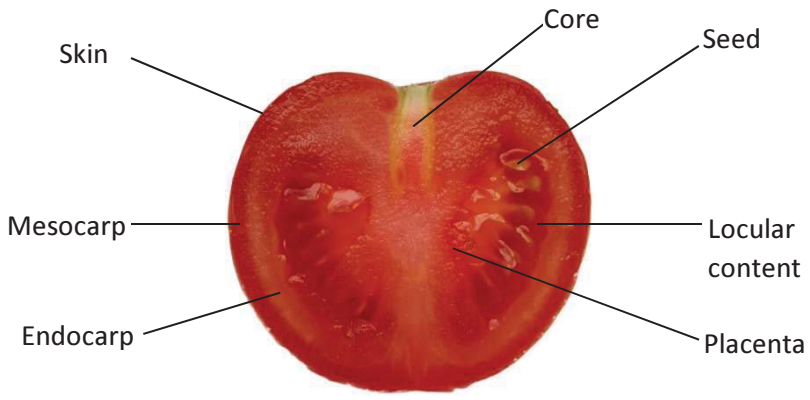

Figure 2-1 - Tomato fruit anatomy.

Generally during processing to tomato paste, the seeds and skin of the tomatoes are separated using a finisher and are not included in the tomato paste product.

2.3 Tomato fruit composition

Tomato fruit contains mainly water with only 5% to 7.5% total solids (Davies *et al.*, 1981). Tomato solids primarily consist of soluble solids (sugar, organic acids, amino acids, volatiles compounds, minerals etc.) and insoluble solids (cellulose, hemicellulose, pectin and protein). The composition of tomato fruit total solids are clearly described in Figure 2.2.

2.3.1 Soluble solids

One of the principal soluble solids components in tomatoes is sugar. This sugar consists of a slightly higher percentage of fructose than glucose, whereas the sucrose content in tomatoes rarely exceeds 0.1% on a fresh weight (Gould, 1992).

Besides sugar, tomato soluble solids contain organic acids which are one of the important flavour components of tomato fruit. The major organic acid in tomato is citric acid, followed by malic acid and traces of tartaric, succinic, acetic, and oxalic acids (Gould, 1992). The average pH of red-ripe tomato was found to be 4.4 – 4.6, depending on the tomato cultivars (Brecht, Keng, Bisogni, & Munger 1976). Table 2.1 shows the composition of organic acids in fresh and processed tomato juice. The processing of tomato causes an increase in organic acids content. This is due to several reactions that occur during processing such as the oxidation of aldehydes and alcohols, deamination of amino acids, and decomposition of sugar during heating in the presence of acids to form acetic, lactic, fumaric, and glycolic acids (Gould, 1992).

Tomato soluble solids also contain amino acids. The major amino acids in fresh tomato juice are glutamic, γ-aminobutyric and aspartic acids, while amides such as glutamine and asparagine are also abundant. Glutamic acids content can range between 50 and 300 mg/100 g of fresh tomato (Davies *et al.*, 1981) Table 2.2 presents the amino acid content of fresh and processed tomato juices. Processing of tomato cause an increase in amino acids particularly glutamic acid, aspartic acids, alanine and threonine. This is attributed to partial hydrolysis of protein.

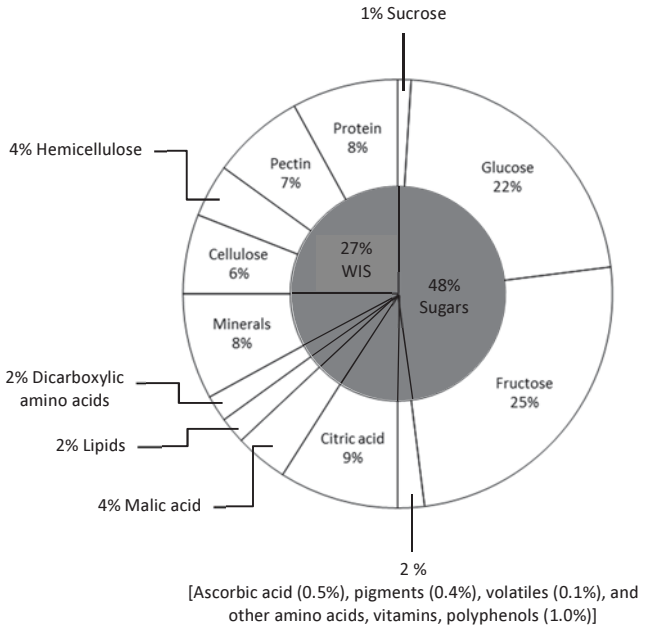

Figure 2-2 - Total solids compositions of fresh tomato fruit (Davies *et al.*, 1981).

Table 2.1 - Composition of organic acids in fresh and processed tomato juice (Gould, 1992).

Organic acids	Fresh (mEq/L)	Processed (mEq/L)
Citric	60.92	66.92
Malic	3.72	5.39
Lactic	1.37	1.46
α-ketoglutaric	1.10	0.53
Acetic	1.06	1.56
Pyrolidone-carboxylic	0.81	8.10
Succinic	0.60	0.49

Table 2.2 - Amino acid content of fresh and processed tomato juice (Gould, 1992).

Amino acids	Fresh (mg/100g)	Processed (mg/100g)
Glutamic acid	21.9	212.5
Asparagime and glutamine	7.8	-
Aspartic acid	5.5	51.6
Serine	2.3	12.7
Phenylalanine	1.4	10.8
Alanine	1.0	9.0
Threonine	1.0	9.0
Lysine	0.9	5.1
Histidine	0.9	7.5
Arginine	0.7	4.4
Isoleucine	0.6	3.8
Leucine	0.6	3.0
Tyrosine	0.5	3.4
Valine	0.4	1.7
Glycine	0.3	1.2
Methionine	0.2	0.9
Proline	0.1	0.4
Unknown	-	0.6
Total	45.1	337.6

The characteristic flavour of tomato results from the reducing sugars (fructose and glucose), organic acids (mainly citric acid), the sugar to acid ratio, aromatic volatiles, and complex interactions between them (Petro-Turza, 1986). The predominant aromatic volatiles of fresh tomato are cis-3-hexenal, 6-methyl-5-hepten-2-one, benzyl alcohol, geranial (citrus and fruity

aroma character) and neral (citrus, fruity volatile) and 2-isobutyl-thiazole (Markovic, Vahcic, Kovacevic Ganic, & Banovic, 2007).

Pigments constitute only 0.4% of tomato total solids. Of these, red-ripe tomato contains 80 – 90% lycopene that is responsible for the visible red colour of ripe tomato fruit. Table 2.3 summarises the amount of lycopene and other carotenoids that are present in tomato fruit. According to Al-Wandawi, Abdul-Rahman, and Al-Shaikhly (1985), tomato skin contains three times higher concentrations of lycopene than in whole mature tomato fruit.

Table 2.3 - Carotenoids content in tomato fruit (Shi & LeMaguer, 2000).

Carotenoid species	Composition (%)
Lycopene	80 – 90
β-carotene	3 – 5
γ-carotene	1 – 1.3
ξ-carotene	1 – 2
α-carotene	0.03
Phytoene	5.6 – 10
Phytofluene	2.5 – 3
Neurosporene	7 – 9
Lutein	0.11 – 1.1

Minerals represent 8% of tomato total solids. Table 2.4 shows the minerals composition in normal ripe tomato fruit.

Table 2.4 - Minerals in normal ripe tomato fruit (Gould, 1992).

Minerals	Composition (mg/ 100g fresh tissue)
Potassium	92 – 376
Phosporus	7.7 – 53
Calcium	4 – 21
Magnesium	5.2 – 20.4
Sodium	1.2 – 32.7
Iron	0.35 – 0.95
Aluminium	0.5 – 2.95
Boron	0.04 – 0.13
Copper	0.05 – 0.2
Lead	0.02 – 0.05
Manganese	0.04 – 0.3
Zinc	0 – 0.25

2.3.2 Water insoluble solids (WIS)

The water insoluble solids (WIS) fraction in tomatoes consists of tomato cell wall materials. The main components of tomato cell wall are cellulose, hemicellulose, pectin and protein (Davies *et al.*, 1981).

2.3.2.1 Cellulose and hemicellulose

Cellulose is a linear polysaccharide of (1,4)-linked β-D-glucan molecules. Whereas hemicelluloses are group of complex polysaccharides that mostly consist of xyloglucan and arabinoxylan. Xyloglucan has a backbone that resembles cellulose but contains xylose branches on 3 out of 4 glucose residues. The xylose can be serially attached with galactose and fucose residues. However, according to York, Kumar Kolli, Orlando, Albersheim, and Darvill (1996), xyloglucan in solanaceous plants (such as tomatoes) has a lower amount of xylose branches and the xylose is mostly extended with galactose and arabinose residues rather than fucose. Arabinoxylan consists of a backbone of (1,4)-linked β-D-xylan molecules that contain arabinose branches (Cosgrove, 2005).

2.3.2.2 Pectin

Pectin is a component of primary cell walls, particularly in the middle lamella that is important in cell-cell adhesion (Thakur, Singh, Handa, & Rao, 1997). Pectin constitutes approximately 25% of the alcohol insoluble solid fraction of the cell wall material (Christiaens *et al.*, 2012, Davies *et al.*, 1981). Pectin molecules contain heterogeneous groups of polysaccharides that are composed of galacturonic acid (GalA) as their backbone. These polysacharides include homogalacturonan, rhamnogalacturonan I (RG I), and smaller amounts of rhamnogalacturonan II (RG II), xylogalacturonan, arabinan, and arabinogalactan I (Cosgrove, 2005).

Homogalacturonan is a linear homopolymer of 1,4-linked α-D-galactopyranosyluronic acid (Gal*p*A) residues with some of the C-6 carboxyl groups being methyl esterified (Figure 2.3). Rhamnogalacturonan I (RG I) is a heteropolymer composed of repeating units of disaccharide [→4)-α-D-GalpA-(1→2)-α-L-Rhap-(1→]. The Gal*p*A residues are presumed to be not methyl esterified, whereas some of the rhamnosyl (Rha*p*) residues are linked to branched and linear oligosaccharides, primarily galactosyl and/ or arabinosyl residues at C4 (Ridley, O'Neill, & Mohnen, 2001) (Figure 2.4). Tomato pectins have low RG content and less branched RG I (Houben, Jolie, Fraeye, Van Loey, & Hendrickx, 2011).

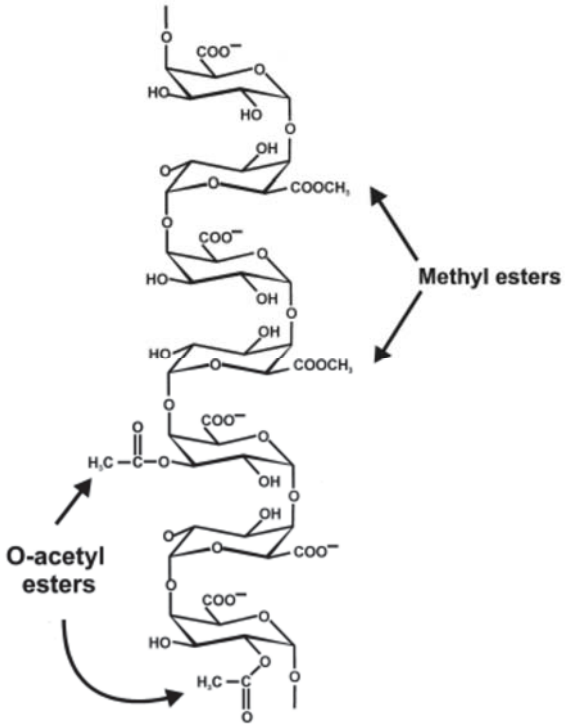

Figure 2-3 - Homogalacturonan primary structure (Ridley *et al.*, 2001).

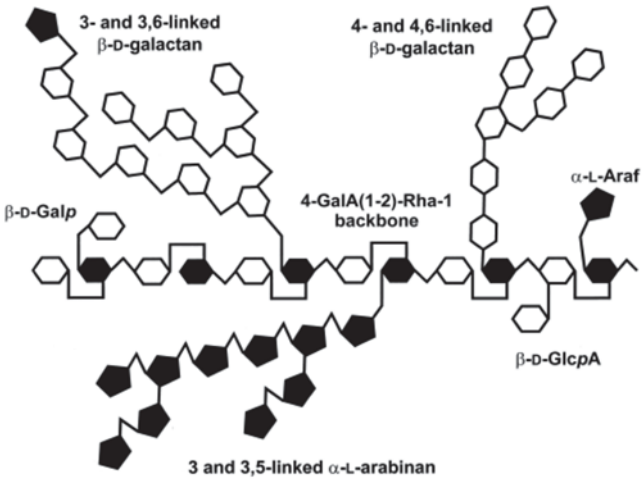

Figure 2-4 - Rhamnogalacturonan I structure (Ridley *et al.*, 2001).

2.3.2.3 Pectin functionalities

The gelation of pectin is due to the formation of continuous three-dimensional networks of cross-linked pectin polymers which consist of junction zones (where polymer molecules are joined together), interjunction segments of polymers that are relatively mobile, and water entrapped in the polymer network (Thakur *et al.*, 1997).

The mechanism of gel formation is influenced by the degree of methylesterification (DM) of the pectin. According to Sila *et al.* (2009) DM can be defined as the total amount of methoxyl groups per galacturonic acid chain. Based on this, pectin can be categorised into high-methylesterified (HM) and low-methylesterified (LM) pectin with DM of 50-80% and 25-50% respectively (Thakur *et al.*, 1997).

2.3.2.4 Pectin-pectin interaction

HM pectins form gels mainly by formation of hydrogen bonds (between functional oxygen atoms and hydroxyl groups) and hydrophobic interactions between methoxyl groups (Thakur et al., 1997). This interaction is favoured at pH below 3.6 and in the presence of cosolutes, generally sucrose at concentration of greater than 55 % (Oakenfull & Scott, 1984). The gel strength of HM pectins obtained from tomato increased with a decrease in pH from 5.0 to 2.0 and with an increase in pectin concentration from 1 to 2% (Sharma, Liptay, & LeMaguer, 1997). Low pH reduced dissociation of hydrogen ions (H+) from pectin carboxyl groups, thus minimizing electrostatic repulsions and consequently increasing the interactions leading to gelation. In the absence of sugar, the methoxyl groups of pectin are surrounded by a cage of water molecules (Walkinshaw & Arnott, 1981). The presence of sugar caused disruption of the cage thus forces pectin methoxyl groups to find alternative hydrophobic sites in order to reduce the energy of the system (Van Buren, 1991). This is accomplished by forming hydrophobic interactions between pectin methoxyl groups. Pectin-pectin interaction and the formation of network zones make the water trapped in the network thus increases the viscosity/ gelling properties of the system.

LM pectins form gels in the presence of Ca^{2+} by forming calcium cross-linkages between free carboxyl groups belonging to two pectin polymers in close contact (Thakur *et al.*, 1997). This interaction can be described by the egg box model that involves two stages. First is the initial dimerization and subsequent aggregation of preformed egg boxes (Figure 2.5). In contrast to HM pectins, higher pH is necessary for gelation of LM pectins because only dissociated carboxyl groups (negatively charged carboxyl groups) are capable of holding calcium ions to form calcium cross-linkages (Thakur *et al.*, 1997). However, the level of Ca^{2+} concentration determines the types of pectin aggregates formed in LM pectin. At low Ca^{2+} concentration, pectins form primary units consisting of two pectin chains with 50% of the carboxyl groups forming calcium cross-linkages. Under this condition, the interaction is favoured by the presence of sugar and low pH. Low pH reduced dissociation of hydrogen ions (H^{+}) from pectin carboxyl groups that unable to form calcium cross-linkages due to the low amount of calcium ions. At the same time sugar promotes hydrophobic interactions. At higher Ca^{2+} concentration, the primary units form sheet like aggregates with excess Ca^{2+} being weekly bound. However, this secondary aggregate only has a small effect on the gel strength. A pH of 3 to 5 is unfavourable under high Ca^{2+} concentration since it increases the calcium cross-linkages to such an extent that pectin is precipitated (Thakur *et al.*, 1997).

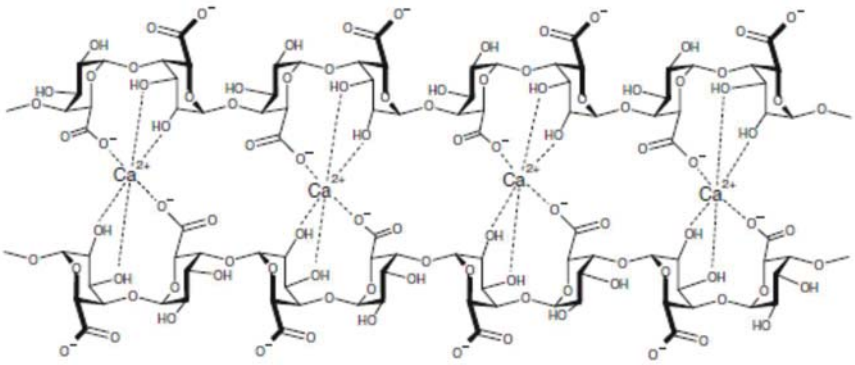

Figure 2-5 - Calcium-pectin-crosslink as egg box model (Voragen, Coenen, Verhoef, & Schols, 2009).

Intact red-ripe tomatoes have an average degree of methoxylation (DM) 63.7–67.5% (Christiaens *et al.*, 2012). This is in agreement with Houben *et al.* (2011) who found that red-ripe tomato fruit possesses very long, linear pectin with DM 61.8%.

2.2.2.4 Pectinmethylesterase (PME) and polygalacturonase (PG)

The changes in pectin structure that occur during ripening or processing are mainly due to the activity of two enzymes that present abundantly in tomato fruit. These are pectinmethylesterase (PME) and polygalacturonase (PG).

PME catalyses the demethylesterification of pectins particularly homogalacturonans (HG), thus producing homogalacturonans with negatively charged carboxyl groups that able to form calcium cross-linkages. The demethylesterified homogalacturonans also become a suitable substrate for depolymerisation by PG (Sila *et al.*, 2009). PG catalyses the hydrolytic cleavage of glycosidic bonds between adjacent demethylesterified galacturonic acid (GalA) residues thus reducing the polygalacturonic acid size and consequently increasing pectin solubility in water (Sila *et al.*, 2009). Figure 2.6 shows a schematic overview of PME and PG activity.

There are two types of PG found in tomato fruits, exo-polygalacturonase and endo-polygalacturonase. The exo-polygalacturonase is the enzyme that removes single galacturonic acid units from the non-reducing end of polygalacturonic acid, whereas endo-polygalacturonase cleaves these polymers randomly (Brummell & Harpster, 2001). Futher discussion in this section about PG refers to endo-polygalacturonase activity.

PG exists in two isoforms which are PGI and PGII, both have optimum catalytic reaction at pH 4.6 (Moshrefi & Luh, 1984). PGI is a complex of PGII and two glycoproteins called β-subunits (catalytically inactive) (Rodrigo et al., 2006). PGI is believed to be a less active form of PGII. The presence of β-subunits modify PGII's properties (reducing PGII affinity towards substrate and increasing its thermostability) (Moshrefi & Luh, 1984; Rodrigo et al., 2006). During ripening, less active PGI is converted to more active PGII by the removal of β-subunits (details about polygalacturonase activity during ripening will be discussed in the next section).

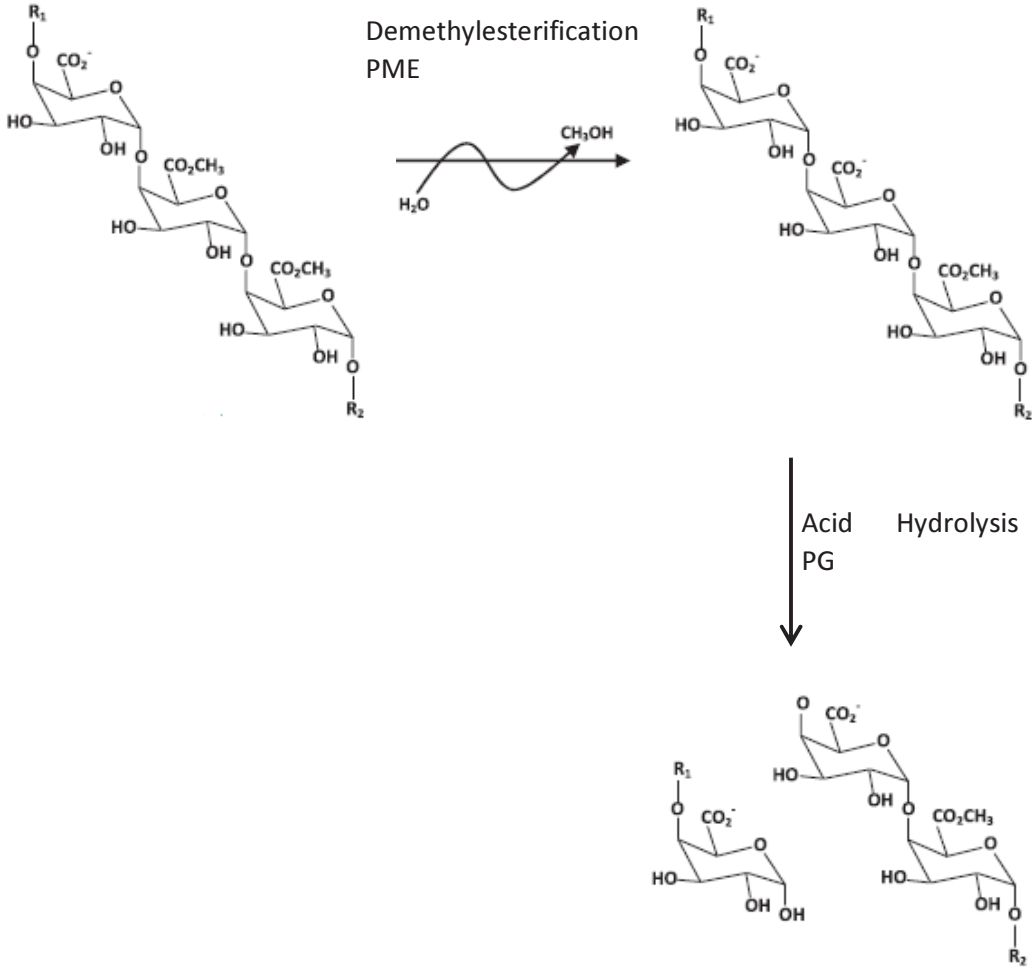

Figure 2-6 - Schematic illustration of pectinmethyesterase (PME) and polygalacturonase (PG) activity upon homogalacturonan (Sila *et al.*, 2009).

In terms of enzyme activity, purified PME and PG from different tomato varieties have different activity levels (Table 2.5). However, there is no difference in the thermal stability for different varieties (Rodrigo *et al.*, 2006). Purified PME can be thermally inactivated at a temperature 70 °C after 5 minutes, whereas purified PG at temperature 90 °C requires 5 minutes for PGI and 65 °C for 5 minutes to inactivate PGII (Rodrigo *et al.*, 2006).

Table 2.5 - Purified PME and PG activity in four different tomato varieties (Rodrigo *et al.*, 2006).

Tomato variety	PME (U[a]/ 500 g tomato)	PGI (U[a]/ 500 g tomato)	PGII (U[a]/ 500 g tomato)
Galeon	126.52	0.070	0.184
Malpica	72.76	0.281	0.294
Perfectpeel	208.60	0.329	0.356
Soto	164.48	0.232	0.346

[a] Enzyme activity units

2.4 Changes in tomato fruit during ripening

Tomato is a climacteric fruit. The ripening process of the tomato begins with ethylene production which is a plant hormonal gas that stimulates ripening at various levels. The ripening process can be distinguished by a change in tomato colour from green to red due to the chlorophyll degradation followed by carotenoid synthesis. According to the U.S. Standards USDA, 1975, tomato fruit can be classified into six ripening stages based on colour (Table 2.6).

Table 2.6 - USDA tomatoes classes (Barrett, Garcia & Wayne, 1998).

Score	Class	Description
1	Green	Fruit surface completely green, varying from light to dark green
2	Breaker	First appearance of external change in colour; pink, red, or tannish yellow colour on not more than 10% of fruit surface
3	Turning	Over 10% but not more than 30% fruit surface is red, pink, or tannish yellow
4	Pink	Over 30% but not more than 60% pinkish or red
5	Light red	Over 60% surface shows pinkish-red or red, but not more than 90% red
6	Red	Over 90% red; desirable table ripeness

Besides changes in colour, tomato fruit also undergo changes in flavour due to the synthesis of aromatic compounds and changes in sugar content and acidity. During ripening, tomato acidity increases rapidly from the green to breaker stages and then decreases as ripening continues (Winsor, Davies, & Massey, 1962). Garcia and Barrett (2006) showed that the pH of tomato fruit increases from the pink (pH 4.24 – 4.32) to red stage (pH 4.42 – 4.78), depending on variety and growing years. According to Davies *et al.* (1981), the main organic acid in immature green tomato is malic acids while citric acid only accounts for 25% of the total acidity. As the ripening progress, citric acid concentration increases and becomes the predominant organic acid in red ripe tomato while malic acid levels decline rapidly. The ripening of tomato fruit is also associated with an increase in reducing sugar content (Winsor *et al.* 1962). However, there is no trend on degree of Brix° (measure of total sugar, acids, and soluble pectin) at different stages of tomato ripeness where the degree of Brix° can range from 5.3 to 6.2 (Srichantra, 2002). This is in agreement with Brecht *et al.* (1976) who found no difference in soluble solid contents in mature green and red ripe tomato fruit.

Apart from the above changes, tomato also undergoes textural changes during ripening that involve the modification of tomato cell wall polysaccharides. This results in weakening of the tomato structure (Brummell, 2006) and a decline in fruit firmness. These modifications mainly involve the depolymerisation and solubilisation of pectin, depolymerisation of hemicellulose, and a loss of neutral sugar.

It has been suggested that pectin is synthesized in a highly methylesterified form and demethylesterified as ripening progresses (Brummell & Hapster, 2001). In tomatoes, the pectin degree of methylesterification (DM) decreases from 90% in the mature green and breaker

stages, to 35% at the pink and ripe stages (Koch & Nevis, 1989). This is due to the activity of pectin methylesterase (PME) that has been shown to increase during ripening before subsequently declining again at the turning stage (Frenkel, Peters, Tieman, Tiznado, & Handa, 1998) (Figure 2.7). Demethyesterification produces pectin with negatively charged carboxyl groups that are able to form intermolecular calcium cross-linkages in the presence of calcium ions (Ca^{2+}) in the cell wall apoplast. The change in pectin structure accompanying tomato ripening can be examined by sequential extraction of isolated cell wall using different extractors. Pectin that is attached to cell wall by calcium cross-linkage can be extracted using chelating agents such as trans-1,2- diaminocyclohexane-N,N,N'N'-tetraacetic acid (CDTA). Pectin that is attached to the cell wall by covalent bonding can be isolated using sodium carbonate (Na_2CO_3). Brummel and Labavitch (1997) reported that the amount of CDTA soluble pectin (CSP) increases during ripening, whereas the amount of Na_2CO_3 soluble pectin decreases.

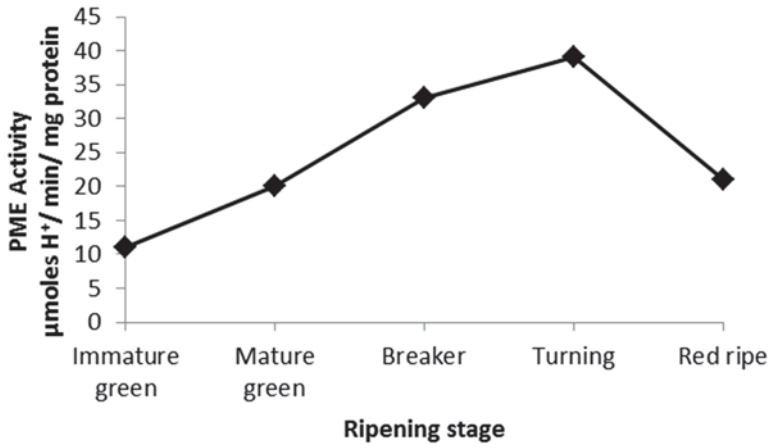

Figure 2-7 - Pectin methyesterase (PME) activity during tomato ripening (Frenkel *et al.*, 1998).

Demethylesterification also causes pectin to become a suitable substrate for depolymerisation by polygalacturonase (PG). Depolymerisation of pectin by PG brings about a reduction in the polygalacturonic acid molecular size and consequently increases pectin solubility in water (Sila *et al.*, 2009). Compared to PME that already shows high activity at the mature green stage (Frenkel *et al.*, 1998), PG activity is first detected at the pink stage of ripening and shows increases as ripening progresses (Huber & O'Donoghue, 1993, Eriksson *et al.*, 2004) (Figure 2.8). In analysis of CSP from ripening tomatoes using size exclusion chromatography on Sepharose CL-2B column, Brummel and Labavitch (1997) found that as ripening progresses the amount of high molecular weight pectin in the CSP decreases concomitant with the increase in intermediate and low molecular weight pectin molecules. A similar result was found by Huber and O'Donoghue (1993) (Figure 2.9). Even though depolymerisation of pectin causes an increase in pectin solubilisation, most of the depolymerized pectin molecules are still attached to the cell wall using ionic bonds and only small amounts of pectin become water soluble. Therefore, solubilisation of pectin is generally defined as an increase in the ease of extractability, measured as an increase in the amount of pectin that can be extracted from the cell wall by chelating agents (Brummel & Harpster, 2001).

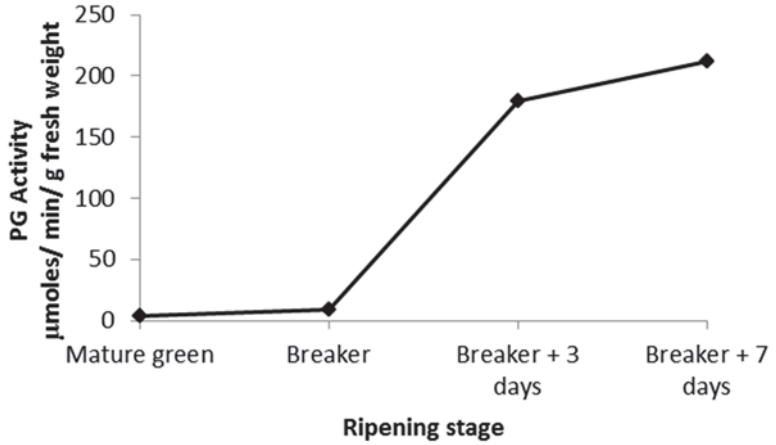

Figure 2-8 - Polygalacturonase (PG) activity during tomato ripening (Eriksson *et al.*, 2004).

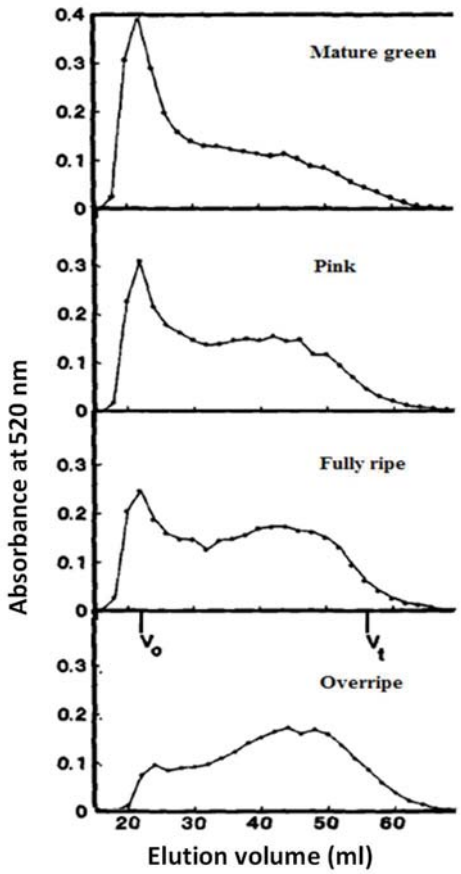

Figure 2-9 - Sepharose CL-28-300 profiles of CDTA soluble pectin derived from Sunny tomato fruit alcohol insoluble solid (AIS) (Huber & O'Donoghue, 1993).

Tomato ripening also associated with the loss of neutral sugars, in particular galactan and arabinan from cell wall polymers. Gross and Wallner (1979) reported that the amount of galactose and arabinose in the isolated tomato cell wall decreases as ripening progressed. This is associated with the activity of β-galactosidase II that increases substantially during ripening (Pressey, 1983). Galactan and arabinan exist in the tomato cell wall mainly as

rhamnogalacturonan I (RG I) side chains. The loss of galactan and arabinan during tomato ripening has been proposed to contribute to pectin solubilisation owing to the loss of pectin attachment to the cell wall. It is suggested that galactan and arabinan anchor pectin to the cell wall by covalent or hydrogen bonding or by physical entanglement with other cell wall polymers (Brummel, 2006). Smith, Abbott, and Gross (2002) suggested an alternative mechanism in that the decrease in galactan and arabinan side chains during ripening cause an increase in cell wall porosity, thus allowing access of degradative enzymes to pectin polymers, and consequently cause pectin solubilisation.

Tomato ripening is also associated with depolymerisation of hemicellulose which is regarded to be the main contributor to the decrease in cell wall rigidity and fruit softening (Brummell, 2006). Hemicellulose exists in the cell wall as a hemicellulose-cellulose network (Cosgrove, 2005). During ripening, a downshift in molecular weight of hemicellulose, particularly molecules that are tightly bound to cellulose has been observed (Brummell et al., 1999). However no solubilisation of hemicellulose was reported during ripening (Maclachlan & Brady, 1994). No degradation of cellulose has been observed during tomato ripening (Gross & Wallner, 1979), however endo-(1→4)β-D-glucanase (EGase) activity (generally known as cellulase) has been reported to increase during ripening (Miedes & Lorences, 2009).

2.5 Tomato product processing

2.5.1 Tomato products

Tomato paste is a product resulting from the concentration of crushed tomatoes after the removal of skins and seeds, and contains not less than 24% natural tomato soluble solids (NTSS) (Hayes, Smith, & Morris, 1998). Table 2.7 describes some useful definitions of processed tomato products. Tomato paste is produced during the tomato harvesting season which is 12 to 14 weeks season per year. Due to this short harvest season, tomato paste is processed for retail or packed aseptically in pre-sterilized bag-in-drum or bag in crate systems of 55 or 300 gallon capacity that can be used up to 18 months later as raw ingredients for processing many other tomato based products such as sauce, ketchup, and soup.

Table 2.7 - Definitions of processed tomato products (Hayes *et al.*, 1998)

Tomato products	Definitions
Tomato pulp	The crushed tomatoes either before or after the removal of skins and seeds
Tomato juice	The juice from whole crushed tomatoes from which the skins and seeds have been removed and is intended for consumption without dilution or concentration
Tomato paste	The product resulting from the concentration of tomato pulp, after the removal of skins and seeds, and contains 24% or more natural tomato soluble solids (NTSS)
Tomato puree	Lower concentration tomato paste (containing 8% to less than 24% NTSS)
Tomato serum	The tomato juice which has been filtered or centrifuged to completely remove suspended solid material
Tomato syrup	The tomato serum which has been concentrated

2.5.2 Tomato paste processing steps

The tomato paste processing diagram is shown in Figure 2.10 and the details about the operation step are discussed in what follows.

2.5.2.1 Reception of tomato from the fields

Tomatoes are transported from the field to the factory in 'lug' or bushel boxes. Tomatoes that arrived in the factory are carefully checked with an emphasis on several criteria such as:

- Uniformity of colour
- Presence of under or over ripe fruit
- Presence of mould growth and insect infestation
- Presence of excessive dirt, mud, and foreign matter
- Cleanliness of containers and conveying vehicle
- Loading faults, damaged containers (which could cause damage to the fruit)
- Presence of fruit of the incorrect variety

Tomato fruit that pass the inspection point are then conveyed to the pre-washing tank (Goose & Binsted, 1973).

2.5.2.2 Washing

At this step, tomatoes are washed by using 5 – 10 ppm chlorinated water (to maintain sterility) (Moresi & Liverotti, 1982) to remove dust, dirt, and foreign matter by means of agitating water in the tank. Subsequently, tomatoes are transferred from the pre-washing tank to the second washing tank before transferred to the sorting area. As tomatoes are transferred to the sorting area they are subjected to a high pressure water rinse from nozzles placed under a protective hood (Goose & Binsted, 1973).

2.5.2.3 Sorting and trimming

At this point, defective tomatoes (rotten, mould, and blemished) are removed and partly defective materials are trimmed. This step is accomplished by using roller type conveyer, where the tomato fruit are turned over in front of the sorters and trimmers to allow all surfaces to be seen (Goose & Binsted, 1973).

2.5.2.4 Crushing or breaking, and preparation of tomato pulp

At this step, washed and sorted tomatoes are crushed to produce a pulp. The tomato pulp is then heated to temperature range from 90 – 95 °C (Moresi & Liverotti, 1982). This method is called as 'hot break' and true 'hot break' conditions can only be achieved if tomato pulp is heated as rapidly as possible after tomatoes are crushed. The main objective of hot break is to inactivate pectinolytic enzymes which would otherwise cause pectin degradation and thus decrease the viscosity of tomato paste produced.

In the 'cold break' method, tomato pulp is held in holding tank for quite long period before being heated to a temperature of 60 °C (Moresi & Liverotti, 1982). Tomatoes that are processed by this method are usually scalded prior to chopping to loosen the skins so better

extraction of tomato pulp can be achieved (Gould, 1992). Past of intermediate viscosity ('warm break') can be produces at conditions (time and temperature) between these two extremes.

2.5.2.5 Juice extraction and refining

Refining is a step that is important to remove skins and seeds and at the same time further break down the tomato plant tissue into smaller and uniform particle size. This unit operation consists of two or three cyclones. The first cyclone is called a 'pulper' and the second and/or third cyclones are called 'finishers' or 'refiners'. The cyclone consists of a rotating paddle inside a large cylindrical screen. When crushed and preheated tomato pulp is pumped to the cyclone, the rotating paddle forces the tomato pulp to flow through the holes in the screen thus separating the pulp from the skins and seeds. The 'pulper' has screen size (holes diameter) of about 1 mm, whereas 'finisher' and 'refiner' has screen size of about 0.7mm and 0.4mm respectively.

2.5.2.6 Concentration of tomato pulp

Tomato juice/pulp is then concentrated under reduced pressure in a series of evaporators. The lower pressure conditions allow lower temperature to be applied to evaporate water and thus produce tomato concentrates that retain most of the colour and flavour of fresh tomato. There are two main types of concentration systems; batch and continuous. In batch systems, the tomato juice is directly concentrated in steam jacketed vacuum pans or pre-concentrated to 12% solid before transferred to the vacuum pans. In continuous system, tomato juice is concentrated in a continuous flow and discharged when the tomato paste reach the desired concentration. In both systems, samples are taken for quality control test as tomato juice is concentrated to the desired concentration (Goose & Binsted, 1973).

Tomato juice can be concentrated different levels of total solids concentration depending of the intended use of the final product. Most of food industry requires tomato paste that has 28-30% NTSS (double concentrate) or 36-40% NTSS (triple concentrate). However, there is also considerable demand for lower concentration tomato pulps (down to 11%) and higher concentrations of tomato concentrate (up to 45% NTSS) (Goose & Binsted, 1973).

2.5.2.7 Tomato paste sterilization and canning

Prior to canning, tomato paste is heated to at least 90 °C to prevent spoilage before hot-filled into packaging. It is then immediately sealed, inverted to sterilize the lid and held about 3 minutes before cooling (Goose & Binsted, 1973). Tomato paste for industrial use is generally subjected to high temperature short time (HTST) treatment (108.9°C for 2.25 min) then cooled to 37.8°C before being packaged aseptically into steam sterilized bag-in-drum or bag in crate systems of 55 or 300 gallon capacity (Hayes *et al.*, 1998). This method allows the tomato industry to process and store product during the tomato harvest season and use it up to 18 months later as raw ingredients for processing many other tomato based products such as sauce, ketchup, and soup.

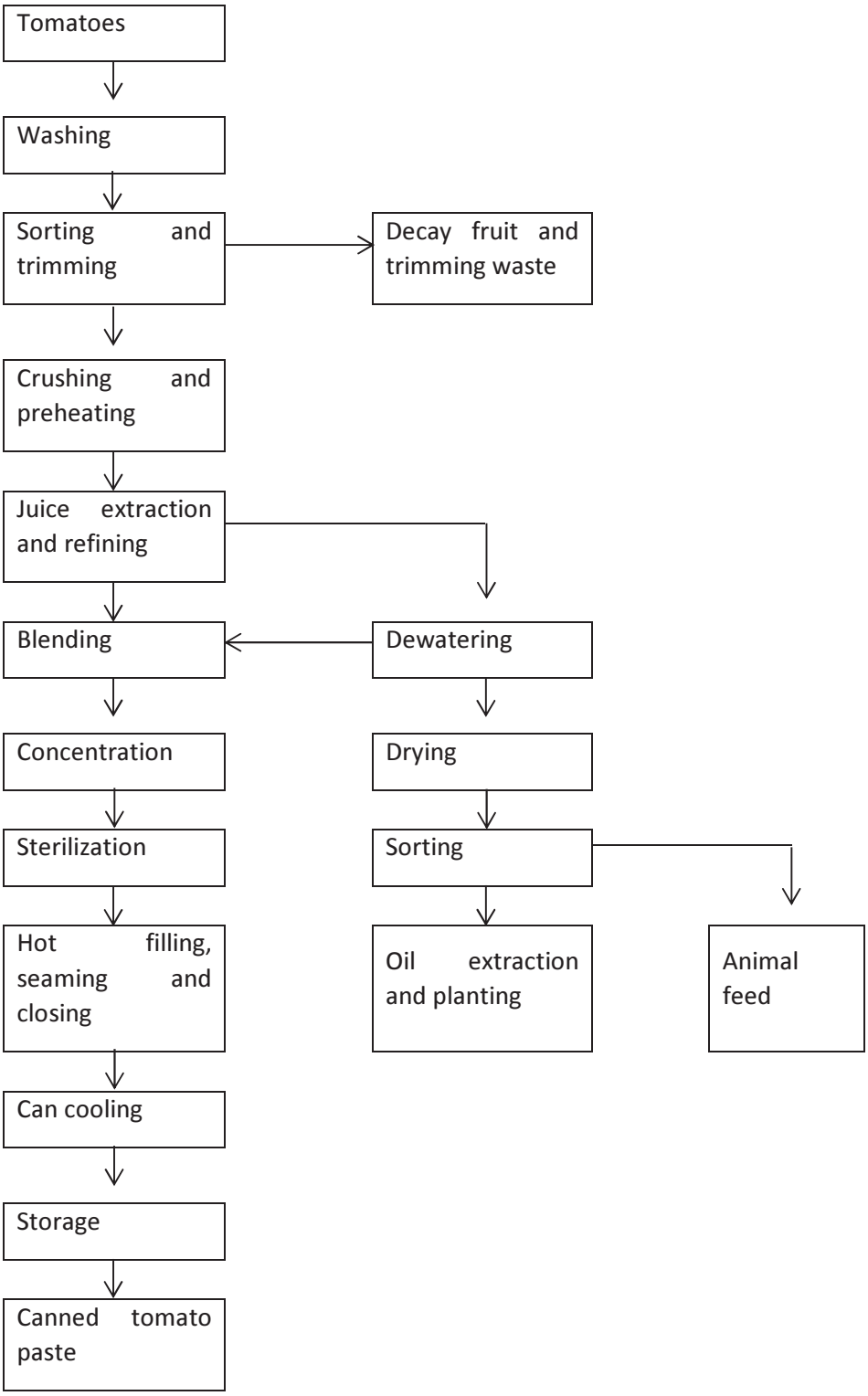

Figure 2-10 - Flow diagram for canned tomato paste production (Moresi & Liverotti, 1982).

2.6 Factors effecting tomato paste rheology

Tomato paste is a dispersion of insoluble plant-tissue-based particles in a continuous serum phase. The dispersed phase consist of disintegrated tomato fruit tissue in the form of cell clusters, intact single cells, or broken cells, and long chain polymers of insoluble pectin, cellulose and hemicellulose (Barrett *et al.*, 1998), while the serum phase is composed of sugars, organic acids, and soluble pectin. Moelants *et al.* (2014c) produced a schematic diagram (Figure 2.11) of a carrot suspension that can be used as an example of other plant-tissue-based food suspensions such as tomato paste or processed tomato products.

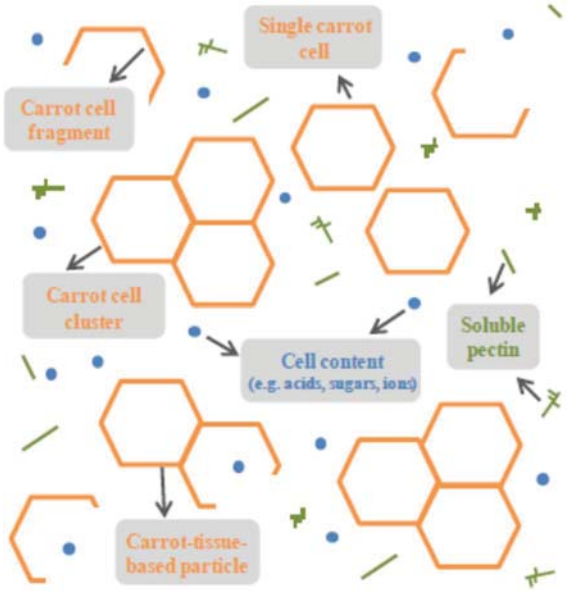

Figure 2-11 - A schematic representation of the composition of plant-tissue-based food suspensions (Moelants *et al.*, 2014c).

The rheological properties of tomato paste are largely determined by the properties of the insoluble phase, in particular its composition, concentration, chemical structure and particle properties such as particle size, particle size distribution, morphology, and deformability. All these factors are in turn dependent on agronomic properties (cultivar and maturity) of the tomato fruit used and the processing conditions applied during tomato paste production.

2.6.1 Chemical properties (composition, concentration, and chemical structure)

The influence of tomato cultivar on tomato paste viscosity has been demonstrated by Xu, Shoemaker, & Luh (1986) in a study conducted to examine the effect of break temperatures on tomato juice and paste viscosity made from four tomato cultivars. They found that at any break temperature, the tomato juice and paste made from cultivar E6203 had the highest viscosity compared to other cultivars. Goodman, Fawcett, & Barringer (2002) also found that different cultivars had a considerable effect on tomato juice viscosity. In their study using three tomato cultivars, they reported that tomato juices prepared from Heinz 9423 and Ohio 9442 using cold or hot break methods had significantly higher viscosity compared to Ohio 8245. In addition to cultivars, growing seasons can also affect tomato paste viscosity. Garcia and Barrett (2006) for example, reported that tomato paste produced in 1996 has higher

viscosity compared to tomato paste produced in 1995 and attributed it to seasonal variation where 1995 was a cooler season than 1996.

In a study that linked tomato cultivars to tomato concentrate composition and rheological properties, Marsh, Buhlert & Leonard (1980) reported that the change in Bostwick value during tomato juice concentration (slope of concentration) was dependent on the tomato cultivar used, and this was later shown to be mainly associated with WIS/TS ratio. Tomato juices made from cultivars that have higher WIS/TS ratio have higher slope of concentration than those having a lower WIS/TS ratio. Sharma, LeMaguer, Liptayb & Poysab (1996) also found that tomato cultivars that have higher WIS content produced tomato thin pulp (diluted pulp) with higher viscosity compared to tomato cultivars with low WIS content. These results indicate the significant contribution of insoluble solids on the viscosity of processed tomato products.

Tomato maturity also has a significant effect on the viscosity of tomato products. Garcia and Barrett (2006) found lower viscosity (higher Bostwick value) of tomato paste produced using tomato fruit at higher maturity stage. The higher amount of low molecular weight pectin compared to high molecular weight pectin at higher maturity stage might contribute to the observed result. Moreover the higher activity of PG enzymes at ripe stage compared to pink stage can result in higher pectin degradation during tomato paste processing. Brummell and Labavitch (1997) reported that the activity of PG in the cell wall is limited. However during tomato processing (crushing to produce pulp), the restriction is removed and PG has greater access to its substrates. Thus higher PG activity at higher maturity stage contributes to greater pectin degradation during tomato processing (even though if hot break method is employed) and consequently lower viscosity of tomato paste produced. Table 2.8 showed the effect of cultivars, maturity, and growing season on the viscosity of tomato paste.

The method of processing also greatly influences the viscosity of tomato products. Sherkat and Luh (1977) showed that tomato paste processed at high break temperature (100 °C) has a higher viscosity compared to tomato paste processed at low break temperature (64.4 °C). High break temperature causes inactivation of PME and PG enzymes and thus prevents pectin degradation. This was confirmed by the greater pectin retention in tomato paste processed at 100 °C compared to 64.4 °C. Similar results were found by Xu et al. (1986) and Thakur, Singh, Tieman, and Handa (1996) who observed higher viscosity and pectin content for tomato juice and paste produced at high break temperature.

Pectin contributes to the viscosity of tomato products by the formation of continuous three-dimensional networks of cross-linked pectin polymers where water and other particles are physically entrapped thus causing an increase in resistance of the fluid to flow. The network is formed by calcium cross-links of low methylesterified (LM) pectin and hydrogen and hydrophobic bonds of high methylesterified (HM) pectin. Inactivation of PME and PG during the hot break method can also result in higher amount of pectin with higher degree of methylesterification (DM) and higher molecular weight compared to the cold break method (Handa, Tieman, Mishra, Thakur, & Singh, 1996). Higher molecular weight pectin contributes to the higher volume occupied by the molecule and increases the extent of molecular association in solution, thus increases the viscosity.

The contribution of other insoluble solid constituents, such as cellulose and protein, on viscosity of tomato products have been demonstrated by Brown and Stein (1977). Enzyme treatment of a 1 % of tomato alcohol insoluble solid (AIS) suspension with cellulase caused a decrease in viscosity, while Pronase (a protease) caused an increase in viscosity.

Table 2.8 - Effect of cultivar, maturity and growing season on tomato paste attributes (Garcia & Barrett, 2006)

Cultivar	Maturity	Soluble solids (°Brix)		Bostwick value (cm/ 30s)		Serum viscosity (Pa.s)	
		1995	1996	1995	1996	1995	1996
FM 9208	Pink	5.05		14.25		9.69	
	Red	4.98	4.8	17.08	15.88	5.41	10.13
	Red + 2	4.78	4.6	16.6	16.19	3.64	6.36
	Red + 3		5.15		15.21		5.54
La Rossa	Pink	5		12.75		9.7	
	Red	5.48	5.25	16.55	13.35	6.03	7.89
	Red + 2	5.35	5.6	16.73	15.51	3.84	6.59
	Red + 3		5.5		17.07		5.36
H 8892	Pink	5.08		10.53		12.35	
	Red	5.25	5.15	13.2	11.65	10.33	11.79
	Red + 2	5.15	4.95	14.08	14.76	7.6	8.79
	Red + 3		5.5		14.13		7.98
Brigade	Pink	5.08		11.25		12.95	
	Red	5	5.4	16.25	14.19	6.17	9.21
	Red + 2	5	4.8	18.1	17.15	4.72	5.79
	Red + 3		5.2		17.68		4.76
Halley 3155	Pink	5.65		12.75		8.08	
	Red	5.53	5.65	15.1	15.11	5.61	8.16
	Red + 2	5.5	5.15	14.38	16.03	4.7	5.36
	Red + 3		5.9		15.55		6.15
N 512	Pink	4.7		11.3		9.47	
	Red	4.83		13.65		10.29	
	Red + 2	4.2		13.63		6.19	

2.6.2 Particle properties (size, size distribution, morphology, and deformability)

The rheological properties of tomato products also have been shown to be influenced by the physical properties of insoluble solid. While the composition, concentration, and chemical structure of insoluble solids are associated with agronomic properties and processing method, the physical properties are mainly due to the processing method only.

Tanglertpaibul and Rao (1987a) investigated the effect of finisher screen size on the rheological properties of tomato juice and concentrate. They found that tomato juice and concentrate produced using an intermediate size screen opening (0.686 mm) had the highest apparent viscosity compared to the others (0.508, 0.838, and 1.143 mm). The use of smaller screen size (0.508 mm) produced tomato juice and concentrates with higher amount of small particle but lower amount of large particle and a narrow particle size distribution. Small particles contribute to the viscosity due to greater surface area, thus causing an increase in particle interactions, while larger particle contributes to the viscosity due to larger aspect ratio. Thus the highest viscosity observed using 0.686 mm screen opening is attributed to the optimum yield of small and large particles. Similarly, Noomhorm and Tansakul (1992) reported that tomato juice and puree produced from intermediate size screen opening (1 mm) has the highest viscosity compared to 0.5 and 1.5 mm screen openings. The lower viscosity of tomato juice and puree produced from 1.5 mm screen opening is reported due to the inclusion of seed and large particle that disrupt the particle-particle interactions.

Lopez-Sanchez et al. (2011) reported that high pressure homogenization (60 MPa) resulted in an increase in the viscosity and yield stress of tomato juice. Even though homogenization decreased the particle size and narrowed the particle size distribution of tomato juice, the increase in the viscosity and yield stress is attributed to the increase in the amount of biopolymers from the cell wall that expand into liquid after homogenization, providing a more fibrous nature to the tomato juice and an increase of phase volume. According to Thakur, Singh, and Handa (1995), homogenization produces linear shape cell walls that exert more resistance to flow thus cause an increase in the viscosity.

2.7 Tomato paste rheology

The inconsistency in tomato paste viscosity has been a major problem to the processing industry. Viscosity can be defined as the internal friction of a liquid or its tendency to resist flow (Bourne, 2002). It can be donated as η, and mathematically described by equation 2.1;

$$\eta = \frac{\sigma}{\gamma} \qquad \text{Equation 2.1}$$

Where;

η = viscosity (Pa.s),
σ = shear stress (Pa), and
γ = shear rate (s^{-1})

Shear stress is the stress component applied tangential to the plane on which the force acts. It is a force vector that has both magnitude and direction. Whereas shear rate is the velocity gradient established in a fluid as a result of an applied stress (Bourne, 2002).

2.7.1 Newtonian and non-Newtonian fluid

Fluids can be divided into Newtonian and non-Newtonian behaviour. For Newtonian fluids, the plot of shear stress versus shear rate shows a linear behaviour where the slope of the plot is the fluid viscosity. Since the viscosity of Newtonian fluids is constant or independent of shear rate, it is called absolute viscosity (η). In contrast, non-Newtonian fluids are fluids that do not obey Newtonian behaviour. The viscosity of non-Newtonian fluid is dependent on the shear rate and called as apparent viscosity (η_{app}) which only applies at a specific shear rate. Non-Newtonian fluids can be further classified into time independent, time dependent, and viscoelastic fluids (Bourne, 2002).

Time independent fluids are defined such that the shear rate is a function of the shear stress only. Whereas for time dependent fluids, the shear rate is depends on the shear stress and duration of shearing. The time allowed for the fluid to rest before successive shearing may also affect the shear rate. Viscoelastic fluids are fluids where an elastic recovery is observed when the shear stress is removed from the material (Holdsworth, 1971).

Time independent non-Newtonian fluids can be divided into shear thinning (pseudoplastic) and shear thickening (dilatant) fluid. For shear thinning fluids, the increase in shear stress gives a higher proportional increase in shear rate. On the other hand, for shear thickening fluids the increase in shear stress gives less than a proportional increase in shear rate. The flow of Newtonian, shear thinning and shear thickening fluids is illustrated in Figure 2.12.

Processed tomato products are non-Newtonian fluids with shear thinning behaviour (Rao, Bourne & Cooley, 1981). The characteristics of shear thinning are considered to be the result of progressive disentanglement of particle aggregates and the orientation of the particles in the direction of shearing. This is supported by the occurrence of Newtonian behaviour at high shear rate due to complete orientation of particles. Likewise, Newtonian behaviour is observed at very low shear rate due to complete disorientation of particles. Another explanation of shear thinning is due to behaviour of highly solvated particles in the dispersed phase. It is suggested that the solvated layers may be progressively sheared away as the shear stress is increased resulting a decrease in the effective size of particles and thus a reduction in apparent viscosity (Holdsworth, 1971).

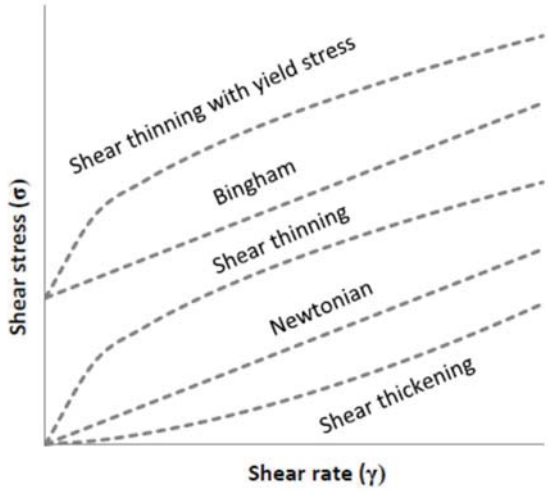

Figure 2-12 - Newtonian fluid and time independent non-Newtonian fluid (Bourne, 2002).

2.7.2 Yield stress

Yield stress is the minimum stress that must be exceeded before the fluid flows (Chhabra & Richardson, 2008). If the applied stress is smaller than the yield stress, the material will deform elastically and behave like an elastic solid. In contrast, if the stress applied is higher than the yield stress, the material starts to flow and behaves like a viscous fluid.

However, questions have been raised about the existence of true yield stress. Barnes (1999) challenged the idea of yield stress by citing that flow occurs even at stresses below yield stress. According to Barnes if stress is applied for a long enough time below the yield stress, the material will show slow but continual steady deformation than can be described by a Newtonian-plateau viscosity. Nevertheless it is agreed that the concept of yield stress is useful and practical in a number of areas such as food science, chemical, and biochemical engineering. In addition, flow models that include yield stress as one of their parameters have been shown to adequately describe the rheological behaviour of many real materials.

2.7.3 Models to describe the non-Newtonian flow behaviour of tomato products

Since the viscosity of non-Newtonian fluids is dependent on the shear rate, the flow behaviour of non-Newtonian fluids cannot be characterised by simple viscosity constant as for a Newtonian fluid. Instead rheological models or constitutive equations are required to describe their flow behaviour. Models that are widely used to describe the flow behaviour of tomato paste and tomato products are explained below.

2.7.3.1 Power Law or Ostwald de Waele

As discussed above, for shear thinning fluids the increase in shear stress gives a higher proportional increase in shear rate. This flow behaviour has been described in Figure 2.12. Correspondingly when shear stress versus shear rate data for shear thinning fluid is plotted on double logarithmic coordinates, the result is a linear graph over a wide range of shear rate values (Figure 2.13). This relationship is expressed mathematically as the power law or Ostwald de Waele model.

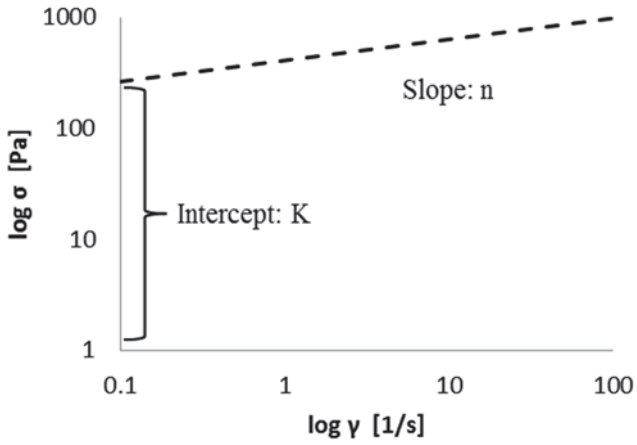

Figure 2-13 - Linear relationship between shear stress and shear rate for shear thinning fluid obeying power law (Holdsworth, 1971).

The power law equation can be written as;

$$\log(\sigma) = n\log(\gamma) + \log(K)$$
$$= \log\gamma^n + \log(K)$$
$$= \log(\gamma^n K)$$

$$\sigma = K\gamma^n \qquad \textbf{Equation 2.2}$$

Where;

K = consistency coefficient or sometimes referred as consistency index (Pa.s^n), and
n = flow behaviour index (dimensionless).

The apparent viscosity (η_{app}) is then;

$$\eta_{app} = \frac{\mathrm{K}\gamma^n}{\gamma} = \mathrm{K}\gamma^{n-1} \qquad \textbf{Equation 2.3}$$

The flow behaviour index (n) reflects the degree of deviation from Newtonian behaviour. For shear thinning fluid n < 1, the smaller the value of n indicates the greater degree of shear thinning. For Newtonian fluid, n=1 while for shear thickening fluids, n > 1. The values of parameters K and n are empirical and obtained by linear regression. It is important to mention that the value of parameter K is dependent on value of parameter n (even the units differ), therefore the values of K must not be compared when the n values differ (Chhabra & Richardson, 2008).

2.7.3.2 Herschel–Bulkley

When the yield stress term is included in the power law model, then the rheological model is known as Hershel-Bulkley model.

$$\sigma = K_H\gamma^{n_H} + \sigma_0 \qquad \textbf{Equation 2.4}$$

Where;

K_H = consistency coefficient or sometimes referred as consistency index (Pa.s^n),
n_H = flow behaviour index (dimensionless), and
σ_0 = yield stress

The value of Hershel-Bulkley model constants can be determined using linear regression if the value of yield stress is known from an independent experiment. If not, non-linear regression techniques are used. For non-linear regression techniques it is important to estimate sensible values for the initial parameters to make sure that the values obtained from the regression are not only best in a least squares scenario but that also reflect the true nature of the sample (Rao, 2007).

2.7.3.3 Casson model

Originally Casson model was develop for describing the flow behaviour of printing ink. However it has been used to describe a number of food dispersion.

$$\sigma^{0.5} = {\sigma_{0C}}^{0.5} + K_C \gamma^{0.5} \quad \textbf{Equation 2.5}$$

The plot of square root of shear stress ($\sigma^{0.5}$) versus square root of shear rate ($\gamma^{0.5}$) gives a straight line, with slope K_C and intercept ${\sigma_{0C}}^{0.5}$. The Casson yield stress (σ_{OC}) is calculated as the square of the intercept;

Where

K_C = Casson consistency coefficient ($Pa^{0.5}.s^{0.5}$),
σ_{0C} = Casson yield stress (Pa)

2.7.3.4 Literature models used for tomato products

Harper & Elsahrigi (1965) studied the flow behaviour of tomato concentrates at 5.8%, 12.8%, 16%, 25% and 30% total solid contents. They found that the power law model can satisfactorily describe the flow behaviour of the concentrates.

Rao, Bourne, and Cooley (1981) compared the use of the power law, Casson, and Herschel-Bulkley models to describe the flow behaviour of tomato concentrate processed from Nova, #475, New Yorker, and #934 varieties at 15% to 36% total solid contents. In the Herschel-Bulkley model, the value of yield stress obtained from Casson model was used and then the value of parameter K_H and n_H was obtained by linear regression analysis of log γ vs. log ($\sigma - \sigma_0$). They found that Casson model did not fit data well at low shear rates. As a consequence the Herschel-Bulkley model also showed a lower correlation coefficient due to the use of the Casson yield stress as one of the parameters in the Herschel-Bulkley model fitting. They reported a higher correlation coefficient for the power law model ($R^2 > 0.880$) compared to Casson ($R^2 > 0.714$) and Herschel-Bulkley models ($R^2 > 0.825$).

Rao and Cooley (1983) investigated the applicability of three models that both include yield stress to describe the flow behaviour of tomato concentrates. The fitting was performed using non-linear regression. These three models were Herschel-Bulkley, Mizrahi-Berk (Equation 2.6), and Vocadlo models (Equation 2.7).

$$\sigma^{0.5} = K_{OM} + K_M \gamma^{n_M} \quad \textbf{Equation 2.6}$$

$$\sigma = ({\sigma_{OV}}^{1/n_V} + K_V \gamma)^{n_V} \quad \textbf{Equation 2.7}$$

The Mizrahi-Berk model is a modification of the Casson model and it becomes Casson model when the parameter (n_M) is equal to 0.5. While the Vocadlo model was developed to be used to describe the rheology of visco-plastic materials. It becomes a simple power law model when the yield stress (σ_{OV}) is zero and simplified to the Bingham Plastic model when the flow behaviour index (n_V) is 1. Rao found that the Herschel-Bulkley and Mizrahi-Berk models satisfactorily represented the flow behaviour of tomato concentrates with Herschel-Bulkley

model showing the highest correlation of the three models. The Vocadlo model did not fit the flow behaviour data at low shear rates.

Tanglertpaibul and Rao (1987a) studied the effect of finisher screen opening on the rheological properties of tomato concentrates. The found that the power law model can be used to describe the flow behaviour of tomato concentrates with correlation coefficient in the range of 0.97 to 1.00. They also determined the value of yield stress for tomato concentrates by using a relaxation method and proposed the use of model that includes yield stress as one of the parameters, such as Herschel-Bulkley model.

Sharma *et al.* (1996) studied the effect of composition on the flow behaviour of tomato thin pulp prepared from five different tomato cultivars. They found that Herschel-Bukley model was the most suitable model to describe the flow behaviour of tomato thin pulps.

Augusto, Falguera, Cristianini, and Ibarz (2010) evaluated two models (Herschel-Bulkley and Falguera–Ibarz model) to describe the steady-state behaviour of commercial tomato juice (5.4 °Brix and 5.96% total solids) at shear rate range from 0.01 to 500s^{-1}. The Falguera–Ibarz model (Equation 2.8), explained the variation in apparent viscosity with shear rate by power decay from zero shear viscosity (η_O) to infinite viscosity (η_∞). They found that the value of R^2 for both models were always higher than 0.99.

$$\eta_{app} = \eta_\infty + (\eta_O - \eta_\infty)\gamma^{-k} \qquad \textbf{Equation 2.8}$$

2.7.4 Instruments used to measure rheological properties of tomato concentrates

The viscosity of tomato concentrates has been widely measured using Bostwick consistometry, especially in food manufacturing plants. The Bostwick consistometer is an empirical method which measures the distance a given amount of fluid will travel down a slanted trough upon being released from a container (Kramer & Szczesniak, 1973). The Bostwick measurement only gives flow behaviour data at one point of measurement (shear rate) and at the same time limited to the measurement of low viscosity tomato concentrates, since higher concentration tomato pastes will not flow in the Bostwick consistometer.

Since tomato concentrate is a non-Newtonian fluid, the measurement flow behaviour at different shear rate or shear stress will give more functional information about the rheological behaviour of tomato concentrates. This can be accomplished by using a viscometer or rheometer. Viscometers offer simple flow behaviour measurement while rheometers provide broader applications for flow behaviour characterisation. Table 2.9 shows the range of shear rates that can be measured using viscometers and rheometers and the relevance of shear rate to practical processing conditions.

Several measuring systems have been used with viscometers or rheometers to measure rheology of tomato concentrates. Rao and Cooley (1992) investigated the steady shear rheological properties of tomato paste using a viscometer with a concentric cylinder (MVII) geometry as the measuring system. Vercet, Cristina, Burgos, Monta & Buesa (2002) studied the flow behaviour of tomato pastes treated by conventional heating or by monothermosonication by using a rheometer equipped with concentric cylinder geometry (C25). Similarly rheometers with concentric cylinder geometries were used by Wu, Gamage, Vilkhu, Simons & Mawson (2008) for the flow behaviour of tomato juice treated with thermal treatment or

thermosonication and by Augusto *et al.* (2010) for the steady shear flow behaviour of tomato juice.

Table 2.9 - Relevant shear rate measurement ranges for viscometers and rheometers (Carrington & Langridge, 2005)

Process	Minimum shear rate (s^{-1})	Maximum shear rate (s^{-1})	Viscometer	Rheometer
Reverse gravure	10^5	10^6		✓
Spraying	10^4	10^5		✓
Blade coat	10^3	10^5	✓	✓
Mixing/stirring	10	10^3	✓	✓
Brushing	10	10^3	✓	✓
Pumping	1	10^3	✓	✓
Extrusion	1	10^2	✓	✓
Curtain coating	1	10^2	✓	✓
Levelling	10^{-2}	0.1		✓
Sagging	10^{-2}	0.1		✓
Sedimentation	10^{-6}	10^{-2}		✓

Xu *et al.* (1986) used a rheogoniometer with a cone and plate geometry to measure the flow behaviour of hot break and cold break tomato juice, however for hot break and cold break tomato paste they used two flat parallel plates (7.5cm diameter). They explained that tomato paste has a higher viscosity than tomato juice and the use of cone and plate that requires small gap can cause loading problems such as sample compacting. Thus a parallel plate is more suitable as a measuring system for the flow behaviour of tomato paste. Sharma *et al.* (1996) measured the flow behaviour of tomato thin pulp using a rheometer with a flat plate system with a gap of 1000 µm.

Yoo and Rao (1994) used a rheometer with a four-bladed vane geometry (diameter 2.1 cm and height 3cm) as the measuring system to determine the yield stress and steady shear flow behaviour of tomato concentrates at 10% to 35% pulp content and particle sizes of 0.34 mm and 0.71 mm. Moelants *et al.* (2014b) measured the flow behaviour of tomato derived suspensions at 25% to 60% pulp contents and different particle sizes using a rheometer with a six-bladed vane geometry (diameter 2.2 cm and height 1.6 cm).

Den Ouden and Van Vliet (2002) compared two measuring systems; a smooth concentric cylinder and rough concentric cylinder (covered with sandpaper) to measure the flow behaviour of tomato suspensions. They found that the shear stress of tomato suspensions measured using smooth concentric cylinder were lower compared to that measured with the sandpaper covered concentric cylinder. They attributed the phenomena to the occurrence of slip in the flow of tomato suspension measured using smooth wall measuring system.

Barnes (1995) explained the occurrence of slip in the flow of two-phase system is due to the displacement of the dispersed phase away from solid boundaries. This is attributed to the steric, hydrodynamic, viscoelastic, chemical, and gravitational forces acting on the dispersed phase adjacent to the solid boundaries. The displacement of the dispersed phase away from the solid boundaries creates a low viscosity layer at the boundaries and explains the lower apparent flow behaviour of the suspension.

The vane geometry has been suggested to able to eliminate slip effects and at the same time offers several advantages, such as minimal disturbance to the microstructure of the sample upon insertion of the vane into the sample. Originally vane geometries were used to measure yield stresses, due to assumption that the liquids entrapped between the blades move together with the vane as a solid body, thus when yielding occurs, it occurs within the fluid itself, thus eliminating slip (Chhabra & Richardson, 2008). According to Barnes and Carnali (1990) for non-Newtonian fluids with flow indexes (n) of power law less than 0.5, the fluid between the blades does move as a solid body, and therefore functions like a bob-in-cup geometry but with the added advantage of eliminating slip. Tomato paste and tomato concentrate has a flow index of 0.13 to 0.35 (Rao & Cooley, 1992) and less than 0.31 (Rao, Bourne, & Cooley, 1981) respectively thus suggesting that vane geometry can be used in this study to eliminate slip.

Table 2.10 summarises the instruments and measuring system used to measure the steady flow behaviour of tomato products.

2.7.5 Functional model of tomato products

Several functional models have been developed to relate the apparent viscosity, yield stress, and flow behaviour model's parameters of tomato products with total solids, pulp content, water insoluble solids, particle size, and serum viscosity.

Rao, Bourne, and Cooley (1981) found that the magnitude of the power law consistency index (K), increased with increasing total solids content in tomato concentrates. They proposed that the relationship between K value and total solid content can be described by a power law model (Equation 2.9) or an exponential model (Equation 2.10). They reported that the power model showed higher correlation compared to the exponential model.

$$K = A(\%Total\ solids)^B \qquad \textbf{Equation 2.9}$$

$$K = A_1 exp(B_1 \times \%Total\ solids) \qquad \textbf{Equation 2.10}$$

Where parameters A, B, A_1 and B_1 are fitted empirical constants.

Table 2.10 - Instruments and measuring systems used to measure the steady flow behaviour of tomato products.

Instrument	Measuring system	Sample	References
Haake RV2 viscometer	Concentric cylinder (MVII)	Tomato paste	Rao and Cooley (1992)
Bohlin CS controlled stress rheometer	Concentric cylinder (C25)	Tomato paste treated by conventional thermal treatment or monothermosonication	Vercet *et al.* (2002)
Rheometer MCR 300	Concentric cylinder (CC27)	Tomato juice treated with thermal treatment or thermosonication	Wu *et al.* (2008)
Haake RS 80 rheometer	Concentric cylinder	Tomato juice	Augusto *et al.* (2010)
Rheogoniometer	Cone and plate	Hot break and cold break tomato juice	Xu *et al.* (1986)
	Parallel plates (7.5cm diameter)	Hot break and cold break tomato paste	
Carri-Med CSL 100 Controlled Stress Rheometer	Parallel plates with a gap of 1000 µm	Tomato thin pulp	Sharma *et al.* (1996)
Deer rheometer III	Four-bladed vane geometry (diameter 2.1 cm and height 3cm)	Tomato concentrates at 10% to 35% pulp content and particle size of 0.34 mm and 0.71 mm	Yoo and Rao (1994)
Stress-controlled rheometer MCR 501	Six-bladed vane geometry (diameter 2.2 cm and height 1.6 cm).	Tomato derived suspension at 25% to 60% pulp content and different particle	Moelants *et al.* (2014b)
Bohlin VOR Rheometer	Serrated plates (diameter 3 cm)	Tomato suspension	Den Ouden and Van Vliet (2002)
Haake Viscometer	Coaxial cylinder measuring system, type P (ribbed outer cylinder)		
	MV3 inner cylinder covered with sandpaper		

Similarly, Fito, Clemente and Sanz (1983) also found that the K value can be related to soluble solids concentration (°Brix) by a power model (Equation 2.11). They also suggested that the flow behaviour index value (n) is related to degree of concentration by a linear equation (Equation 2.12).

$$K = A_2(°Brix)^{B_2} \quad \textbf{Equation 2.11}$$

$$n = A_3 - B_3(\log °Brix) \quad \textbf{Equation 2.12}$$

Where A_2, B_2, A_3 and B_3 are empirically fitted constants.

Rao and Cooley (1983) proposed that the logarithm of tomato yield stress can be related to total solid by a quadratic equation (Equation 2.13)

$$\ln \sigma_O = A_4 + B_4(\%Total\ solids) + C_4(\%Total\ solids)^2 \quad \textbf{Equation 2.13}$$

Where A_4, B_4 and C_4 are empirically fitted constants.

Tanglertpaibul and Rao (1987b) centrifuged tomato juice at 11,700 x g to separate tomato juice serum and pulp. The serum (5.6 °Brix) obtained from the centrifugation was then concentrated to 10, 15 and 20 °Brix. After that, the pulp was combined with the prepared serum to produce tomato concentrate with different pulp contents at every serum concentration (°Brix). They proposed that the apparent viscosity of tomato concentrates is related to the pulp content and serum viscosity (Equation 2.14). They suggested that the serum viscosity is dependent of the soluble pectin content (Equation2.15)

$$\eta_{100} = A_5(Pulp\ content)^{B_5} + \eta_{serum} \quad \textbf{Equation 2.14}$$

$$\eta_{serum} = A_6 + B_6(Soluble\ pectin)^{C_6} \quad \textbf{Equation 2.15}$$

Where A_5, B_5, A_6, B_6 and C_6 are empirically fitted constants.

Rao and Cooley (1992) suggested that relative viscosity of tomato paste cannot be satisfactorily described by solid volume fraction (ϕ_{solid}) only. Since tomato paste is a more concentrated form of tomato suspension, they proposed that tomato pastes strong network structure is due to the contribution of; 1) network structure contributed by solid phase, in proportion to (ϕ_{solid}), 2) network structure contributed by viscous serum phase, in proportion to (ϕ_{liquid} = 1 − ϕ_{solid}). Thus the functional model for tomato paste should include the network structure contributed by both solid phase and viscous serum phase. They proposed Equation 2.16 for the power law consistency coefficient (K) and Equation 2.17 for the Casson yield stress (σ_{O_C});

$$\frac{1}{K} = \frac{\phi_{solid}}{A_7} + \frac{1-\phi_{solid}}{B_7} \quad \textbf{Equation 2.16}$$

$$\frac{1}{\sigma_{O_C}} = \frac{\phi_{solid}}{A_8} + \frac{1-\phi_{solid}}{B_8} \quad \textbf{Equation 2.17}$$

Where A_7, B_7, A_8 and B_8 are empirically fitted constants.

Sharma *et al.* (1996) found that the magnitude of yield stress obtained from fitting of the flow behaviour of tomato thin pulp with Herschel-Bulkley model can be related to water insoluble solid (%WIS) content using Equation 2.18.

$$\sigma_O = A_9 exp(B_9 \times \%WIS) \qquad \textbf{Equation 2.18}$$

Where A_9 and B_9 are empirically fitted constants.

Moelants *et al.* (2014b) suggested that an increase in the yield stress of tomato suspension with the increase in pulp content could be fitted to a power law model (Equation 2.18).

$$\sigma_O = A_{10}(\%\mathrm{Pulp})^{B_{10}} \qquad \textbf{Equation 2.19}$$

Where A_{10} and B_{10} are empirically fitted constants.

Although these attempts have been made to link compositional properties of tomato products to the rheological properties, it is likely that the fitting parameters will vary with variety and processing method due to the resulting differences in pectin solubilisation and particle size reduction.

2.8 Conclusions

There has been substantial study of tomato products and how raw material and processing variations cause differences in composition and functionality. Much research has been done on the solubilisation of pectins and their impact on properties. Insoluble solids play an important role in the rheological behaviour of tomato products. The particle size of the insoluble material is also a key factor that can be controlled to some extent by the finisher size. In addition, soluble pectins affect the serum phase viscosity.

A variety of different rheological techniques have been used to measure paste flow behaviour. Of these, rheometry with a vane geometry seems to be the most applicable to tomato paste. Similarly, a range of flow models have been used to describe the flow. Of these, the power law and Herschel Bulkley models have been successfully applied to describe tomato paste flow by several different research groups.

There has been some attempt to link flow behaviour model parameters (such as K or σ_O) to compositional properties of tomato pastes. These approaches offer a useful starting point for this research. Because these relationships are likely to be dependent on the raw materials and processing methods used to produce the paste, it is likely that the functional model parameters will be product specific. As such, this research should identify the simplest overall model and how it can be applied in an industrial context. Of particular relevance is how the flow behaviour will change on dilution of the paste in subsequent food processing operations.

Chapter 3

Evaluation of flow models for tomato paste production

3.1 Introduction

The Power law and Herschel-Bulkley models have been shown to satisfactorily describe the flow behaviour of tomato products (Augusto et al., 2012; Harper & ElSahrigi, 1965; Rao & Cooley, 1983; Sharma et al., 1996; Tanglertpaibul & Rao, 1987). However, it is preferable to choose only one model to be used in this entire study. For this reason, in this chapter the performance of the power law and Herschel-Bulkley models are compared for five commercial tomato pastes. This will provide the basis for future work aimed at finding relationships between the parameters of the chosen model and the compositional properties of tomato paste (total solids content, °Brix, water insoluble solids content, and pulp content).

3.2 Materials

Commercial tomato pastes from five different manufacturers were purchased in a local New Zealand supermarket and used in this study. To assure the standardization of the samples, tomato paste packages with the same batch number were used within each brand. Samples from the same batch number for each brand were assumed to have the same compositional and flow behavior properties. Table 3.1 shows the brand, designation, batch number, and basic compositional properties (from the label) of the tomato pastes used in this study.

Table 3-1 - General information of tomato paste used in this study

Brand	Code	Batch number	Country of manufacture	Ingredients	% Composition			
					Protein	Carbohydrate	Sugar	Sodium
Delmain	TP1	L1867 07 2015 14:44	France	Tomato	4.2	11.3	6.1	1.6
Homebrand	TP2	3302/ 01046	China	Tomato paste (99%), and salts	4.1	15.7	12.1	0.21
Watties	TP3	TV 31131940 H2	New Zealand	Concentrated tomatoes, and citric acid	3.5	13.9	10.8	0.4
Mutti	TP4	B/B 01/07/2016	Italy	99.5 % tomato, and salts	4.2	17	12.3	3.4
Leggos	TP5	B/B 030416 1229	Australia	Tomato paste (99%), and salts	3.4	10.1	9.8	4.6

3.3 Methods

The physicochemical properties (total solids, Brix°, water insoluble solids, and phase volume fraction) and flow behaviour of tomato pastes were measured using the following methods.

3.3.1 Total solids

The total solids content of the tomato paste samples were determined using a vacuum oven following the AOAC Official Method 964.22 with a few modifications. The vacuum oven method has been shown to give the least variation between results for tomato paste samples (Campbell, 2004). Aluminium dishes and lids were dried at 108°C in an air forced oven (Contherm) for 1 hour and then cooled down in a desiccator containing dry silica gel for 1 hour. The dishes and lids were weighed with a Metler Analytical Balance (AE 200). About 2.0 gram of tomato paste was accurately weighed into the aluminium dishes and spread into a thin layer as rapidly as possible to avoid moisture loss. The aluminium dishes were placed in the vacuum oven at 70°C for 12 h. After drying, the aluminium dishes were quickly covered with their lids and put in the desiccator for 1 hour and weighed as soon as possible after samples reached room temperature. The percentage total solids in the tomato paste were calculated as;

$$\%\,\boldsymbol{Total\ solids} = \frac{\boldsymbol{Tomato\ paste\ weight\ after\ drying}}{\boldsymbol{Tomato\ paste\ weight\ before\ drying}} \times \mathbf{100}\% \qquad \textbf{Equation 3.1}$$

Total solids evaluations for each tomato paste sample were performed with five replicates. Total solids were reported in units of kg total solids.kg tomato paste^{-1}.

3.3.2 Soluble solids (° Brix)

The presence of insoluble solids in tomato paste has been shown to affect the Brix° reading (Campbell, 2004). Therefore, tomato paste and diluted tomato pastes were centrifuged at 8000 rpm for 60 minutes before Brix° measurement to separate the insoluble solids. After centrifugation, the serum phase was decanted and used to determine the Brix° value of the paste using a bench-top refractometer (RFM 330, Bellingham Stanley Ltd) at 20 °C. The experiments were done in triplicate. This method provides soluble solids measurements measured in °Brix (kg soluble solids.kg solution^{-1}). Note that this unit does not include the insoluble solids component in its basis. For this reason, equation 3.2 was used to covert the units to have a total paste basis (kg soluble solids.kg paste^{-1}).

$$\%\,\boldsymbol{Soluble\ solids} = \frac{^{\circ}\boldsymbol{Brix}}{\mathbf{100} - ^{\circ}\boldsymbol{Brix}} \times (\mathbf{100} - \%\,\boldsymbol{Total\ solids}) \qquad \textbf{Equation 3.2}$$

3.3.3 Water insoluble solids content

Water insoluble solids content was determined from a total mass balance as given by the following equation;

$$\%\,WIS = \%\,Total\ solids - \%\,Soluble\ solids \quad \textbf{Equation 3.3}$$

Substitution of Equation 3.2 into Equation 3.3 and rearrangement gives;

$$\%\,WIS = \frac{\%\,Total\ solids - °Brix}{100 - °Brix} \times 100 \quad \textbf{Equation 3.4}$$

3.3.4 Pulp fraction

The serum separation method based on Rao & Cooley (1992) was used in this study to characterise the pulp fraction of the paste. According to Rao, a centrifugal force of 100, 000 x g is required to satisfactorily separate the serum and dispersed phase of tomato paste. A 25 g sample of tomato paste was weighed into a pre-weighed centrifuge tube. Tomato pastes were centrifuged at 101, 000 x g (37, 500 rpm) for 90 minutes using an ultracentrifuge (WX Ultra 80) equipped with a T865 rotor. The serum fraction was decanted off the top and the remaining pallet was weighed. The pulp fraction was determined using the following equation;

$$\%\,\boldsymbol{Pulp\ fraction} = \frac{\boldsymbol{Mass\ of\ pallet}}{\boldsymbol{Mass\ of\ tomato\ paste}} \times \mathbf{100}\% \quad \textbf{Equation 3.5}$$

The experiments were done in triplicate.

3.3.5 Flow behaviour

The flow behaviour of tomato pastes and suspensions were measured using a rheometer (MCR 302, Anton Paar) at temperature of 25 °C. A cup (diameter 28.930 mm) with a four-bladed vane (diameter 22 mm and height 40 mm) was used as the measuring system. The sample was pre-sheared for 1 minute at a shear rate (γ) of 100 s^{-1} followed by 2 minutes of rest (γ = 0 s^{-1}) before all measurements to eliminate the effect of loading history on the sample structure. The sample was then sheared at increasing shear rate (γ) from 0.1 to 100 s^{-1} with fifty equally spaced measurement points. For each original tomato paste, the experiment was run in duplicate. All experiments were performed on fresh samples to avoid any influence of the shear history.

3.4 Results and discussion

3.4.1 Compositional characteristics

Table 3.2 shows the compositional properties of the tomato paste types used in this study. Tomato paste is a concentrated form of tomato dispersion. As can be seen from the table, all samples had total solid contents and soluble solid contents higher than 22.1% and 21.0 °Brix, respectively, with TP1 being the most concentrated. Tomato paste 3 had the highest levels of water insoluble solids and Tomato paste 5 had the highest pulp content.

Table 3-2 Compositional properties of tomato paste.

Tomato paste	Total solids (% total basis)	Soluble solids (°Brix)	Water insoluble solids (% total basis)	Pulp content (% total basis)
TP 1	30.7 ± 0.2	29.7*	1.4	31.42 ± 0.12
TP 2	26.2 ± 0.4	25.4*	1.1	33.97 ± 0.94
TP 3	23.5 ± 0.2	21.7*	2.3	26.21 ± 0.17
TP 4	30.3 ± 0.7	29.6*	0.9	30.72 ± 0.10
TP 5	22.1 ± 0.2	21.0*	1.4	34.50 ± 0.52

Mean ± standard deviation *All replicated °Brix readings were identical at the precision of the instrument.

From the table, it also can be seen that the pulp content is not dependent on the water insoluble solids content alone since there was no correlation between % WIS and % pulp content was observed. Beresovsky, Kopelman, and Mizrahi (1995) reported that the volume of pulp (precipitated by centrifugation) depends not only on the mass of insoluble solids but also on the extent of inter-particle interactions. Whereas Takada and Nelson (1983) proposed that the weight ratio of precipitate to the initial sample weight after centrifugation (precipitate weight ratio) is a measure of water holding capacity of the water insoluble solids that is influenced by the amount and physical properties of the water insoluble solid. However, they did not discuss in detail what physical properties of the water insoluble solid contributed to the higher precipitate weight ratio.

3.4.2 Flow behaviour of tomato paste

Figure 3.1 shows the comparison between the flow curves measured for each tomato paste sample.

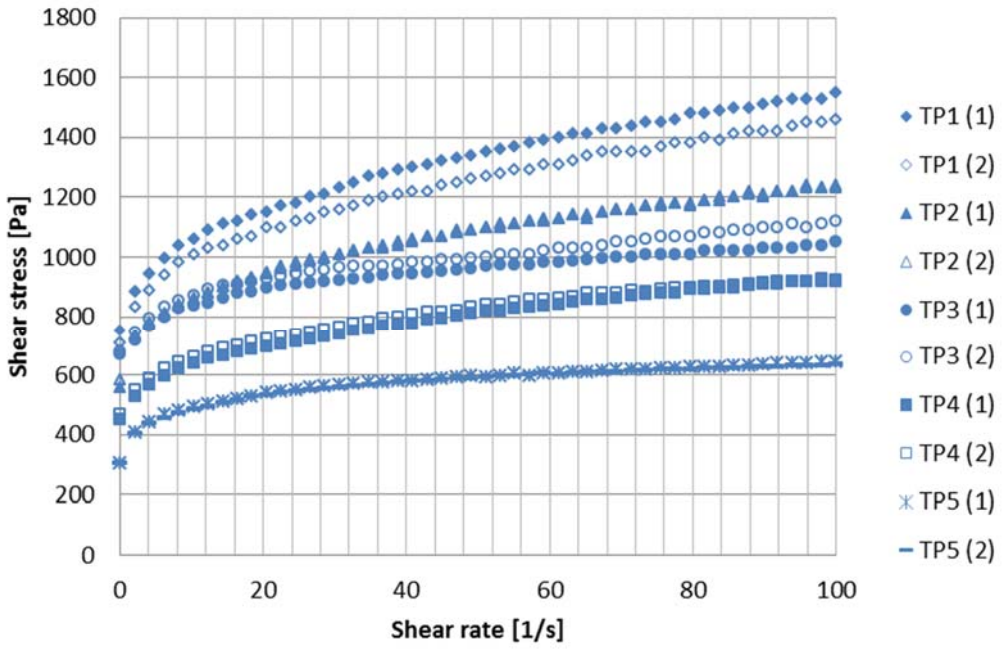

Figure 3.1- Plot of shear stress vs shear rate of tomato pastes including replicates.

In this study, the flow behaviours of tomato pastes were measured by subjecting them to shear rates ranging from 0.1 to 100 s^{-1}. Figure 3.1 shows that all tomato pastes have similar flow behaviours, showing an increase in shear stress as shear rate increases. There is clear shear thinning behaviour as previously reported by other researchers (Augusto et al., 2012; Rao & Cooley 1992; Sharma et al., 1996; Xue et al., 1986). It is possible that the pastes exhibit a yield stress at very low shear rates as has also been reported (Bayod, Mansson, Innings, Bergenstahl, & Tornberg 2007; Rao & Cooley 1992; Sharma et al., 1996; Yoo & Rao, 1995) and for this reason it is likely that the Hershel Bulkley model may be appropriate. It is clear that tomato paste is a non-Newtonian fluid with shear thinning behaviour and the possible occurrence of a yield stress.

While there are small differences between the replicate flow curves for each paste, there are much larger differences between different pastes. Figure 3.1 also illustrated that TP1 has the highest shear stress versus shear rate data. This equates to the highest apparent viscosity. This is followed by TP2, TP3, TP4, and the lowest apparent viscosity is TP5. Some of the flow behaviour differences may be linked to the compositional differences between the pastes (e.g. TP1 has the highest apparent viscosity and the highest total solids content, TP5 has the lowest apparent viscosity and the lowest total solids content). It is evident however, that such simple comparisons are not useful due to the broad differences in total solids and insoluble to soluble solids ratios.

3.4.3 Flow behaviour model

The power law and Herschel-Bulkley models have been shown to satisfactorily describe the flow behaviour of tomato concentrates (Rao et al., 1981; Sharma et al., 1996). Thus, in this study, the flow behaviour data of tomato pastes were fitted to these two models; the power law model (Equation 2.2) and the Hershel-Bulkley model (Equation 2.3).

The parameters K and n for the power law model and K_H, n_H, and σ_o for the Herschel-Bulkley model were obtained for each replicate by linear and non-linear regression methods, respectively, using the solver function in Excel. This was achieved by minimizing the sum of the squared errors (SSE), which is the square of the difference between experimental shear stress and the predicted shear stress at each shear rate. In this fitting method, one constraint was introduced, which was that the value of flow behaviour indexes (n, n_H) for both models should be less than or equal to 1.

Since the initial or guessed value for the parameters (K, n, K_H, n_H, and σ_o) in the models are important, all initial parameters were obtained from Rao, Bourne, & Cooley (1981) for tomato concentrates at 36% total solids.

The parameters obtained from fitting the flow behaviour data to power law and Hershel-Bulkley model for each replicate are shown in Table 3.3. The correlation coefficients ranged from 0.958 to 0.997 and 0.997 to 0.999 for the power law and Hershel-Bulkley models, respectively. This shows that both models satisfactorily described the flow behaviour of the tomato pastes. The Hershel-Bulkley model shows higher correlation coefficients compared to power law model and at the same time includes yield stress parameter in the equation. Thus it is preferable to use Hershel-Bulkley model in this study to describe the flow behaviour of tomato paste and diluted tomato paste.

Tomato pastes show shear thinning behaviour, with all tomato pastes showing a flow behaviour index value less than 1. In this study the flow behaviour index (n_H) values varied in range from 0.13 to 0.38, while the consistency coefficient (K_H) value ranged from 111 to 311 $Pa.s^n$.

Table 3-3 - Power law and Hershel Bulkley parameters for each tomato paste

Tomato paste	Power Law			Hershel-Bulkley			
	K (Pa.s^n)	n	R^2	K_H (Pa.s^n)	n_H	σ_o (Pa)	R^2
TP 1	766	0.15	0.959	149	0.38	692	0.999
	725	0.15	0.958	138	0.38	657	0.999
TP 2	628	0.14	0.979	199	0.29	467	0.999
	634	0.14	0.975	175	0.31	501	0.999
TP 3	700	0.08	0.962	145	0.25	573	0.993
	711	0.09	0.950	124	0.30	614	0.988
TP 4	459	0.15	0.960	92	0.38	412	0.999
	492	0.13	0.970	130	0.31	394	0.997
TP 5	380	0.11	0.998	313	0.13	69	0.998
	377	0.11	0.997	311	0.13	67	0.997

The yield stress (σ_o) value of tomato paste ranged from 69 to 594 Pa. Table 3.4 showed the value of Herschel-Bulkley parameters reported by other researchers for tomato concentrates. The values were slightly different from this study. This might be due to different tomato paste types and compositions or the measuring system used (vane vs cylindrical geometries).

3.4.4 Correlation between physicochemical properties of tomato paste and Herschel-Bulkley parameters

Correlations between the Herschel-Bulkley parameters fitted above and compositional properties of different brands of tomato paste were determined by plotting K_H, n_H and σ_o against total solid content (% TS), °Brix, water insoluble solid content (% WIS), and pulp content (% Pulp). These are shown in Figure 3.2.

Figure 3.2 showed no clear trends on the effect of total solids content, °Brix, water insoluble solids content, and pulp content on K_H, n_H, and σ_o. These plots should be interpreted carefully. This can be seen from the graph of flow behaviour index (n_H) against total solids or °Brix, that suggests that increased concentrations cause an increase in flow behaviour index (n_H). An increase in flow behaviour index indicates a move towards more Newtonian behaviour which is not intuitive. It may be expected that an increase in water insoluble solids would increase the shear thinning nature of the fluid, and to some extent this is evident in figure 3.2. The trend is not strong however, suggesting that the nature of the water insoluble solids may be different for each paste (e.g. more or less cell wall clumps or different pectin chain lengths or structure).

The observed result might be due to the narrow range of each independent variable. Thus to better elucidate the effect of total solids content, °Brix, water insoluble solid content, and pulp content on K_H, n_H and σ_o, the samples were diluted to four concentrations (0.75, 0.5, 0.25, and 0.125, relative to the original strength w/w). This was done by manually mixing a certain amount of tomato paste with reverse osmosis (RO) water. The diluted tomato paste (0.75, 0.5, 0.25, and 0.125, w/w) were measured for Brix° value and flow behaviour data. The data for total solids, water insoluble solids, and pulp content for diluted tomato pastes were calculated by multiplying the value of the original tomato pastes data by its dilution factor. The measurement was done at the same day of sample preparation and the prepared tomato paste dilutions were covered with aluminium foil to avoid moisture losses while waiting to be analysed.

Table 3-4 - Values of Herschel-Bulkley parameter reported by other researchers.

Reference	Sample	Designation	Concentration	Instrument	Model fitting	n_H	K_H	σ_o
Rao et al. (1981)	Tomato concentrate	New Yorker	5.6 – 36% total solid	Viscometer; Concentric cylinder MVI	Hershel-Bulkley; Linear regression using Cason yield stress	0.39-0.66	0.6 - 30.6	3 – 121
		#475				0.33-0.64	1 - 167.4	6 – 149
		Nova				0.47-0.64	0.3 - 188	3 – 51
		#934 HB				0.43-0.59	0.5 - 33.5	2 – 118
		#934 CB				0.27-0.63	0.1 - 33.9	3 – 122
Rao and Cooley (1983)	Tomato concentrate	New Yorker	5.6 – 36% total solid	Viscometer; Concentric cylinder MVI	Hershel-Bulkley	0.52	0.2 - 16.7	3 – 100
		#475				0.53	0.3 - 79.7	6 – 157
		nova				0.54	1.2 - 63.2	3 – 63
		#934				0.51	0.1 - 33.9	2 – 111
Sharma et al. (1996)	Tomato concentrate		0.7 – 1.4% WIS	Controlled stress rheometer; flat plate system	Hershel-Bulkley	0.42 - 0.54	1.28 - 3.66	13 – 28
Bayod et al. (2007)	Tomato paste	HB-28/30	6.5% WIS	Controlled stress rheometer; four-bladed vane	Time dependent rheological measurement	-	-	89
		HB-22/24	6.9% WIS			-	-	89
		CB-36/38	5.9% WIS			-	-	211
Correia and Mittal (1999)	Tomato paste			Concentric cylinder	Hershel-Bulkley	0.5	28	159

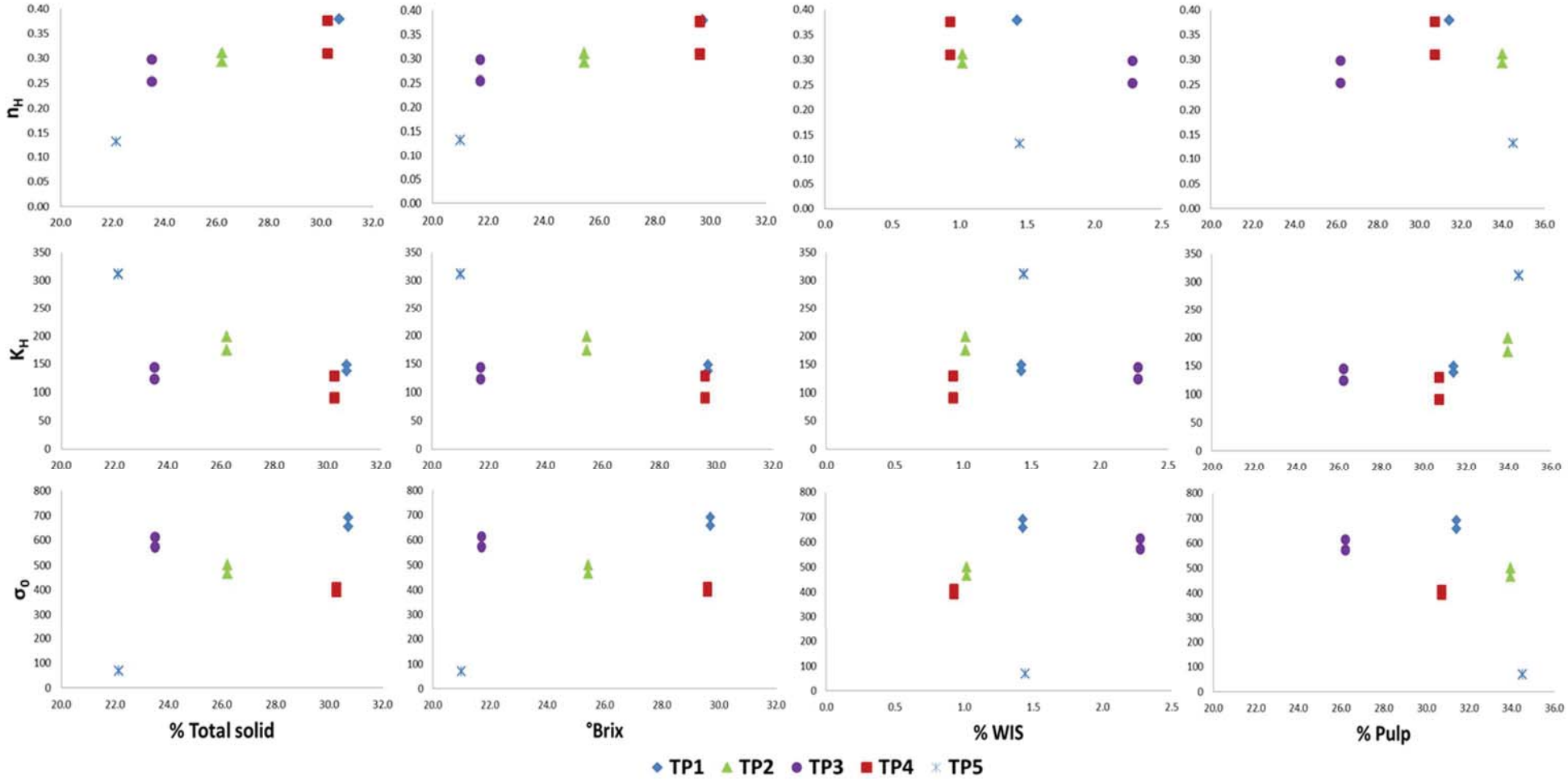

Figure 3.2 - Correlation between Herschel-Bulkley parameters and compositional properties.

3.4.5 Effect of dilution on Herschel-Bulkley parameter

Table 3.5 below shows the compositional and Herschel Bulkley model parameters fitted to the flow curves for the diluted paste TP5. For diluted tomato paste samples, only tomato pastes TP3 and TP5 were run in duplicate. Both sets of results showed good reproducibility (data for TP3 not shown). For other diluted tomato paste samples, the experiment was run only once due to this good reproducibility and the significant time required to measure the rheological properties of the samples.

Table 3-5 - °Brix, total solid content and Herschel-Bulkley parameters of tomato paste TP5 at different concentrations.

Dilution	°Brix	Total solid (%)	K_H (Pa.s^n)	n_H	σ_o (Pa)	R^2
Original	21	22.1	172	0.20	220	0.993
			168	0.20	213	0.991
0.75	15.6	16.6	26	0.40	127	0.998
			28	0.38	124	0.997
0.50	10.4	11.1	3	0.59	37	0.996
			3	0.60	38	0.996
0.25	5.1	5.5	0.11	0.75	2	0.997
			0.12	0.74	2	0.993
0.125	2.6	2.8	0.01	1.00	0.05	0.983
			0.01	1.00	0.04	0.981

Table 3.5 shows that the values of K_H, n_H, and σ_o are a function of concentration. As the concentration of tomato paste decreased by dilution, the values of n_H increase and the values of K_H and τ_0 decrease (the same result was obtained for other tomato pastes). As has been proposed by Harper and ElSahrigi (1965), n_H is the measure of the extent of departure of a fluid from Newtonian behaviour, while K_H is the measure of magnitude or consistency. Thus, when the concentration of tomato paste in this study was reduced by dilution, the result shows that flow behaviour of tomato paste was changed from non-Newtonian to nearly Newtonian and the viscosity was decreased.

For tomato pastes at a dilution 0.125 x the original concentration, the correlation coefficient (0.988) is lower compared to other samples (original, 0.75, 0.5, and 0.25) and the graph is not as smooth as other samples. This might be because at lower concentration, the viscosity is low (in this case the viscosity of diluted tomato paste at concentration 0.125 ranged from 0.012 to 2 Pa) and according to Barnes and Nguyen (2001), the vane geometry cannot give accurate results when used to measure low viscosity liquid due to inertial effects. This explained the flow behavior data of low concentrated tomato paste. As a consequence of this, data for diluted tomato paste at this concentration was not taken into consideration.

Figure 3.3 shows the fitted Herschel Bulkley parameters for each paste as a function of the various compositional factors. For each individual paste there are clear trends observed in each parameter as a result of dilution. Simple trendlines were fitted. For the relationship

between the independent variables (composition) and n_H, a linear relationship was applied while for K_H and σ_o a power relationship was applied. As has been discussed above, the value of n_H decreased and the values of K_H and σ_o increased as the concentration increases, as expected. The parameters from the model changed with dilution in similar ways for all the pastes however the dependency differed substantially between brands. Figure 3.3 shows that tomato paste TP1 was the most sensitive to changes in concentration for both n_H and K_H but had only a small effect on yield stress (σ_o). Tomato paste TP3 behaved similarly except there was a strong effect of concentration on yield stress. Tomato pastes TP4 and TP5 were the least sensitive to changes in concentration for all Herschel Bulkley model parameters. TP2 behaved between these two extremes in all aspects.

The reason for these trends is not clearly explained by the composition of these paste samples. Tomato paste TP1 and TP3 had had relatively high insoluble solids content however tomato paste TP5 had similar insoluble solids content to TP1, yet had very different behaviour in Figure 3.3. Pastes with the highest insoluble to total solids ratios were TP3 (9.8%) and TP5 (6.3%) while TP1 (4.6%) and TP2 (4.2%) had similar concentrations and TP4 (3.0%) had the lowest fraction of solids being insoluble.

By diluting the paste samples in this way, all component concentrations are lowered by the same amount. As such it is not possible to identify which components are responsible for the changes in rheological parameters. Water soluble pectins could contribute to serum viscosity which in turn could impact on paste viscosity. It is likely that the insoluble solids fraction is the principal contributor to overall paste rheology. It seems from the data collected here, that the nature of these insoluble solids is different for each of the pastes. It is possible that differences in insoluble solids structure could occur through variations in fruit cultivar, ripeness during processing, conditions for further enzyme hydrolysis in the break process and in general damage during breaking, pumping and filling operations. More systematic investigation into how different fractions and their component ratios in the tomato paste are required to answer these questions.

A general correlation between compositional properties of tomato concentrates and Herschel-Bulkley parameters was explored irrespective of the tomato paste brand. These plots of Herschel-Bulkley parameters against total solids content, °Brix, water insoluble solids content, and pulp are shown in Figure 3.4. The result shows higher correlation coefficients for plots of K_H and σ_o against total solids content and n_H against pulp content. Rao et al., (1981) reported similar results in that the consistency coefficient (K_H) of tomato concentrate is a function of total solids content and proposed an exponential (Equation 2.8) and power (Equation 2.9) model to describe the relationship between both variables. As has been mentioned before, they found that power model has a higher correlation coefficient compared to the exponential model.

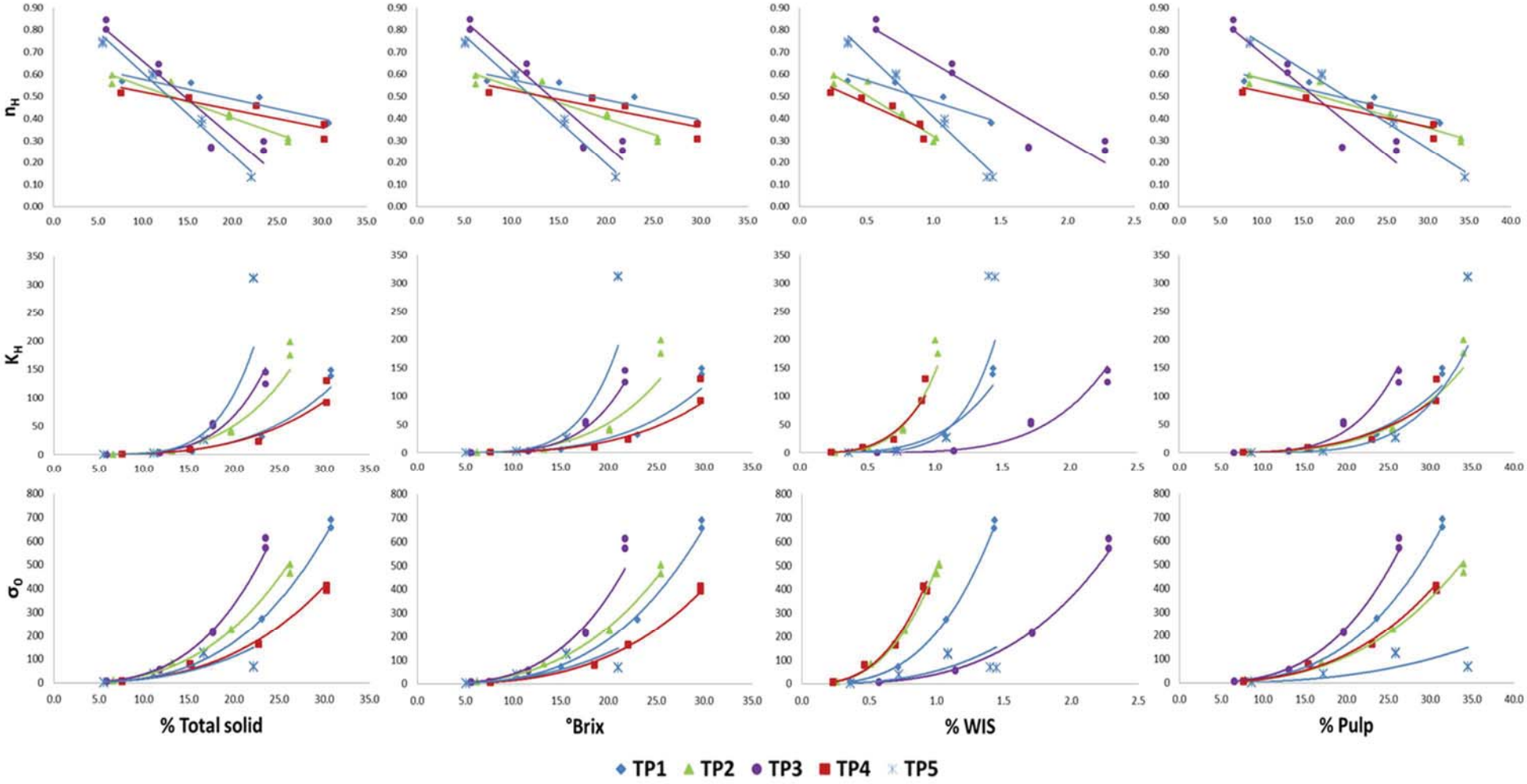

Figure 3.3 - Effect of dilution on Herschel-Bulkley parameters.

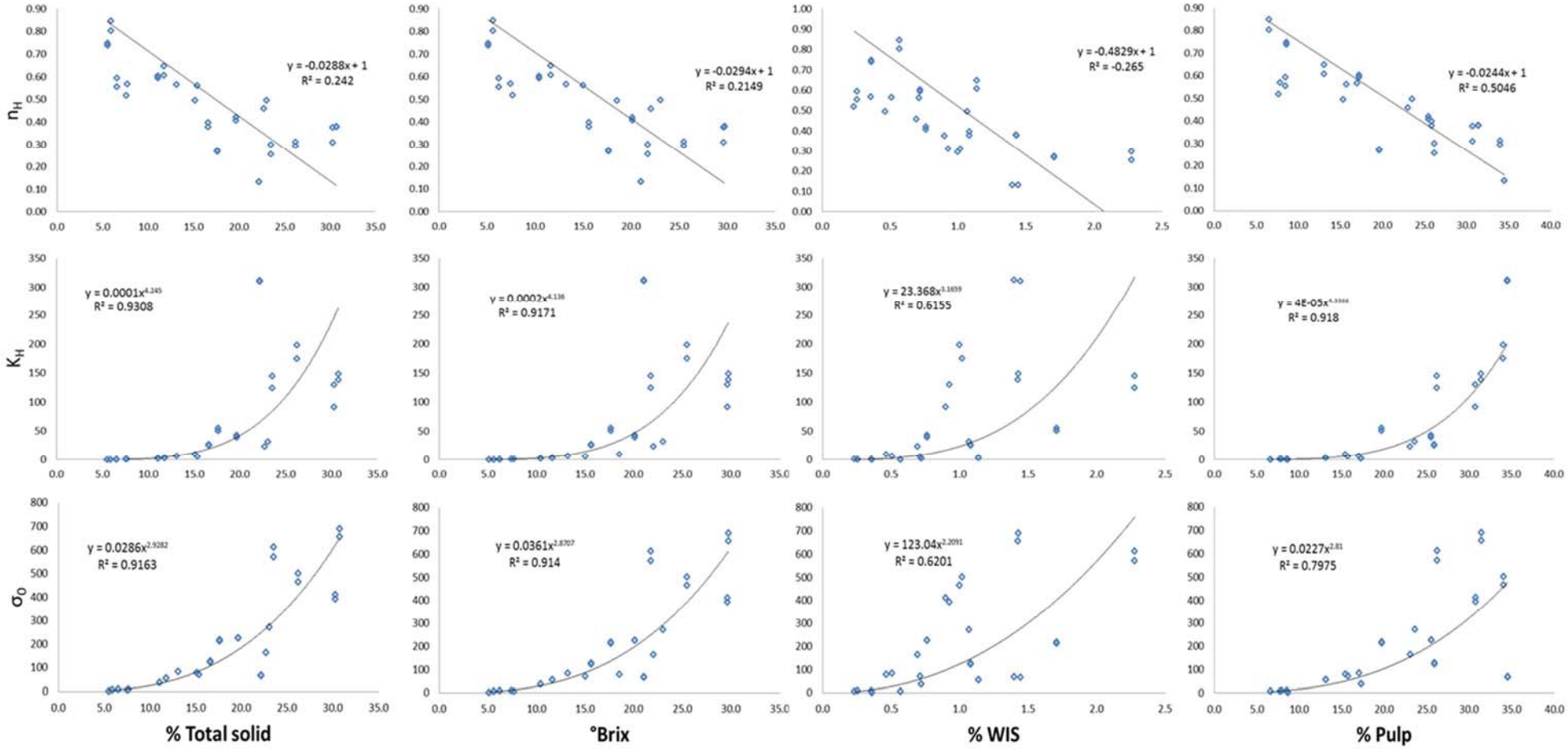

Figure 3.4 - Relationship between physicochemical properties of tomato concentrates and Herschel-Bulkley parameters.

3.5 Conclusions

Five different tomato paste samples, made by different manufacturers were characterised for compositional and rheological differences. For each paste, the Herschel-Bulkley model could explain the rheological behaviour better than the simple power law and was selected to describe the flow behaviour of tomato pastes and diluted tomato pastes for the remainder of this study.

The total solid content shows a strong contribution to the Herschel-Bulkley parameters. However, to verify this, further characterisation is required since upon dilution all variables (total solid, °Brix, water insoluble solid, and pulp content) were also changed. Thus, the aim of the next chapter was to change one variable while make other variables constant so the effect of specific variables on rheological properties of tomato concentrate could be elucidated. In addition, the contribution of serum phase to the flow behaviour of tomato phase was investigated.

Chapter 4

The effect of the serum phase on tomato paste rheology.

4.1 Introduction

Tomato products can be considered as a suspension of insoluble plant-tissue-based particles that composed of finely-divided cellular debris, including lignin, cellulose, hemicellulose and insoluble pectin in a continuous serum phase that consist of soluble pectin, sugar, and organic acid (Holdsworth, 1971). Tanglertpaibul and Rao (1987b) reported that the contribution of continuous phase to the rheological properties of tomato concentrate is less compared to the suspended phase.

Pectin presence in the suspended particles has been shown to contribute to the viscosity of tomato juice (Luh, Sarhan, & Wang, 1984; Beresovsky et al., 1995). In pure pectin solution, pectin-pectin interaction is dependent on the various factors such as pH, sugar and ions. However, there is much less information on the influence of sugar and ions on pectin-pectin interaction in a suspension of insoluble plant-tissue-based particles like tomato product. Since serum contain sugar and ions among others, it is interesting to investigate the contribution of serum and its components to the rheological properties of tomato suspensions.

The aim of this chapter was to determine the role of serum fraction on the rheological behaviour of tomato paste. This was done by substituting tomato paste serum with water. Then a complimentary experiment was done to determine which constituent in the serum that contributes to the observed result. The main constituents that were investigated are sugar and calcium ions.

4.2 Materials

In this and the next chapters, tomato pastes TP1 and TP4 were used. Due to insufficient amounts of the materials used in chapter 3, paste samples with different batch numbers were used. Table 4.1 shows the batch number and compositional properties of the new tomato paste samples TP1 and TP 4 used and compares them to the properties of the previously used batches.

Table 4.1 - Batch number and chemical properties of tomato paste TP1 and TP4.

Tomato paste	Batch number	Soluble solids (°Brix)	Total solids (% TS)	Water insoluble solids (% WIS)
TP1*	L1867 07 2015 14:44	29.7	30.7	1.4
TP1	L148T 1/5/2016	29.5	30.6	1.6
TP4*	B/B 01/07/2016	29.6	30.3	0.9
TP4	MR1 L-T 245	29.3	29.6	0.4

TP1* and TP4* were the original pastes used in chapter 3

The table shows that the Brix and total solids levels are relatively consistent between samples, although differences in water insoluble solids were observed for tomato paste TP4. Generally, the two pastes had similar brix levels while having different levels of water insoluble solids, making these pastes interesting for comparison in future work. These pastes had quite different rheological behaviour as shown in Figure 3.1.

4.3 Methods

Sample preparation and analyses were conducted using the following methods.

4.3.1 Preparation of pulp and serum fractions

Tomato paste TP1 was centrifuged at 30, 000 x g (15,900 rpm) for 30 minutes using Sorvall RC 6+ Centrifuge equipped with F21S-8X50 rotors. The serum was decanted and the pulp was washed by mixing with reverse osmosis water and left at room temperature for 30 minutes before being recentrifuged. This process was repeated until the decanted supernatant reached approximately 0 °Brix. To achieve this, four washes with reverse osmosis water was required. To prevent mould growth and chemical changes that might alter the physical and chemical properties of the pulp and serum, both fractions were vacuum-packed and stored at 4 °C prior to being used. The sample preparation is illustrated in Figure 4.1.

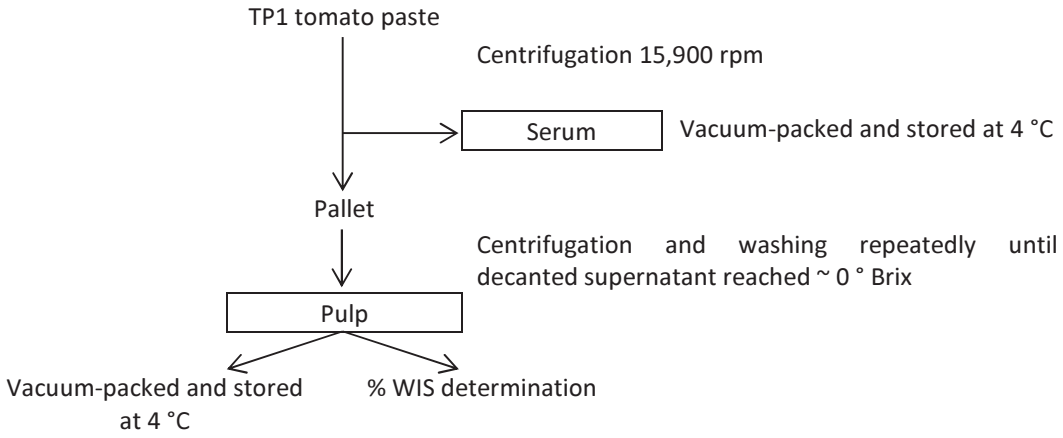

Figure 4.1 - Schematic overview of tomato pulp fraction separation.

4.3.2 Serum viscosity

The viscosity of serum collected from step 4.3.1 was measured using a rheometer (MCR 302, Anton Paar) at temperature 25 °C. A cup (diameter 28.930 mm) and a concentric cylinder (diameter 26.637 mm and height 40.009 mm) was used as the measuring system. The serum was sheared at linearly increasing shear rates (γ) from 0.1 to 100 s^{-1}. The experiment was run in triplicate. All experiments were performed on a fresh sample to avoid any influence of the shear history.

4.3.3 Water insoluble solid (% WIS) determination

20 g tomato paste was weighed into pre-weighed centrifuged tube then the steps in method 4.3.1 were followed. Pulp was weighed into aluminium dishes and placed in the vacuum oven at 70 °C for 12 h. The percentage of WIS/ tomato paste and WIS/ pulp was calculated as;

$$\%\,\boldsymbol{WIS} = \frac{\boldsymbol{Mass\ of\ dried\ washed\ pallet}}{\boldsymbol{Mass\ of\ original\ tomato\ paste}} \times \mathbf{100}\% \qquad \textbf{Equation 4.1}$$

and;

$$\%\,\boldsymbol{WIS_{pulp}} = \frac{\boldsymbol{Mass\ of\ dried\ washed\ pallet}}{\boldsymbol{Mass\ of\ wet\ washed\ pallet}} \times \mathbf{100}\% \qquad \textbf{Equation 4.2}$$

The experiments were done with five replicates.

4.3.4 Reconstituted tomato paste prepared with its own serum (PS)

To determine the effect of pulp preparation methodology, particularly due to centrifugation and washing, samples with the same percentage of WIS as the original tomato paste were prepared by mixing pulp with its own serum. The sample was then left at room temperature for 30 minutes before being centrifuged. This process was repeated until the decanted serum reaches the °Brix value of the original tomato paste.

4.3.5 Variation of serum phase properties at fixed WIS content

Under fixed water insoluble solids concentration (the same concentration as the original TP1), reconstituted tomato paste was prepared using different continuous phases (see Table 4.2). From this experiment the contribution of serum to the flow behaviour of the tomato paste could be elucidated. Fructose solution at the same soluble solids concentration was added for samples PF18 and PF28. This scenario tested the interaction between the main sugar present in serum and the pectic substances in the WIS fraction. Samples PC and PCX tested the role of calcium on pectic substance interactions.

Table 4.2 - Reconstituted tomato paste using different continuous phase

Sample	WIS content (%)	Continuous phase
PW	5.1	Reverse osmosis water
PF18	5.1	Fructose solution
PF28	5.1	Fructose solution
PC	5.1	Calcium chloride ($CaCl_2$) solution
PCX	5.1	Calcium chloride ($CaCl_2$) solution

4.3.5.1 Preparation of reconstituted tomato paste with water as the continuous phase (PW)

Tomato pulp was mixed with reverse osmosis (RO) water instead of serum.

4.3.5.2 *Preparation of reconstituted tomato paste at 18 °Brix and 28.5 °Brix (PF18 and PF28)*

Fructose solution was prepared using D (-) Fructose obtained from Sigma Chemical Co. Two reconstituted tomato paste were prepared by mixing pulp with 23 and 33 °Brix fructose solution to produce reconstituted tomato paste at 18 and 28.5 °Brix, respectively. The reduce value of °Brix after reconstitution is due to the presence of water in the tomato pulp.

4.3.5.3 *Preparation of reconstituted tomato paste with added Ca^{2+} ion (PC and PCX)*

This sample was prepared with the prior information about mineral content in tomato paste, pulp, and serum. The mineral content analysis was performed by Hill Laboratories. The calcium, magnesium, potassium, sodium, phosphorus, sulphur, and iron contents were determined using inductively coupled plasma optical emission spectrometry (ICP-OES) and boron, copper, manganese, and zinc contents were determined using inductively coupled plasma mass spectrometry (ICP-MS).

A calcium chloride solution was prepared by using calcium chloride dihydrate ($CaCl_2.2H_20$) obtained from Biolab (Aust) Ltd. 1 M $CaCl_2.2H_20$ was prepared by mixing $CaCl_2.2H_20$ with reverse osmosis water. Samples with added Ca^{2+} ion were prepared by adding 0.2 ml of 1 M $CaCl_2.2H_20$ solution to reconstituted tomato paste. Sample with excess calcium ion was prepared by adding 1.6 ml of 1 M $CaCl_2.2H_20$ solution to reconstituted tomato paste. Both samples were prepared so that the percentage of WIS were the same as the original tomato paste with one have the same calcium ion concentration as the original and another one with calcium in excess.

4.3.6 Flow behaviour measurements

The flow behaviour of the samples were measured using method 3.3.6 with the rheometer was set to measure at logarithmic intervals. The sample then was sheared at the increasing shear rate (γ) from 0.1 to 100 s^{-1} and 100 measurement points were determined. All the prepared samples were left overnight before flow behaviour measurement.

4.4 Results and discussion

The results were discussed in sections as below.

4.4.1 Water insoluble solid (% WIS)

Table 4.3 - Water insoluble solid content (WIS) of tomato pastes TP1 and TP4 obtained by the drying method.

Tomato paste	WIS/ tomato paste (Drying method) (%)	WIS/ tomato paste (Equation 3.4) (%)	WIS_{pulp} (%)
TP1	5.1 ± 0.02	1.6	14.0 ± 0.16
TP4	4.2 ± 0.09	0.4	10.1 ± 0.06

Mean ± standard deviation

In this chapter the amount of WIS (%) and WIS_{pulp} (%) in tomato paste samples TP1 and TP4 were obtained experimentally. Both values were important to determine the amount of pulp needed to prepare tomato suspension studied in this chapter. In Chapter 3 and Table 4.1 the % WIS was obtained using Equation 3.4. It was expected that both procedure (equation and experiment) would give the same value. Contrary to expectation, the % WIS obtained experimentally showed much higher values compared to the values obtained through the equation (Table 4.3).

A possible explanation for this might be that Equation 3.4 was not valid. To validate whether the equation can satisfactorily be used to determine water insoluble solid content in tomato paste, % WIS was calculated using a hypothetical tomato paste model (Figure 4.2).

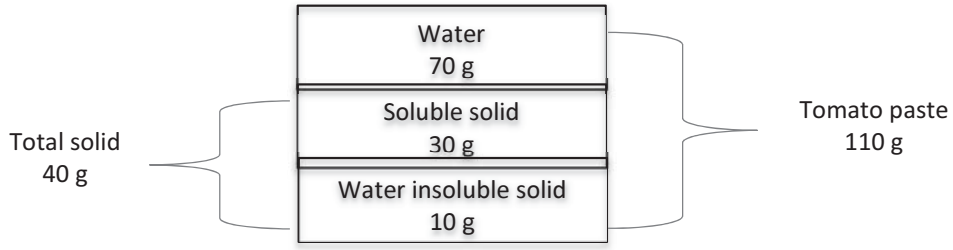

Figure 4.2 - Tomato paste model.

From Figure 4.2, % WIS was calculated as;

$$\%\,\boldsymbol{WIS} = \frac{\boldsymbol{Water\ insoluble\ solid\ (g)}}{\boldsymbol{Tomato\ paste\ (g)}} \times \mathbf{100}\% \qquad \textbf{Equation 4.3}$$

$$= \frac{10}{110} \times 100\%$$

$$= 9.090909\%$$

To compare percentage of WIS/ tomato paste calculated from above with Equation 3.4, two values (°Brix and % Total solids) need to be calculated using the information in Figure 4.2.

The soluble solids (°Brix) value of tomato paste model was calculated as;

$$^{\circ}\boldsymbol{Brix} = \frac{\boldsymbol{Soluble\ solid\ (g)}}{\boldsymbol{Soluble\ solid + water\ (g)}} \times \mathbf{100}\% \qquad \textbf{Equation 4.4}$$

$$= \frac{30}{100} \times 100\%$$

$$= 30.0\%$$

and % total solid was calculated as;

$$\%\,\boldsymbol{Total\ solids} = \frac{\boldsymbol{Total\ solid\ (g)}}{\boldsymbol{Tomato\ paste\ (g)}} \times \mathbf{100}\% \qquad \textbf{Equation 4.5}$$

$$= \frac{40}{110} \times 100\%$$

$$= 36.36364\%$$

Thus, from Equation 3.4, % WIS was;

$$\%\,WIS = \frac{\%\,Total\ solids - °Brix}{100 - °Brix} \times 100 \qquad \textbf{Equation 4.4}$$

$$= \frac{36.36364 - 30}{100 - 30} \times 100\%$$

$$= 9.090909\%$$

This showed that Equation 3.4 was adequate to be used to determine the % WIS. Thus another possible explanation for the different between values obtained from calculation and experimental is might be due to the misinterpretation of °Brix value measured using refractometer as actual soluble solid content. °Brix is the measure of the sucrose concentration in a water solution on a weight for weight basis of solution, ignoring insoluble materials. Thus, 1 °Brix is equal to 1 g of sucrose in 100 g of solution. °Brix value has been generally used as approximation of the amount of soluble solids in tomato and tomato products. In tomato paste, soluble solids consist of sugar (mainly glucose and fructose), acid, salts, and soluble pectin. Thus, the presence of these soluble solids (primarily soluble pectin) rather than pure sucrose might slightly contribute to an error in measuring soluble solids content in tomato paste using the refractometer. To test this, soluble solids in tomato paste TP1 was measured using a drying method. Soluble solids were determined by drying tomato serum and diluted tomato serum at concentrations 0.85, 0.70, 0.55, 0.40 x that of the original paste, using the vacuum oven method following AOAC Official Method 964.22 with a few modifications (Method 3.3.1). The value of soluble solids obtained from drying methods was the compared against values obtained using refractometer (see Figure 4.3).

It is clear from Figure 4.3 that the soluble solids measured using the refractometer gave higher soluble solids reading than the actual values. This difference was by a constant factor of 1.1194. This could be explained by the fact that refractometer measured the refractive index of tomato soluble solids but gives the °Brix reading based on refractive index of pure sucrose solution. Besides sugar, tomato soluble solids consist of other soluble polysaccharides, in particular soluble pectin. According to Tanglertpaibul and Rao (1987b), 5.6 and 20 ° Brix tomato serum contained 0.2% and 0.8% soluble pectin respectively. The higher molecular mass of soluble polysaccharides compared to sucrose, might contribute to the higher refractive index of tomato soluble solids solutions than sucrose solutions at the same concentration and therefore causes over estimation of tomato soluble solid concentrations in a solution when the °Brix reading is calibrated based on refractive index of pure sucrose solutions.

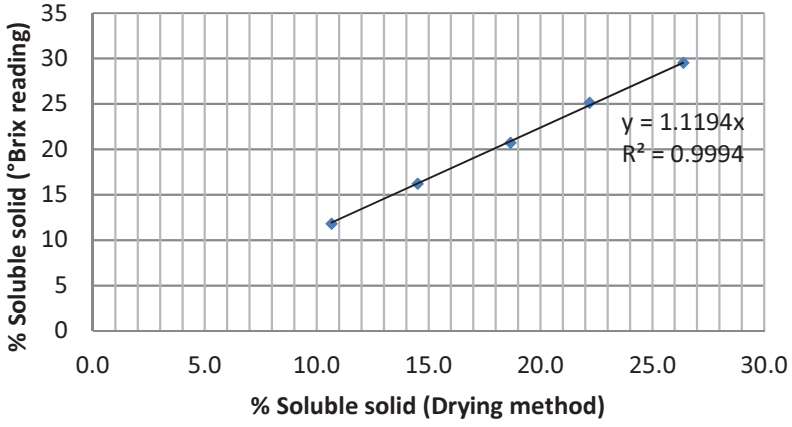

Figure 4.3 - Comparison of percentage of soluble solid determine using drying method with refractometer.

Moelants et al. (2013) showed molecular mass distribution of soluble polysaccharides in tomato serum (Figure 4.4). The figure shows that soluble polysaccharide in tomato serum have higher molecular mass than sucrose (342 Dalton) thus might explain the higher refraction and consequently higher Brix reading.

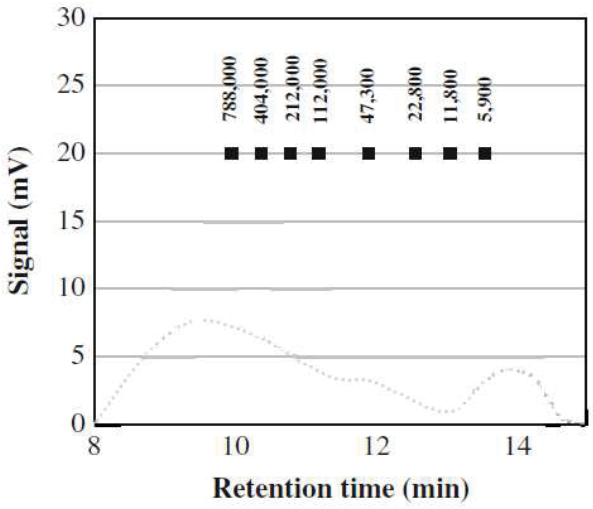

Figure 4.4 - Molar mass distributions of soluble polysaccharides in tomato serum. Elution times of pullulan standards are indicated to allow for a rough estimation of the molar masses (in Dalton) (Moelants et al. 2013).

Using % soluble solids obtained from the drying method, % WIS in tomato paste TP1 was calculated using Equation 3.4.

$$\%\,WIS = \frac{\%\,Total\ solids - °Brix}{100 - °Brix} \times 100 \qquad \textbf{Equation 4.4}$$

$$= \frac{36.36364 - 26.4}{100 - 26.4} \times 100\%$$

$$= 5.8\%$$

This value is in close approximation to the value obtained from experiment which was 5.1 ± 0.01%. The slightly lower value of % WIS TP1 obtained from experiment might be due to the loss of small amount of water insoluble solids during the washing and centrifuging process.

This section gave a brief explanation on the reason for the differences found in the % WIS obtained from Equation 3.4 and experiment. In conclusion Equation 3.4 can be used to determine % WIS of tomato products on the condition that the actual soluble solids content is obtained. This may be achieved by more appropriately calibrated °Brix measurement by refractometer. There is a potential that differences between serum compositions (e.g. water soluble pectin concentration) could mean the correction factor found in this work may be different for other pastes. For further preparation of reconstituted tomato pastes from pulp solids in this work, the experimentally derived % WIS solids levels were used.

4.4.2 Effect of pulp preparation method on reconstituted tomato paste rheology

Figure 4.5 shows the flow behaviour of original and reconstitued tomato paste TP1.

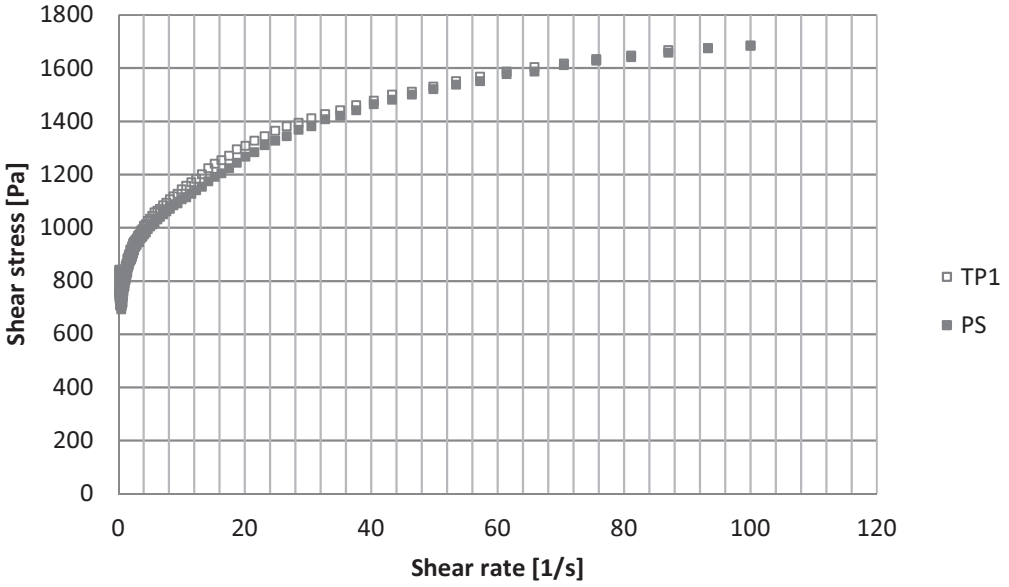

Figure 4.5 - Shear rate versus shear stress curves of original tomato paste TP1 and reconstituted tomato paste with its own serum (PS). The data was plotted as the average of three replicates.

Reconstitued tomato paste was prepared from pulp obtained from centrifuging and washing of water insoluble solid from the original tomato paste. Then the tomato pulp was added to the original tomato serum at the same concentration of water insoluble solid as the original one. As washed pulp contained residual water, the addition of pulp to the serum decreases the °Brix value of the reconstitued tomato paste. Thus to prepare reconstitued tomato paste that exactly resembled the original tomato paste, the suspension was centrifuged and washed again with serum. This step was repeated until the serum of the reconstitued tomato paste reached the °Brix value of original tomato paste (which was 29.5 °Brix). The process of washing and centrifuging was done carefully to make sure that there were no pulp losses during the process and therefore the concentration of water insoluble solid in the reconstitued tomato paste was maintained.

Figure 4.5 shows that reconstitued tomato paste has the same flow behaviour as the original one. This result suggests that the process of isolating and reconstituting the pulp (involved washing and centrifugation steps), do not effect the flow behaviour of the reconstitued tomato paste.

This result was the basis of for futher experiments where pulp was added at different continuous phase properties and used at different concentrations (Chapter 5). Thus the result that was obtained would be solely dependent on the treatment given rather than on the changes to the nature of the solids during sample preparation.

4.4.3 The contribution of serum on the flow behaviour of tomato paste

Tomato serum is a low viscosity Newtonion fluid with viscosity range from 0.0043 to 1.4 Pa.s (Rao & Cooley 1992). In this study, the viscosity of tomato serum is 0.0042 and 0.0031 Pa.s for tomato serum TP1 and TP4, respectively measured using concentric cylinder.

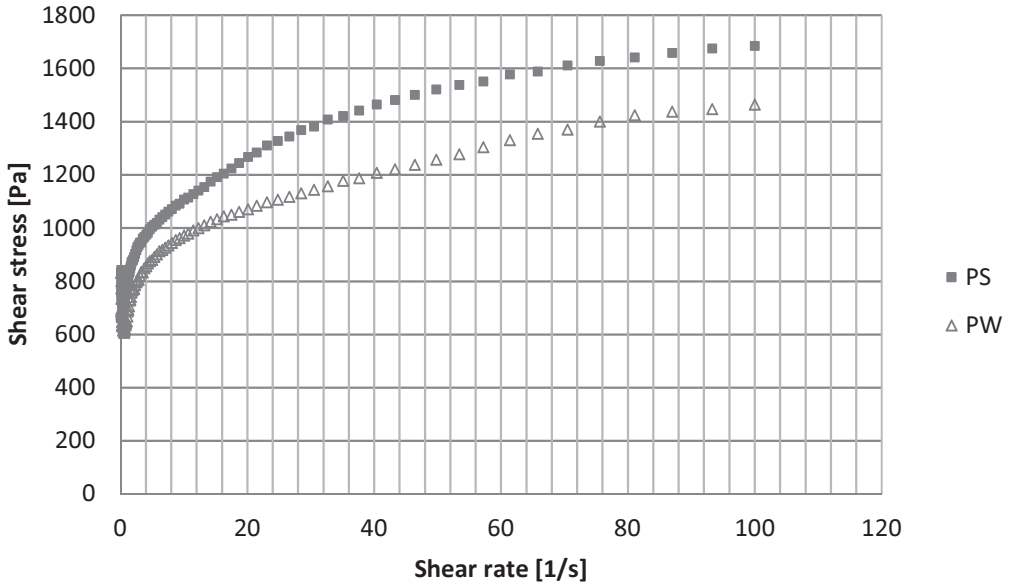

Figure 4.6 - Shear rate versus shear stress plots of reconstituted TP1 prepared with serum (PS) and water (PW). The data was plotted as the average of three replicates.

Reconstituted tomato paste prepared with serum has higher viscosity compared to reconstituted tomato paste in water. This may be explained by the fact that serum TP1 has higher visocity (0.0042 Pa.s) compared to water (0.00089 Pa.s). However from the above result, it is impossible to conclude that the difference in the flow behaviour of PS and PW is due to the serum viscosity only because of its low serum viscosity (0.0042 Pa.s). Another explanation for the observed result is due to the presence of soluble pectin, sugar, and ions in the serum that enhance tomato paste insoluble solid particle interactions; in particular pectin-pectin interactions, thus increase the viscosity of reconstituted tomato paste in serum (PS).

In contrast, Whittenberger and Nutting (1958) found that the reconstitution of washed insoluble solids from tomato juice, with distilled water caused an increase in viscosity almost double of the original tomato juice (Table 4.4). The result showed that serum has a negative effect on the flow behaviour of tomato juice. They explained this is due to the presence of ions in serum that are sufficient to keep the viscosity of tomato juice at a low level. The differences in the observed results might be due to the different tomato product used in the study. In their study, tomato juice with the °Brix value around 4 to 9 °Brix was used. At the low sugar content, it is anticipated that the negative effect of ions in the serum will be dominant. However, at higher °Brix values, such as in the tomato paste TP1 serum (29.5 °Brix), the presence of high sugar concentration might overrule the negative effect of ions. This can be supported by result obtained by Benitez, Genovese, and Lozano (2009). They reported that at critical sugar

concentration (>0.004 mol/mol), the particle-sugar interaction is more important than particle-particle interaction, thus cause increase in the stability and viscosity of the system.

Table 4.4 - Viscosity of tomato juice and reconstituted tomato juice (Whittenberger & Nutting, 1958).

Sample	Apparent viscosity (Pa.s)
Original tomato juice	0.24
Reconstituted tomato juice (distilled water)	0.50

To futher elucidate the contribution of each constituent of serum in tomato paste viscosity, reconstituted tomato paste in fructose and $CaCl_2$ solutions were prepared. As has been determined by the drying method, tomato paste TP1 had 26.4% soluble solids content. According to Figure 2.2, 65% of tomato fruit soluble solids consist of simple sugars. Thus it can be calculated that ~17.3% of tomato paste TP1 is composed of sugars. In order to investigate the effect of sugar on tomato paste, two samples of reconstituted tomato paste were prepared. The first sample was 18 °Brix reconstituted tomato paste (PF18) where the sugar content was the same as tomato paste TP1 (this was done by mixing TP1 tomato pulp with fructose solution so that the PF18 had 18 °Brix which is ~17.3% sugar content) and the second sample is 28 °Brix reconstituted tomato paste (PF28) where the sugar content is much higher than in TP1 but the soluble solids content was similar. The results in Figure 4.7 showed that PF18 had almost the same flow behaviour as PS. These results indicate the significant contribution of sugar to the flow behaviour of tomato paste and it is likely that the higher apparent viscosities of the PS sample is mainly due to the contribution of sugar. Futhermore at the higher sugar contents (but the same °Brix as the original paste), sample PF28 showed higher flow behaviour.

As has been discussed, low pH and the presence of sugar are important for high-methylesterified (HM) pectin interaction. Low pH reduced dissociation of hydrogen ions (H^+) from pectin carboxyl groups, thus minimized electrostatic repulsions while sugars stabilize hydrophobic interactions between pectin molecules (Oakenfull & Scott, 1984). Under the same conditions (low pH and the presence of sugar) low-methylesterified (LM) pectin can also form networks by the same mechanism that governs HM pectin interactions (Thakur et al.,1997).

The degree of methylesterification (DM) of pectin in tomato paste depends on the processing method employed. According to (Handa et al., 1996) the cold break processing method produces LM pectin with 14 % DM while the hot break method produces HM pectin with 50 % DM. However in this study, the information on processing method employed for the production of tomato paste TP1 is not known. In spite of the lack of information, the presence of sugar is important for both pectin types (LM and HM pectin) to form pectin-pectin interaction under low pH conditions such as in tomato serum which has pH 4.2 (Table 4.6). Thus it can be concluded that the higher viscosity of reconstituted tomato paste with serum (PS) might be due to the presence of sugar in the serum that provides better conditions for pectin-pectin interactions.

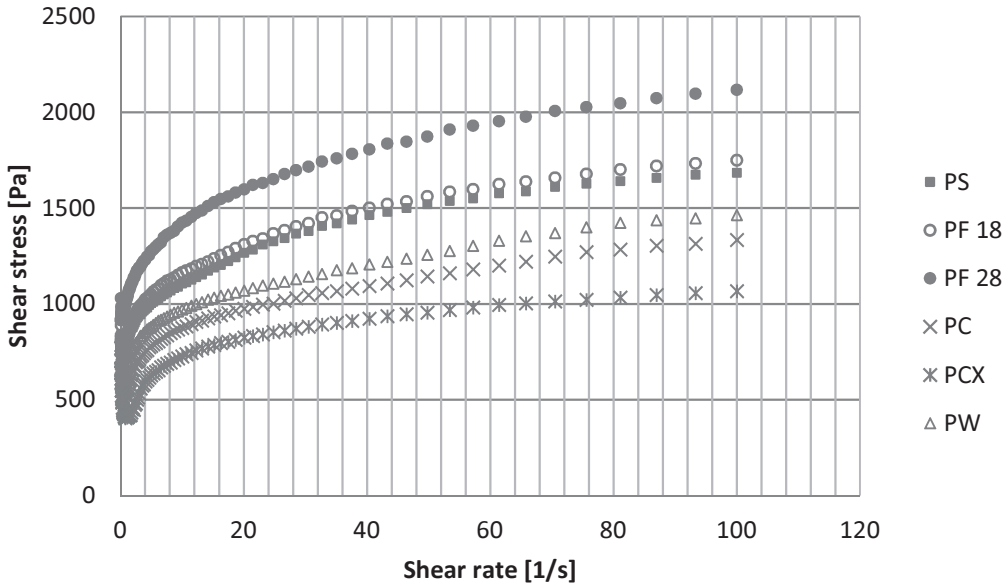

Figure 4.7- Shear rate versus shear stress plot of reconstituted TP1 prepared with serum (PS), 18°Brix fructose solution (PF18), 28 °Brix fructose solution (PF28), matched calcium concentration (PC), excess calcium (PCX). The data are plotted as the average of three replicates.

Contrary to reconstituted tomato paste in fructose solution, reconstituted tomato paste in $CaCl_2$ solution showed a decrease in the flow behaviour. Reconstituted tomato paste in $CaCl_2$ solution was prepared with prior information of calcium ion content in tomato paste, tomato pulp and serum of TP1 (Table 4.5). Two samples were prepared. The first sample was reconstituted tomato paste that had the same amount of Ca^{2+} as TP1 (PC) and the second sample is reconstituted tomato paste with an excess amount of Ca^{2+} (PCX). The result in Figure 4.7 showed that PC and PCX has lower flow curve compared to the whole recombined paste (PS). This result suggests that in the absence of sugar, the presence of Ca^{2+} in the serum causes the decrease in the flow behaviour of tomato paste. A similar result was observed by Whittenberger and Nutting (1958) who found that cations and anions in the serum cause a decrease in tomato juice viscosity. Treatment of tomato juice with synthetic ion-exchange resins to remove cations and anions from the serum, caused an increased in the viscosity of tomato juice. Similarly Sherkat and Luh (1977) found that the addition of 0.8 % sodium chloride caused a decreased in the consistency of tomato paste.

Table 4.5 - Concentration of metal ion in tomato paste, pulp and serum of tomato paste TP1.

Metal ion	Tomato paste (g/ 100g)	Tomato pulp (g/ 100g)	Tomato serum (g/ 100g)
Calcium	0.04	0.07	0.02
Magnesium	0.05	0.01	0.05
Potassium	1.35	0.14	1.40
Sodium	0.02	0.00	0.02
Phosphorus	0.08	0.04	0.07
Sulphur	0.06	0.04	0.05

Table 4.5 shows that even after tomato pulp was washed until the decanted supernatant reached approximately 0 °Brix, the tomato pulp still contained calcium (Ca^{2+}). This suggets that tomato pulp contains intrinsic Ca^{2+} that bound to pectin by calcium cross-linkages. Mixing tomato pulp with $CaCl_2$ solution may cause deprotonation of pectin carboxyl groups. This is supported by the measured decrease in pH of the PC and PCX samples (Table 4.6). Even though it was expected that these negatively charged pectin carboxyl groups will form additional calcium cross-linkages and thus enhance pectin-pectin interactions and consequently increase the viscosity of PC and PCX, different result was obtained. The presence of Ca^{2+} in the solution caused a decrease in the viscosity of reconstituted tomato paste.

This is in agreement with Moelants et al. (2014a) who found that that addition of Ca^{2+} decreased the networks stiffness (measured as storage modulus) of a carrot suspension. At pH higher than the pKa of pectin, hydrogen ions will be disassociated from the carboxyl group thus forming negatively charged pectin that able to bind Ca^{2+} thus forming calcium cross-linkages. However, instead of showing higher storage modulus, carrot suspension at higher pH than pKa showed lower value of storage modulus after addition of calcium ions. They explain the observed result is due to the screening of Ca^{2+} at the particle surface of pectin polymers rather than forming calcium cross-linkages thus causing a reduction in the electrostatic repulsion between pectin polymers. Another possible explanation is due to the formation of calcium cross-linkages to the extent where the network precipitates.

Table 4.6 - pH of sample used in the study.

Sample	pH
TP1	4.2 ± 0.01
PS	4.2 ± 0.03
PW	4.3 ± 0.02
PF18	4.2 ± 0.00
PF28	4.2 ± 0.01
PC	4.0 ± 0.01
PCX	3.6 ± 0.03

4.5 Conclusion

Overall, the results in this chapter indicate that serum contributes to the flow behaviour of tomato paste due to the presence of soluble solids in the serum. In particular, it was found that primarily sugars cause this effect, potentially by enhancing the pectin-pectin interactions in the WIS component of the paste. This suggests the importance of °Brix (close approximation to sugar content) as one independent variable in the development of a tomato paste flow behaviour model.

The methodologies developed in this chapter to separate WIS and serum fractions were shown to be reversible. This offers the ability to independently change the relative amounts of WIS and soluble solid in recombined tomato pastes, to explore their relative contributions to past rheology. This idea is investigated in the following chapter.

CHAPTER 5

Development of a model for predicting rheology.

5.1 Introduction

In Chapter 3 strong relationships between total solids and Herschel-Bulkley parameters were observed for a range of tomato pastes at different dilutions (see Chapter, Figure 3.4). In Figure 3.4 there was a large scatter when comparing yield stress to %WIS. In Chapter 4 (section 4.4.1), a correction factor (1.1194) was found to relate the Brix reading to soluble solids, and thereby affected the %WIS calculation used in chapter 3. Figure 5.1 is a redrawn version of Figure 3.4 with this correction made and it shows much less variation between tomato pastes once compositional variations are considered.

In Chapter 4 serum has been shown to contribute to the viscosity of tomato concentrates and suggested due to the presence of sugar that enhances pectin-pectin interaction. In the literature, there have been a number of functional models suggested to predict rheology from composition (reviewed in Chapter 2.7.5). Some models link power law rheological model parameters to total solids, soluble solids or tomato pulp concentrations (Rao *et al.,* 1981; Fito *et al.,* 1983; Tanglertpaibul & Rao, 1987b), while other researchers fitted functions to link composition to yield stress (Rao & Cooley, 1983; Sharma *et al.,* 1996; Moelants *et al.,* 2014b).

A methodology to separate and wash WIS fraction of whole tomato pastes from the serum fraction was developed in Chapter 4. Furthermore, it was shown that the original paste rheological behaviour can be recovered by appropriate mixing back together for these two fractions. This provides the opportunity to create paste samples with widely varying %WIS to Soluble solids rations at a range of dilutions. Charactersation of the rheology of these samples could provide the basis for a wide ranging functional model linking composition to flow behaviour.

The aim of this chapter was to prepare well-characterised samples to determine the effect of %WIS and °Brix (as a close approximation of sugar content) to the flow behaviour and consequently Herschel-Bulkley parameters of tomato concentrates. Based on this data, an overall functional model for flow behaviour of tomato pastes could be developed.

5.2 Materials and Methods

In this chapter, tomato pulp and serum prepared from tomato paste TP1 and TP4 as defined in Table 4.1 were used. For each paste, the method outlined in Chapter 4, section 4.4.1 was used to produce separate samples of washed pulp and undiluted serum. Table 5.1 summarises the composition of the washed pulp produced by this process.

Table 5.1 - Composition of the washed pulp samples produced from Tomato pulps 1 and 4.

Sample	% WIS/ tomato paste	% WIS/pulp	%Pulp/tomato paste	% Water/ Pulp
TP1	5.1	14.0	36.2	86.0
TP4	4.2	10.1	41.5	89.9

Five different amounts of water insoluble solid content were mixed with serum to produce samples with five different °Brix values. This produced twenty-five samples or with different soluble and insoluble solids concentrations from each tomato pulp. The results in Table 5.1 were used to calculate the amounts of pulp to be added to prepare these samples

In each case the pulp was weighed into pre-weighed centrifuge tubes and original serum was added at half the amount of serum required to produce a sample with its desired %WIS. The mixture was then mixed using a spatula. Then the rest of serum was added and at the same time used to wash the pulp that had stuck onto the spatula back to the mixture. This process was done carefully to make sure that there are no pulp loss during the process thus maintained desired concentration of water insoluble solids. The sample was then left at room temperature for 30 minutes before being centrifuged. This process (washing with serum) was repeated until the sample reached the required Brix value. To prepare samples with Brix values lower than original serum (29.5 °Brix for TP1 and 29.3 °Brix for TP4), the second wash was done with diluted serum. The samples used in this chapter are summarised below in Table 5.2.

Table 5.2 - Summary of target compositions for 25 different samples produced for TP1 and TP4

TP1	°Brix				
%WIS	5.6	11.6	16.3	22.7	29.5
5.8	x	x	x	x	x
5.1	x	x	x	x	x
4.3	x	x	x	x	x
3.5	x	x	x	x	x
2.8	x	x	x	x	x

TP4	°Brix				
%WIS	4.5	11.6	16.1	22.7	29.3
4.8	x	x	x	x	x
4.2	x	x	x	x	x
3.6	x	x	x	x	x
2.9	x	x	x	x	x
2.3	x	x	x	x	x

The flow behaviour of duplicates of each sample was measured using the method described in section 4.3.6. After flow measurement, the °Brix of sample was measured using the method described in section 3.3.2.

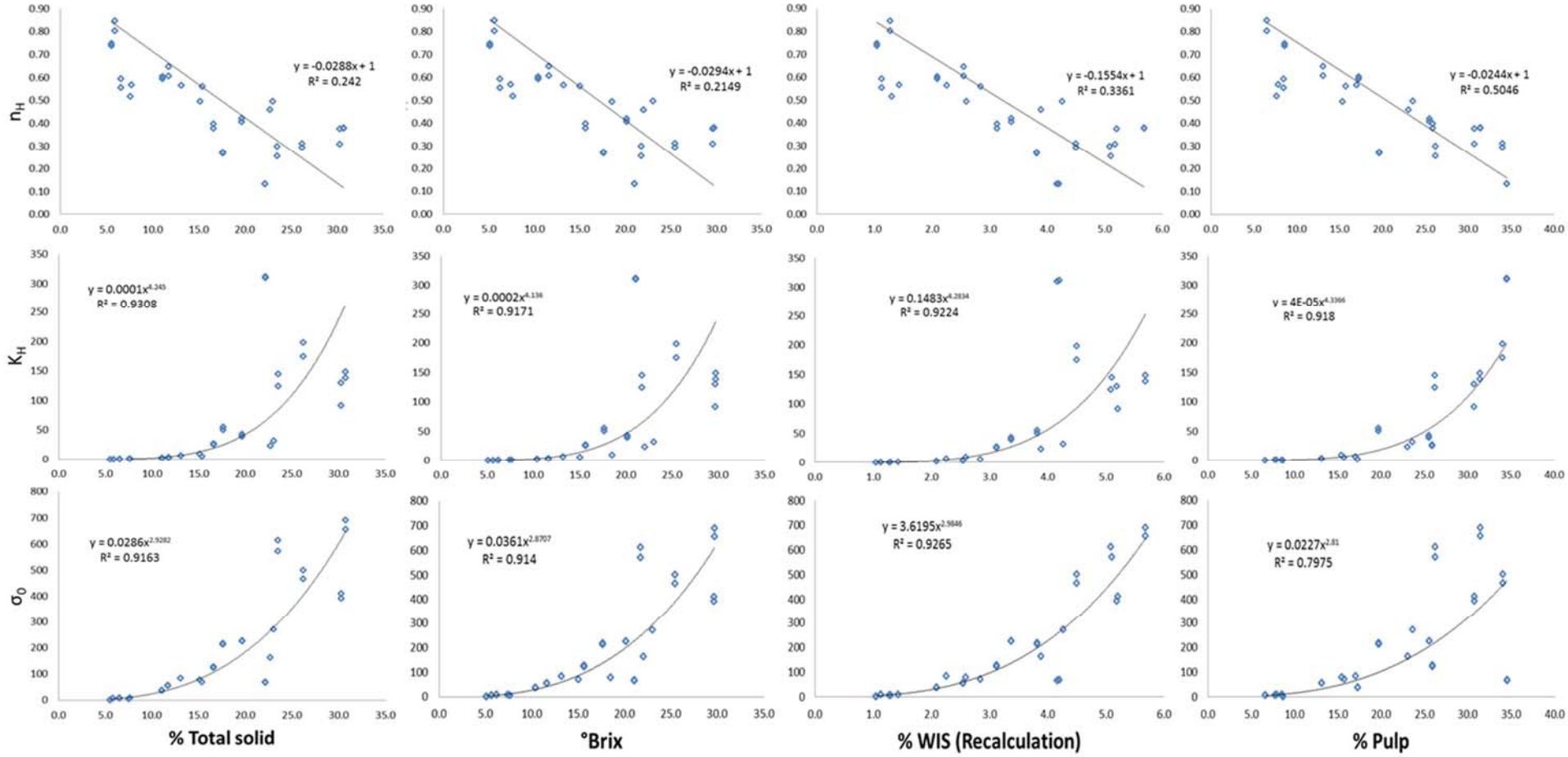

Figure 5.1 - Relationship between physicochemical properties of tomato concentrates and Hershel-Bulkley parameters. (Figure 3.4 after %WIS data recalculation for adjusted °Brix).

5.3 Results and Discussion

Figure 5.2 shows the raw flow curve data collected during the experiment. The dataset is the most complete set currently available in terms of variation in concentrations of each phase. Some combinations are well outside industrially available pastes. For example, a tomato paste sample with 5.8% water insoluble solids and only 5.6°Brix would have to involve separation of the serum phase before or after dilution. Pastes with high °Brix but low %WIS could occur by dilution of tomato paste with a sugar solution and may occur in some product formulations. In this study, the wide-ranging composition allows evaluation of the interactions between the two components. In chapter 3, these interactions could not be explored as dilution of samples, lowered the concentration of both soluble and insoluble solids by the same proportion.

5.3.1 Effect of %WIS and °Brix on flow behaviour data

Figure 5.2 presents the flow behaviour measurements of the reconstituted tomato concentrates at different %WIS and °Brix prepared from tomato pulp TP1 (Figure 5.2 A) and TP4 (Figure 5.2 B). As can be seen from graphs A, a decrease in %WIS from 5.8 %WIS to 2.8 %WIS caused a marked decrease in the shear stress versus shear rate data of the tomato concentrates. The same phenomena observed in tomato concentrates prepared tomato pulp TP4 (graph B).

Figure 5.2 also showed that for tomato concentrates at the same %WIS (each graph), a decrease in °Brix caused a decrease in the shear stress versus shear rate data of the tomato concentrates. This effect was identified in Chapter 4 and attributed to soluble solids interacting with the insoluble solids fraction. It is apparent from Figure 5.2, that the effect of °Brix on the flow behaviour data is considerably smaller compared that of %WIS, but still notable. In addition, the effect of °Brix is found to be more pronounced at high %WIS. At low %WIS a decrease in °Brix only shows a slight decrease in the flow behaviour data.

More quantitative analysis can be achieved by using the Herschel Bulkley model to collapse the full flow curve into three model parameters (n_H, K_H, and σ_o). This allows direct comparison of how %WIS and °Brix to affect the flow properties of the paste samples. This was investigated next.

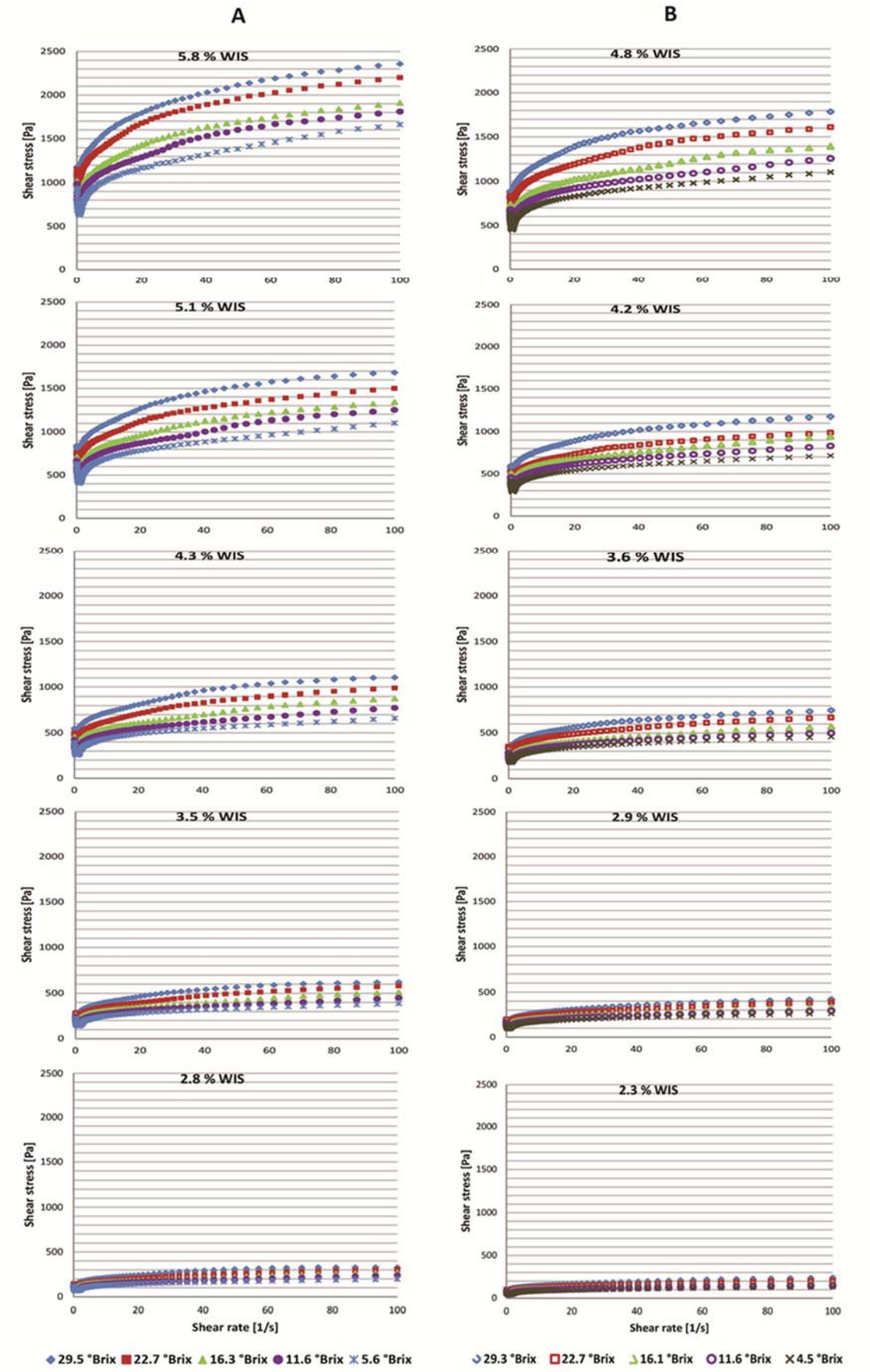

Figure 5.2 - Shear stress versus shear rate data for reconstituted tomato concentrates at different % WIS and °Brix prepared from tomato pulps TP1 (A) and TP4 (B).

5.3.2 Effect of %WIS and °Brix on Herschel-Bulkley parameters

The Herschel Bulkley model was fitted to each flow curve using nonlinear regression as outlined in Chapter 3, section 3.4.3. The effect of %WIS and °Brix to the Herschel-Bulkley parameters are shown in Figure 5.3. As a preliminary analysis, a best fit line that can describe the data for each sample was applied by using the trendline feature in MS Excel. For relationship between %WIS and n_H, a linear relationship was applied while for K_H and σ_o power relationships were applied. For the relationships between °Brix and n_H, K_H, and σ_o, linear relationships were applied.

Generally, it can be seen from Figures 5.3 and 5.4 (A) that an increase in %WIS caused a linear decrease in n_H, at least over the range of %WIS present in the samples. There is some scatter in this trend but there is a stronger dependence of $n_H$on %WIS than on °Brix (see Figures 5.3 and 5.4 B). This observation is interesting as the literature models showing concentration dependency for n_H, link it to °Brix (see Chapter 2 Equation 2.12). Since $n_H$is a measure of the deviation from Newtonian behaviour with n =1 for Newtonian fluid and n < 1 for non-Newtonian fluid, thus it was anticipated that as the %WIS tended to zero (infinite dilution), the suspension will become more Newtonian and $n_H$will become 1. Consequently, it was proposed that the plot of $n_H$against %WIS has y-intercept at 1.

Figures 5.3 and 5.4 (A) also showed that K_H and $\sigma_o$can be related to %WIS using power or exponential relationships. This trends has been used in literature models using power or exponential equations to describe how K_H varies with Total solids (Chapter 2 Equations 2.9 and 2.10), and how σ_0 varies with %WIS (Chapter 2 Equations 2.18 and 2.19). In Figures 5.3 and 5.4 (B) there is some evidence of K_H being linearly dependent on °Brix. It also can be seen from the graph that the effect of °Brix on K_H is more pronounced for samples with higher %WIS (5.1% and 5.8%). This support the result obtained in section 5.3.1. One model in the literature uses a power law model to link K_H to °Brix (Chapter 2 Equation 2.11). No relationship between yield stress and °Brix was observed. Similarly, Moelants *et al.* (2014b) found that serum did not affect the dynamic yield stress (σ_{oD}) which is the yield stress obtained by the extrapolation of the flow curves to zero shear rate such as in fitting Herschel-Bulkley model.

Following this it was proposed that a model to describe the overall trends could be based on;

- n_H is linearly dependent on %WIS and independent of °Brix. Because n_H will approach 1 on dilution, it is proposed that the intercept should be 1.

K_H and $\sigma_o$are dependent on %WIS and can be described with either a power or exponential relationship

- K_H is linearly dependent on °Brix.

From this basis, the next step was to formulate this mathematically and obtain overall fits to the model using non-linear regression for the data sets for each tomato paste (TP1 and TP4).

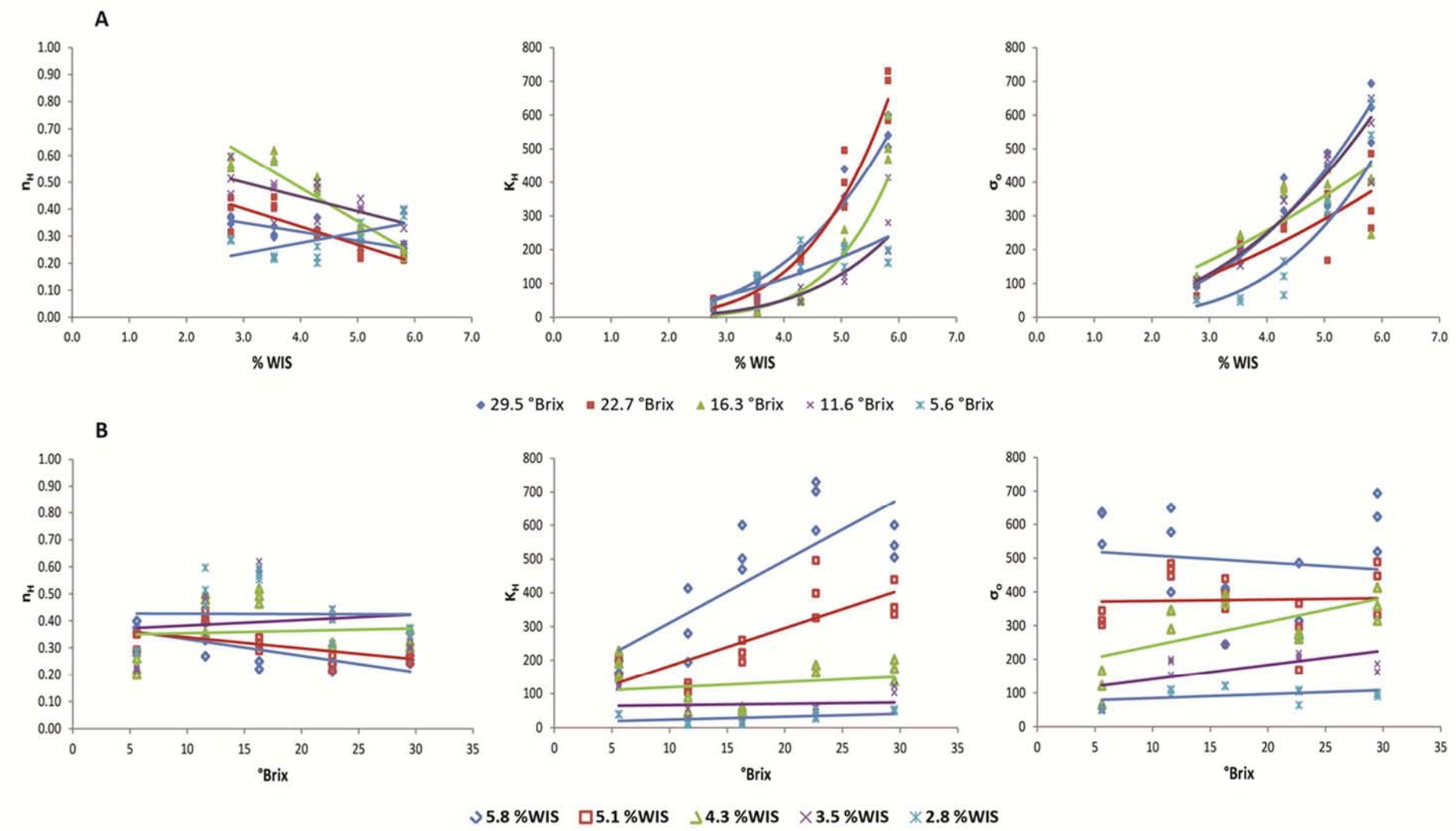

Figure 5.3 - Effect of % WIS (A) and °Brix (B) on Herschel-Bulkley parameters for tomato concentrates prepared from tomato pulp TP1.

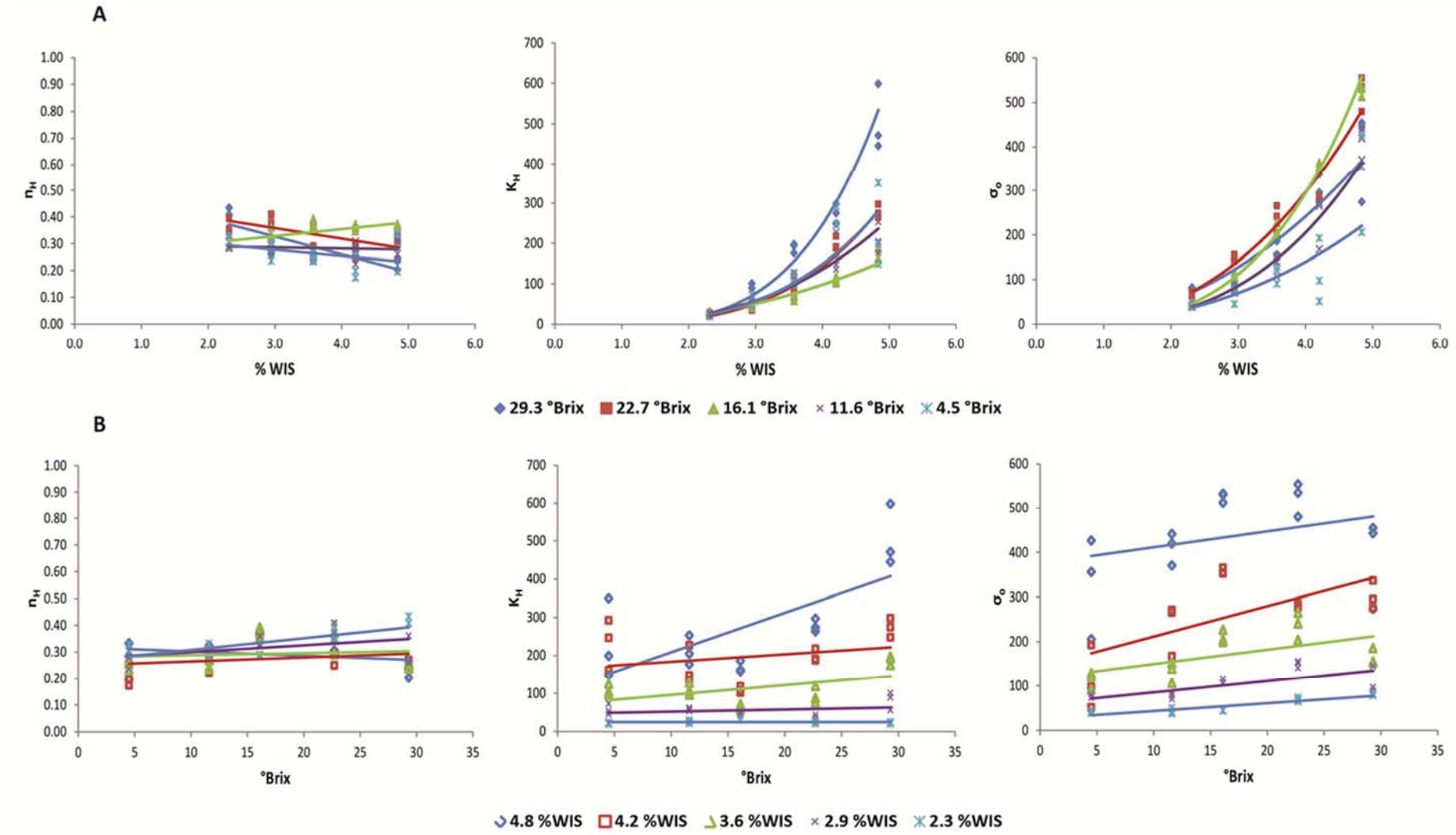

Figure 5.4 - Effect of % WIS (A) and °Brix (B) on Herschel-Bulkley parameters for tomato concentrates prepared from tomato pulp TP4.

5.4 Mathematical model development

The experimental results outlined in section 5.3 gave a better understanding on how %WIS and °Brix affect the flow behaviour and the Hershel-Bulkley parameters of tomato concentrates. Using the trends observed from this data, mathematical models were developed as below.

5.4.1 Mathematical model Set 1 (Exponential model)

Following the approach of equations 2.10 and 2.18, the dependence of Herschel Bulkley parameters K_H and $\sigma_o$as a function of %WIS were assumed to follow an exponential relationship.

$$n_H = 1 - n_{slope}(\%WIS) \qquad \textbf{Equation 5.1}$$

$$K_H = K_{slope}(°Brix)\times\exp(K_b\times\%WIS) \qquad \textbf{Equation 5.2}$$

$$\sigma_o = \sigma_{oslope}\times\exp(\sigma_{ob}\times\%WIS) \qquad \textbf{Equation 5.3}$$

5.4.2 Mathematical model Set 2 (Power model)

Equations to predict $K_H$and $\sigma_o$as a function of %WIS and °Brix can also be described by a power equation (as in Equations 2.9 and 2.19). Thus, another set of mathematical model equations were constructed by maintaining Equation 5.1 and substituting Equation 5.2 and Equation 5.3 for Equation 5.4 and 5.5, respectively.

$$n_H = 1 - n_{slope}(\%WIS) \qquad \textbf{Equation 5.1}$$

$$K_H = K_{slope}(°Brix)(\%WIS)^{K_b} \qquad \textbf{Equation 5.4}$$

$$\sigma_o = \sigma_{oslope}(\%WIS)^{\sigma_{ob}} \qquad \textbf{Equation 5.5}$$

5.5 Model fitting

A total of five parameters were required to be fitted from the experimental data for each set. Each model equation set was fitted separately to the raw viscosity data using a nonlinear least square solver (lsqnonlin) in Matlab R2015a. The values of parameters n_{slope}, K_{slope}, K_b, σ_{oslope}, and $\sigma_{ob}$from fitting exponential model and power model are shown in Tables 5.3 and 5.4, respectively.

Table 5.3 - Values of model parameters for tomato concentrate TP1 and TP4 for exponential model.

Sample/ Coefficients	n_{slope}	K_{slope}	K_b	σ_{oslope}	σ_{ob}	SSerr
TP1	0.1051	0.0194	1.09	24.37	0.64	43.07
TP4	0.1287	0.0114	1.35	14.99	0.80	41.72

Table 5.4 - Values of model parameters for tomato concentrate TP1 and TP4 for power model.

Sample/ Coefficients	n_{slope}	K_{slope}	K_b	σ_{oslope}	σ_{ob}	SSerr
TP1	0.1118	0.0028	4.73	9.82	2.55	17.24
TP4	0.1359	0.0035	4.93	9.46	2.66	22.77

Figures 5.5 to 5.8 compare the viscosity of tomato concentrates predicted from the mathematical model Set 1 (exponential model) and mathematical model Set 2 (power model) to those of experiment, respectively for both TP1 and TP4. In general, both models give good predictions of tomato concentrate viscosity at all concentration ranges studied for both TP1 and TP4. However, it is apparent from the graphs that lower values of R^2 were observed for samples at low °Brix for both exponential and power model models.

The lower R^2 values for samples at low °Brix is supported by higher value of relative error of these samples (±0.2) compared to other compositions. This can be seen in both exponential (Figure 5.5) and power model fits (Figure 5.6). For samples at low °Brix, the relative error seems to be affected by the shear rate applied for both TP1 and TP4. At low shear rates the model overestimates the tomato concentrate viscosity, whereas at high shear rate the model underestimates tomato concentrate viscosity. The models give more accurate predictions of tomato concentrate viscosity for samples at high °Brix regardless of the shear rate applied, except for a few samples where the model overestimates the viscosity at high shear rates.

The power model fitting has higher values of R-squared for almost every sample for both TP1 and TP4 (compared to exponential model). This is supported by the lower values sum of square error (SSerr) of power model which is 17.2 for TP1 and 22.8 for TP4 (Table 5.4) compared to 43.1 for TP1 and 41.7 for TP4 when using exponential model (Table 5.3). This result suggests a better prediction of tomato concentrate viscosity when using the power model compared to the exponential model.

The parameters in table 5.4 are similar for the two different tomato pastes investigated. To assess if the parameter is paste specific or whether it can share a common value between pastes, a sensitivity analysis was carried out. For example, if a parameter is paste specific, the change in its parameter value can have significant effect on model prediction. If a parameter can be fitted with a shared value, valid for both tomato pastes, then this simplifies the overall model. A model with minimal paste specific values would provide greater utility.

5.6 Sensitivity analysis

The purpose of a sensitivity analysis is to identify variables that do not significantly influence the model outcome. Because each they differ in magnitude for each prospective model, a scaling approach was taken where an upper and a lower value was identified for each model parameter. The range was set such that the difference between the fitted values for TP1 and TP4 were within, but near the extremes of the ranges. Tables 5.5 and 5.6 summarise the parameter ranges included in the sensitivity analysis.

Table 5.5 - Range of parameters value used in the sensitivity analysis (exponential model)

Sample/ Coefficients	n_{slope}	K_{slope}	K_b	σ_{oslope}	σ_{ob}
TP1	0.1051	0.0194	1.0875	24.3672	0.6362
TP4	0.1287	0.0114	1.3502	14.9927	0.7975
Lower range	0.09	0.01	1	14	0.6
Upper range	0.14	0.02	1.5	26.5	0.85

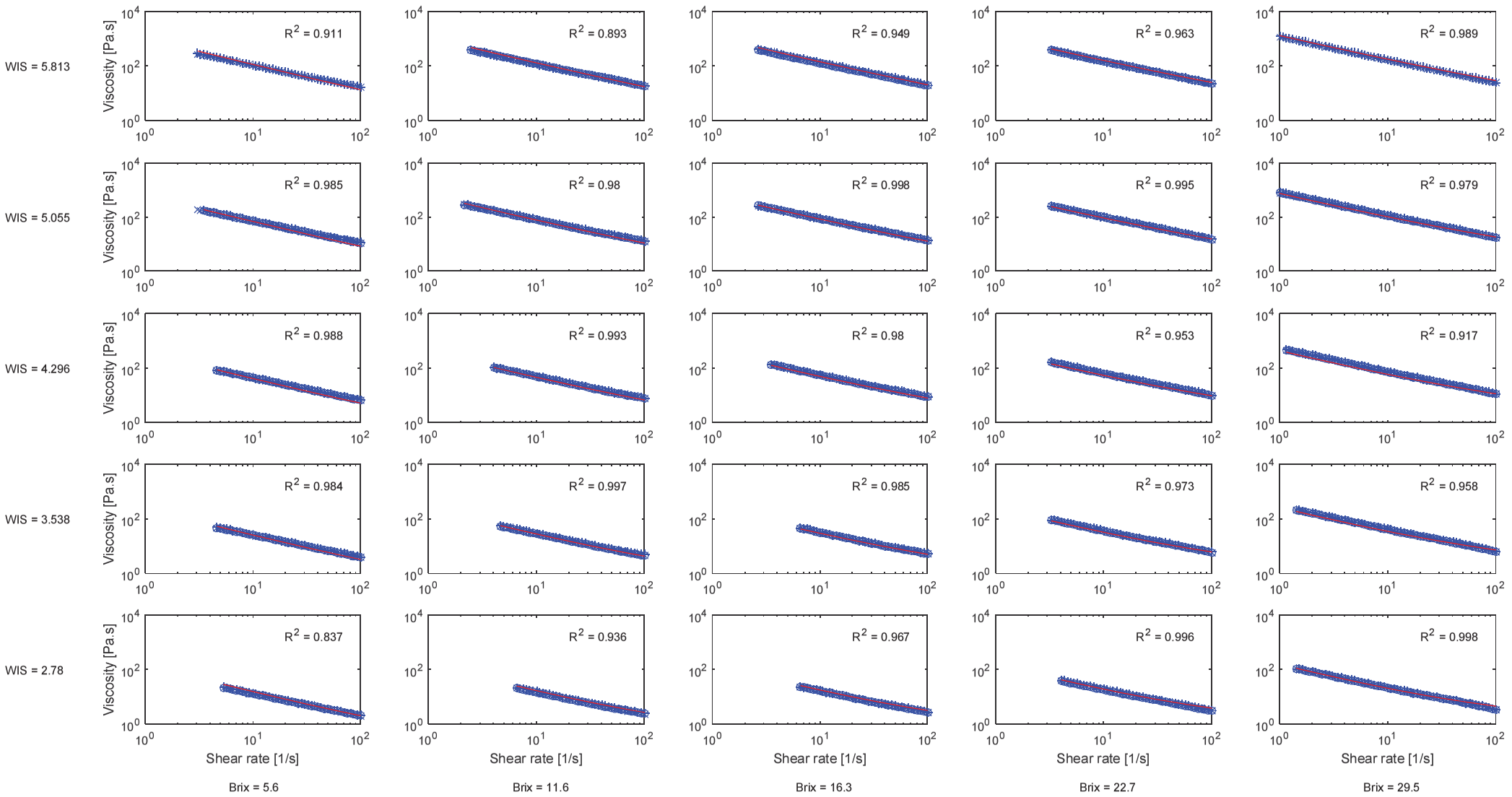

Figure 5.5 - Comparison of tomato concentrates viscosity obtained from experiment (***) and from fitting exponential model (_____) for TP1.

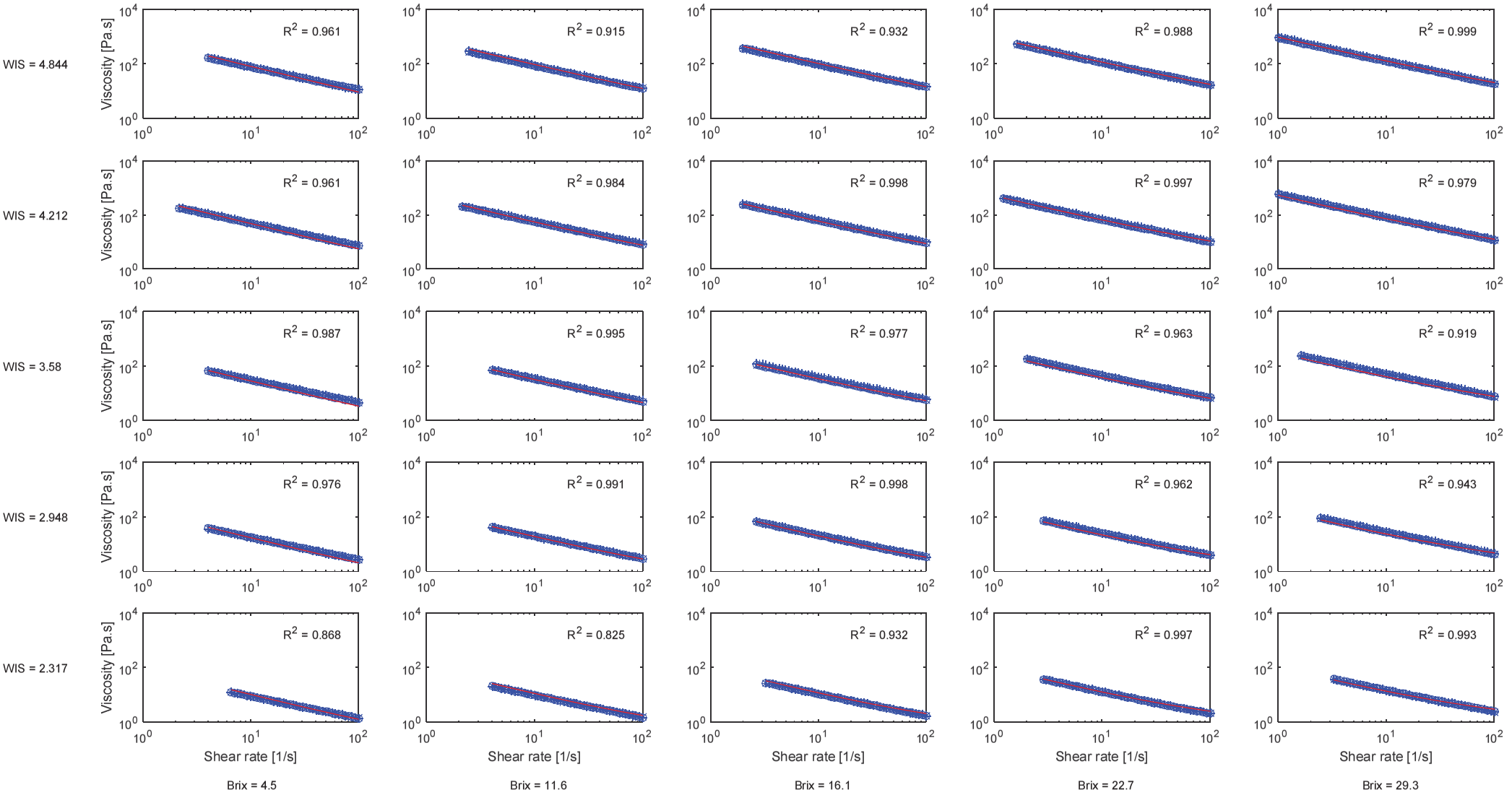

Figure 5.6 - Comparison of tomato concentrate viscosity obtained from experiment (***) and from fitting exponential model (_____) for TP4.

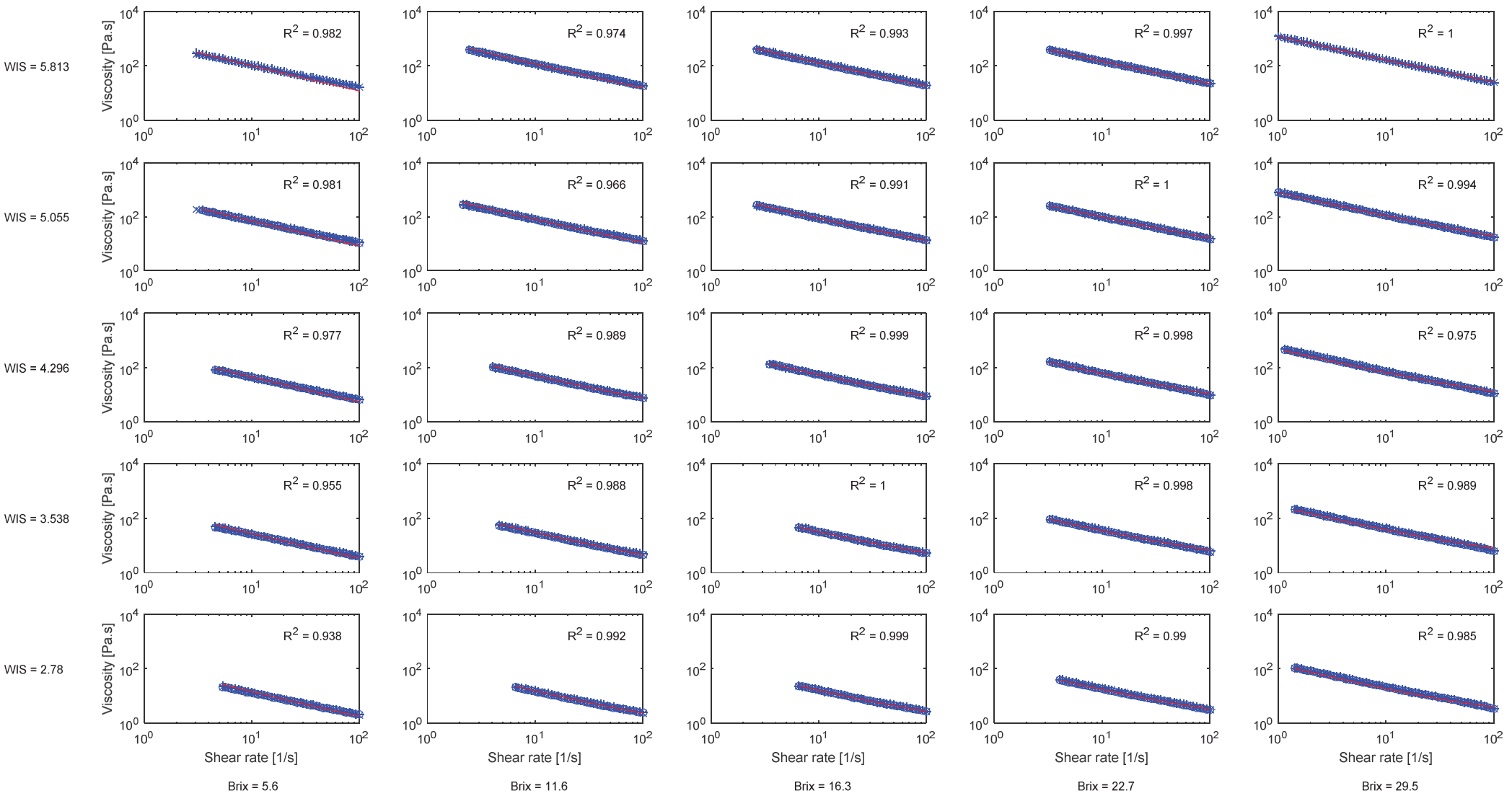

Figure 5.7 - Comparison of tomato concentrates viscosity obtained from experiment (***) and from fitting power model (_____) for TP1.

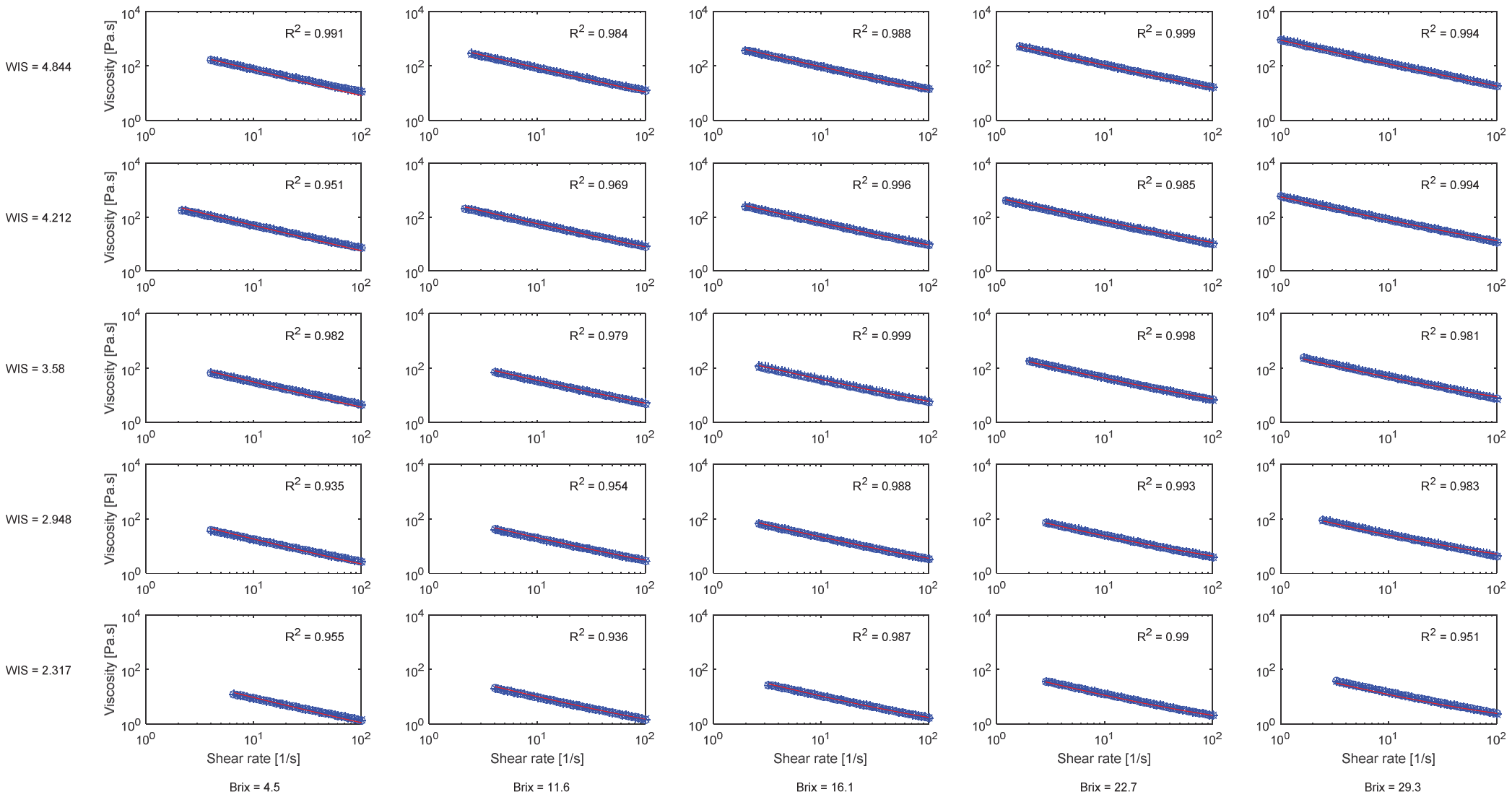

Figure 5.8 - Comparison of tomato concentrates viscosity obtained from experiment (***) and from fitting power model (_____) for TP4.

Table 5.6 - Range of parameters value used in the sensitivity analysis (power model)

Sample/ Coefficients	n_{slope}	K_{slope}	K_b	σ_{oslope}	σ_{ob}
TP1	0.1118	0.0028	4.7336	9.8181	2.5464
TP4	0.1359	0.0035	4.9282	9.4564	2.6611
Lower range	0.09	0.0026	4.7	9.4	2.5
Upper range	0.14	0.0036	4.95	9.9	2.7

Based on the ranges defined in Tables 5.5 and 5.6, Figures 5.9 and 5.10 were produced by normalising the change in variable from the lower value (scaled to 0), to the highest value in the range (scaled to 1). The resulting figures show the relative change in viscosity given a change in one input parameter at a time over these ranges. For comparison, the fitted values are drawn for each parameter curve as a circle (TP1) and square (TP4).

For the exponential model (Figure 5.9), only parameters $K_b$and σ_{ob} are highly sensitive to changes. This suggests the others in the model can be kept the same for both pastes. This makes sense in that these describe how the consistency coefficient (K) and yield stress are not only a function of WIS concentration but its properties. The °Brix parameter (K_{slope}) is not sensitive as would be expected as it is dominated by fructose and glucose and only small differences in soluble pectin may cause some differences. The WIS fractions of each paste could be quite different in physical properties (particle size distribution, and shape such as single cell or cell debris) and chemical nature (pectin content, degree of methylesterification (DM), and molecular weight) so parameters accounting for the contribution to the WIS fraction on the rheology ($K_b$and σ_{ob}) are expected to change.

For the power model, it is apparent that only the parameter σ_{ob} is sensitive to changes. This suggests that only the σ_{ob} factor needs to be a function of paste type.

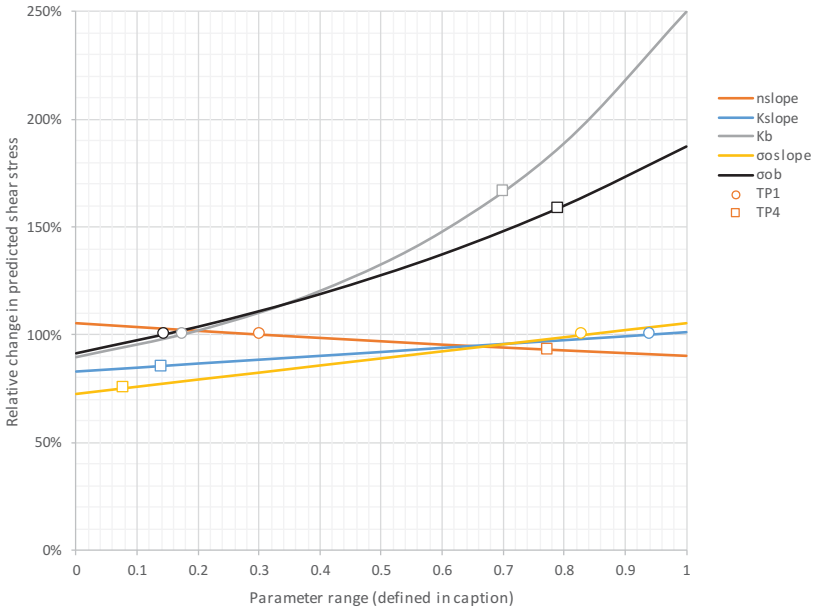

Figure 5.9 - Effect of parameter change on exponential model predictions. - Each parameter range was scaled from 0 to 1, corresponding to the range specified in Table 5.5.

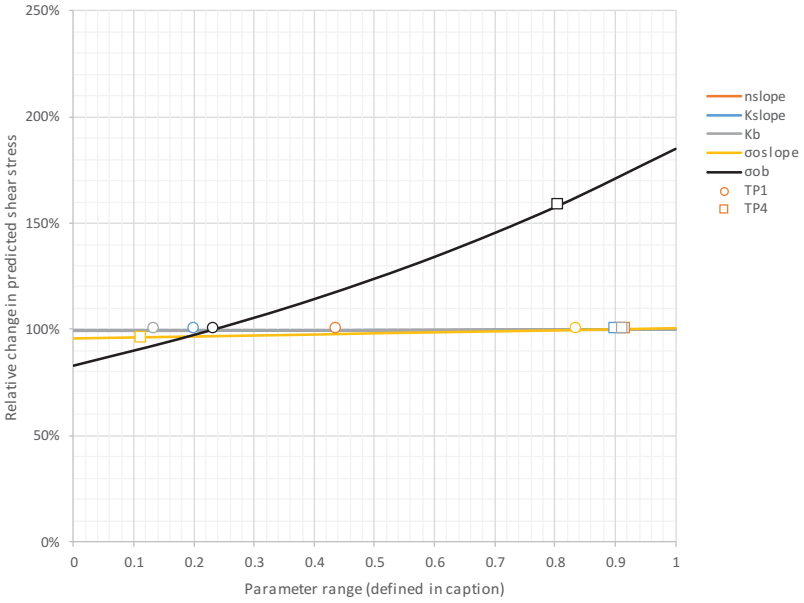

Figure 5.10 - Effect of parameter change on power model predictions. - Each parameter range was scaled from 0 to 1, corresponding to the range specified in Table 5.6.

Based on the results of sensitivity analysis, revised fits were applied for each model to the data from both pastes at once. For the exponential model, the parameters n_{slope}, K_{slope} and σ_{oslope} were fixed to be the same for both pastes but the other parameters K_b and σ_{ob} were fitted for each paste differently (giving a total of 7 fitted parameters). The parameters obtained are shown in Table 5.7. The viscosity prediction obtained from fitting these new parameters compared to the experimental data are presented in Figure 5.11 and 5.12.

Table 5.7 - Exponential model values obtained from common parameters n_{slope}, K_{slope} and σ_{oslope} and paste specific parameters K_b and σ_{ob}.

Sample/ Coefficients		n_{slope}	K_{slope}	K_b	σ_{oslope}	σ_{ob}	SSerr
Previous fit TP1		0.1051	0.0194	1.0875	24.3672	0.6362	43.0744
Previous fit TP4		0.1287	0.0114	1.3502	14.9927	0.7975	41.7221
Fitted together	TP1	0.110	0.0143	1.1699	8.6446	1.2223	53.1090
	TP4			1.2223		2.7677	

Figures 5.11 and 5.12 show that although there was a small increase in the sum of squared residuals, the combined model explained that data well. As was found for the exponential model fitted for each paste individually, there was a slightly steeper predicted slope of the shear stress versus shear rate plot at low °Brix.

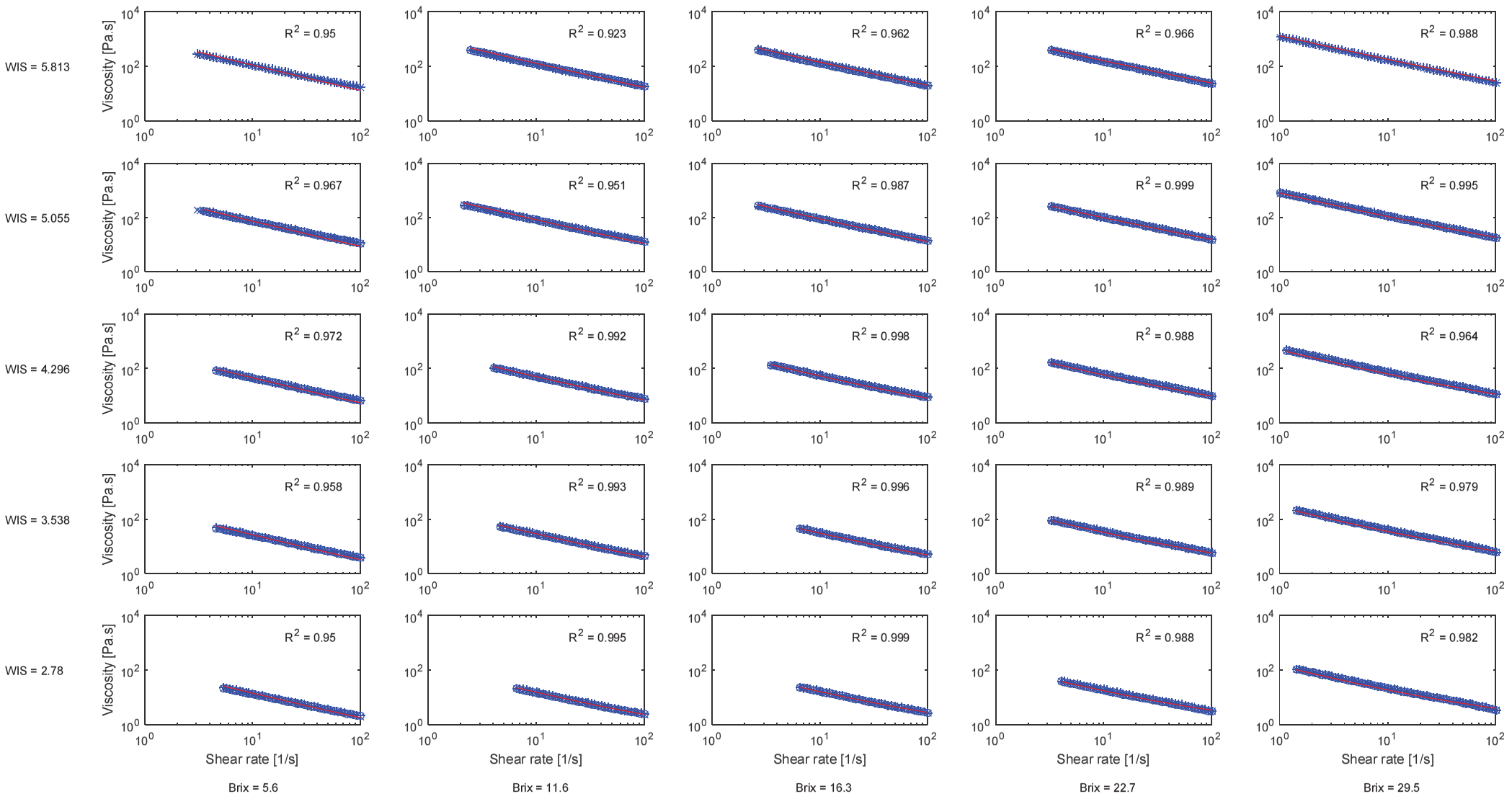

Figure 5.11 - Comparison of tomato concentrates viscosity obtained from experiment (***) and from fitting exponential model using combined parameters in Table 5.7 (_____) for TP1.

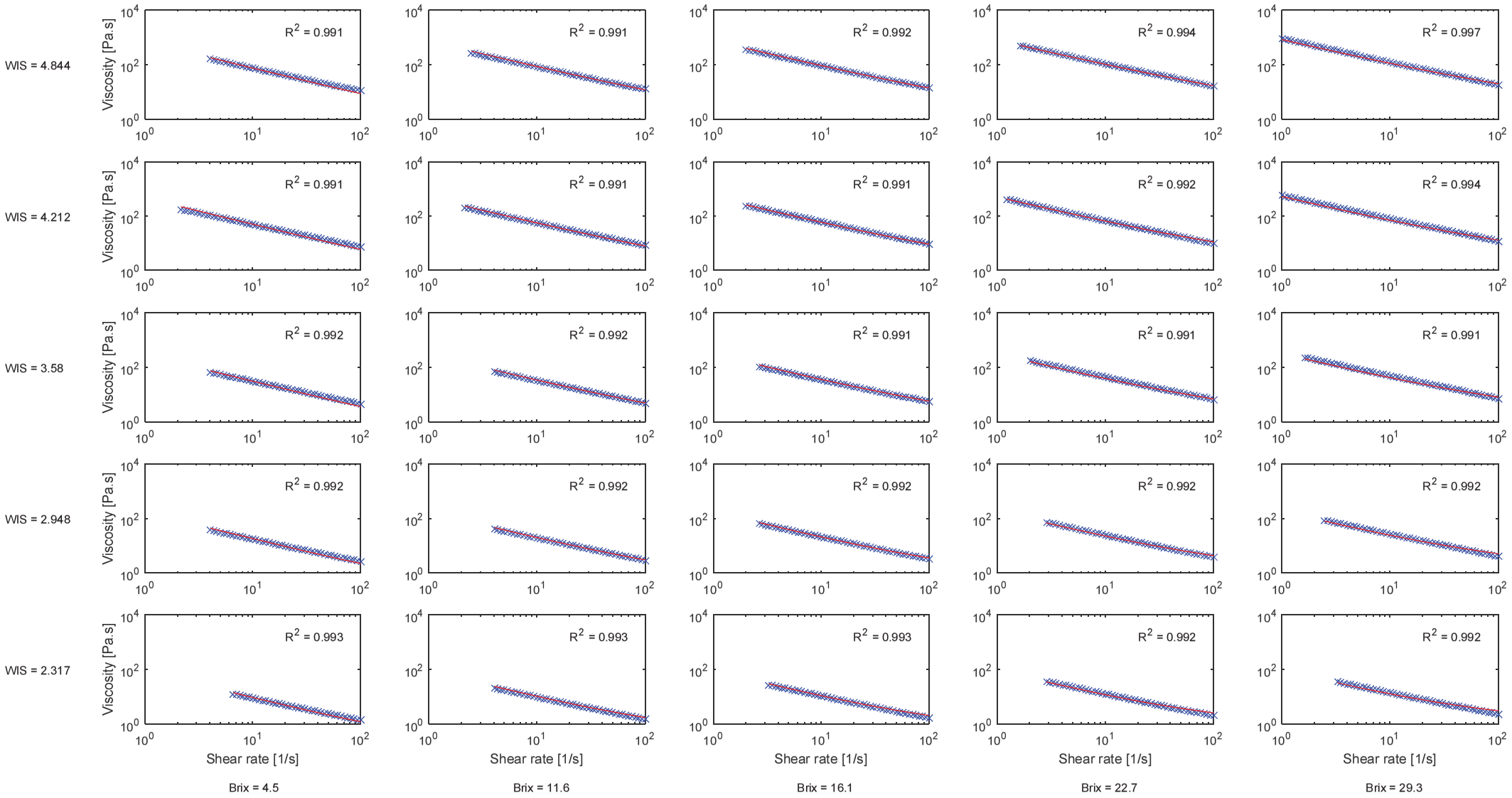

Figure 5.12 - Comparison of tomato concentrates viscosity obtained from experiment (***) and from fitting exponential model using combined parameters in Table 5.7 (_____) for TP4.

A similar analysis was carried out based on the results of the sensitivity analysis carried out for the power model. Table 5.8 shows the result of parameters obtained from fitting only parameter σ_{ob} for each paste differently while fitting common values for the other parameters (a total of 6 parameters). Figures 5.13 and 5.14 show the viscosity predictions using this combined model.

Table 5.8 - Exponential model values obtained from common parameters n_{slope}, K_{slope}, σ_{oslope} and K_b and paste specific parameter σ_{ob}

Sample/ Coefficients	n_{slope}	K_{slope}	K_b	σ_{oslope}	σ_{ob}	SSerr
Previous fit TP1	0.1118	0.0028	4.7336	9.8181	2.5464	17.2353
Previous fit TP4	0.1359	0.0035	4.9282	9.4564	2.6611	22.7653
Fitted TP1	0.1202	0.0034	4.7264	9.2468	2.5624	42.4719
together TP4					2.7136	

This model describes the data very well, with only small increases in the sum of squared residuals. It offers the potential for using a general model to predict paste flow behaviour with only one parameter to be fitted specifically for each paste. This would be a very valuable tool for industrial applications as only one parameter needs to be fitted for any new tomato paste sample. There is the possibility however, that the selected pastes TP1 and TP4 could have had very similar particle properties (particle size distribution and shape) but different interparticle forces. It has been suggested that consistency index K is a function of particle packing (Servais, Jones, & Roberts, 2002) and therefore particle size and shaped dependent. Yields stress however is also dependent on interparticle forces (Lopez-Sanchez, Chapara, Schumm, & Farr, 2012) which may depend on the chemical nature of the WIS fraction. Because the analysis was carried out for only the two paste samples, it is not clear whether the modelling approach can be extended beyond these materials.

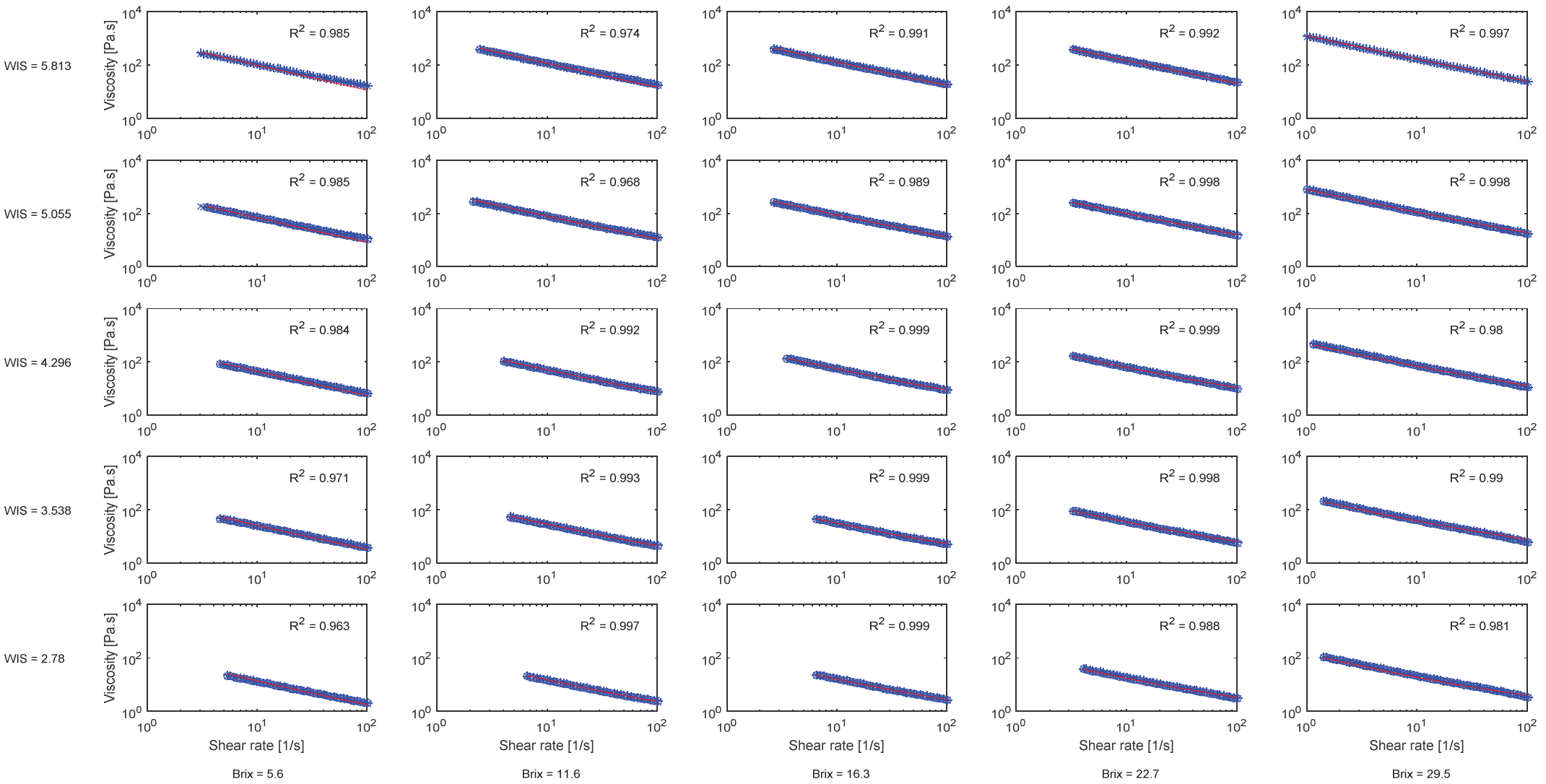

Figure 5.13 - Comparison of tomato concentrates viscosity obtained from experiment (***) and from fitting exponential model using combined parameters in Table 5.8 (_____) for TP1

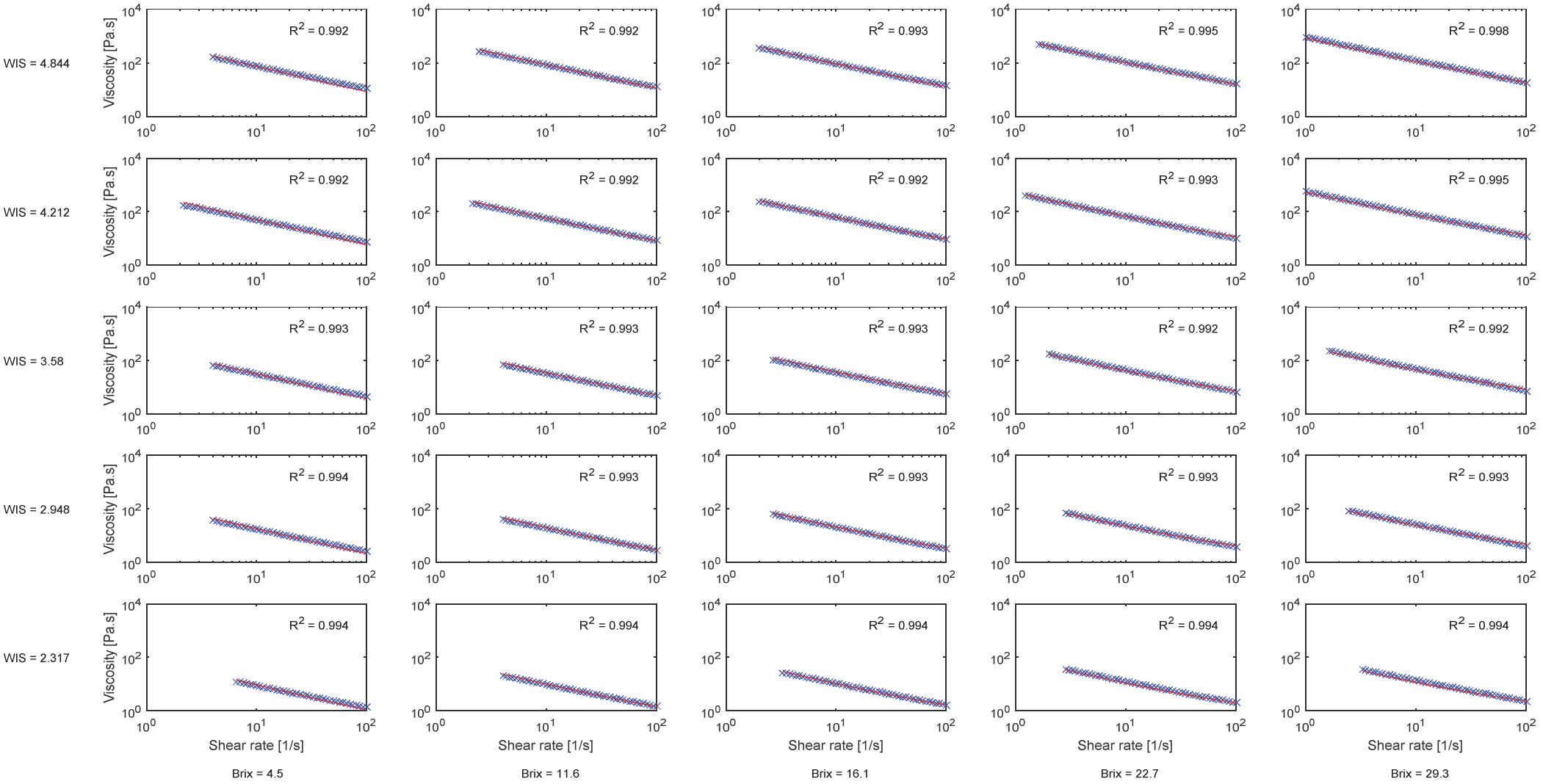

Figure 5.14 - Comparison of tomato concentrates viscosity obtained from experiment (***) and from fitting exponential model using combined parameters in Table 5.8 (_____) for TP4

5.7 Validation against blends of TP1 and TP4

To test the modelling approach a partial validation was carried out by creating mixtures of tomato pastes TP1 and TP4.

5.7.1 Methods

Triplicate blends comprising 25, 50 and 75% TP1 mixed with TP4 were created by mixing by hand using a spatula in a beaker and leaving them to stand overnight. Each blend was then diluted to 0.85, 0.7 and 0.55 times the original strength. The resulting twelve tomato paste samples are summarised in Table 5.9.

Table 5.9 - Summary of blended paste compositions

Ratio TP1:TP4	Dilution (Fraction of original strength)							
	1		0.85		0.7		0.55	
	%WIS	°Brix	%WIS	°Brix	%WIS	°Brix	%WIS	°Brix
0.25	4.4	29.5	3.8	24	3.1	19.7	2.4	16
0.5	4.6	29.5	3.9	25	3.2	20.5	2.5	16
0.75	4.8	29.5	4.1	24.2	3.4	20.5	2.7	15.4

Each tomato paste blend was then analysed in the rheometer following the procedure outlined in Chapter 4 section 4.3.6.

5.7.2 Model fitting and performance

The power model (model set outlined in section 5.4.2) was fitted to each blend and its dilutions together using a nonlinear least squares fitting method in Matlab as explained in section 5.5. The simplified power model where common values of n_{slope}, K_{slope}, $\sigma_{oslope}$and K_b are used and there is only one paste specific parameter (σ_{ob}) fitted. The values of n_{slope}, K_{slope}, $\sigma_{oslope}$and K_b were set and maintained at the values found previously for TP1 and TP4 as outlined in Table 5.8. The resulting fits are summarised in Table 5.10 below.

Table 5.10 - Exponential model values obtained from common parameters n_{slope}, K_{slope} , $\sigma_{oslope}$and K_b and paste specific parameter σ_{ob}

Sample/ Coefficients	n_{slope}	K_{slope}	K_b	σ_{oslope}	σ_{ob}
0% TP1: 100% TP4	0.1202	0.0034	4.7264	9.2468	2.7136
25% TP1: 75% TP4	0.1202	0.0034	4.7264	9.2468	2.6876
50% TP1: 50% TP4	0.1202	0.0034	4.7264	9.2468	2.6068
75% TP1: 25% TP4	0.1202	0.0034	4.7264	9.2468	2.5590
100%TP1: 0% TP4	0.1202	0.0034	4.7264	9.2468	2.5624

Figure 5.15 shows the performance of the model to predict the experimental data. The figures show that very good performance is achieved except for the most diluted pastes at low shear rate.

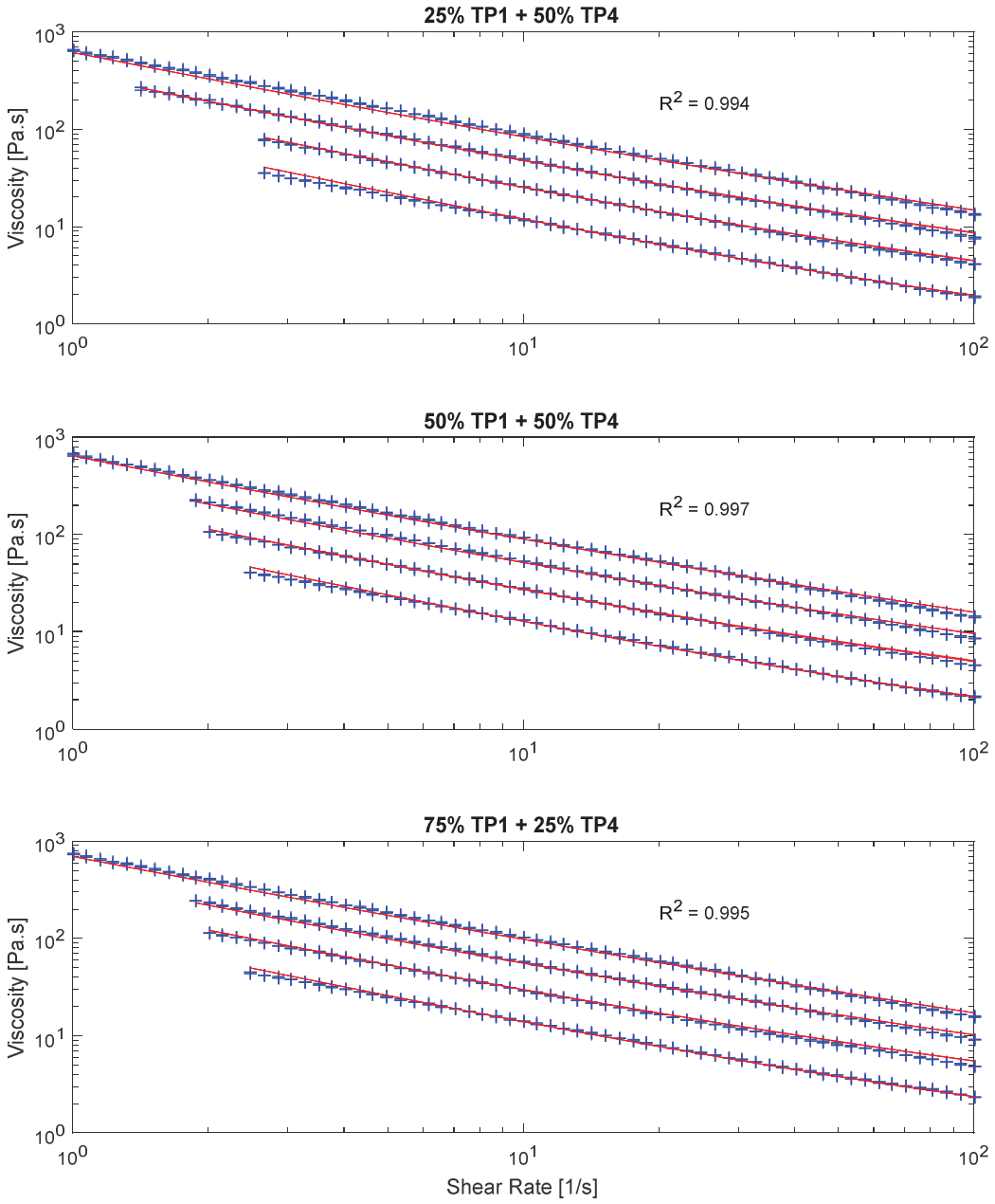

Figure 5.15 - Predicted and experimental viscosity for blends of TP1 and TP4 using parameters summarised in Table 5.10. Note that the four curves on each plot are for dilutions (most concentrated pastes are uppermost).

Figure 5.16 shows that for the blended pastes, the fitted parameters (σ_{ob}) lie between the parameters fitted for the unblended pastes. The relationship between the value of σ_{ob} and the proportion of each paste is not linear.

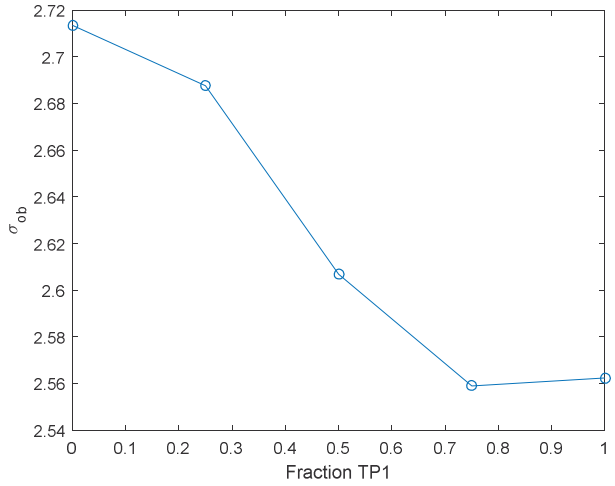

Figure 5.16 - Relationship between σ_{ob} and the proportion of TP1 and TP4 for blends.

This analysis shows that the model can be applied to different paste samples and in this case only one parameter needed to be adjusted, although in this case the pastes were made from water insoluble solids fractions that the original model was fitted for. The model would have greater application if it could be applied to completely different paste materials.

5.8 Validation against TP2, TP3 and TP5 at different dilutions

In chapter 3, five different tomato pastes were analysed. For these samples, the water insoluble solids and °Brix levels were analysed. The flow curves for each paste, for the original strength material as well as for a range of dilutions (section 3.4.2). Two of these three pastes were further investigated in this chapter to construct the functional rheological model. Application of the model to the remaining three pastes (TP2, TP3 and TP5), especially if only one or two parameters need adjusting, would show the universality of the model.

The power model was fitted to tomato pastes TP2, TP3 and TP5 in a similar way to what was done for the blended tomato paste samples (section 5.7). Four parameter arrangements were used to fit the models were investigated. Firstly, for each paste and its dilutions, the full model will all parameters adjustable was fitted. Secondly, the simplified power model was fitted where only the σ_{ob} parameter was fitted and the other parameters were maintained at the values found for TP1 and TP4. In the third approach, n_{slope} was also allowed to change (in addition to σ_{ob}). Figures 5.17-5.19 show the resulting fits between experimental and predicted data for these four scenarios respectively.

It can be seen for all three pastes, that fitting the power model with fully adjustable parameters results in very good predictions. Care must be taken with this approach however because the model contains three parameters that account for the contribution of the WIS fraction and two other parameters that account for °Brix. In this experiment, for each paste, the ratio of WIS and °Brix do not vary and they both decrease proportionately on dilution. Thus, many overall fits for the model with widely different parameters could be possible. An example of this is for TP2 where the low σ_{ob} value is compensated for by the much higher σ_{oslope}.

Table 5.11 - Summary of model fits to TP2, TP3 and TP5 (common parameters indicated in italics)

Paste	Fitting parameters	n_{slope}	K_{slope}	K_b	σ_{oslope}	σ_{ob}	R^2
TP2							
	All parameters	0.1851	0.0028	5.8483	57.4727	0.7305	0.998
	σ_{ob}	0.1202	*0.0034*	*4.7264*	*9.2468*	2.6741	0.992
	n_{slope} and σ_{ob}	0.1420	*0.0034*	*4.7264*	*9.2468*	2.8373	0.994
TP3							
	All parameters	0.1645	0.0008	5.8993	5.0579	1.6304	0.997
	σ_{ob}	0.1202	*0.0034*	*4.7264*	*9.2468*	1.8317	0.805
	n_{slope} and σ_{ob}	0.1286	*0.0034*	*4.7264*	*9.2468*	2.8373	0.884
TP5							
	All parameters	0.1849	0.0078	4.6243	4.2370	2.9599	0.994
	σ_{ob}	0.1360	*0.0034*	*4.7264*	*9.2468*	2.7136	0.919
	n_{slope} and σ_{ob}	0.1202	*0.0034*	*4.7264*	*9.2468*	2.2889	0.960

In the second case, only σ_{ob} was allowed to change and the other parameters were fixed at the values found for TP1 and TP4 above. As shown in Figure 5.18, the model predicts the order of magnitude of the apparent viscosity within reason and does a good job of predicting the flow behaviour for TP2 and TP5. The predictions for TP3 were much poorer, especially at low shear rates. This shows that although the broad rheological behaviour can be predicted using only one paste specific parameter, the variations in the nature of the WIS fraction from different pastes requires more fitting parameters. This makes sense as it is known that the processing conditions and finishers affect the particle size distribution and shape of the WIS and that these in turn effect the flow behaviour.

The model fits are improved by allowing n_{slope} to also change during the fitting (see Figure 5.19). This makes sense in that it is hypothesised that in suspensions the nature of particles is important. Longer or non-spherical particles need extra energy to slide pass each other, thus increase energy dissipation. Alignment of the particles during flow at higher shear rates results in more shear thinning and consequently the n_{slope} parameter must change to allow this. A similar argument can be made about the particle size distribution where the proportion of large and small particles will contribute differently since small particles can act as a lubricant and thus decrease the viscosity.

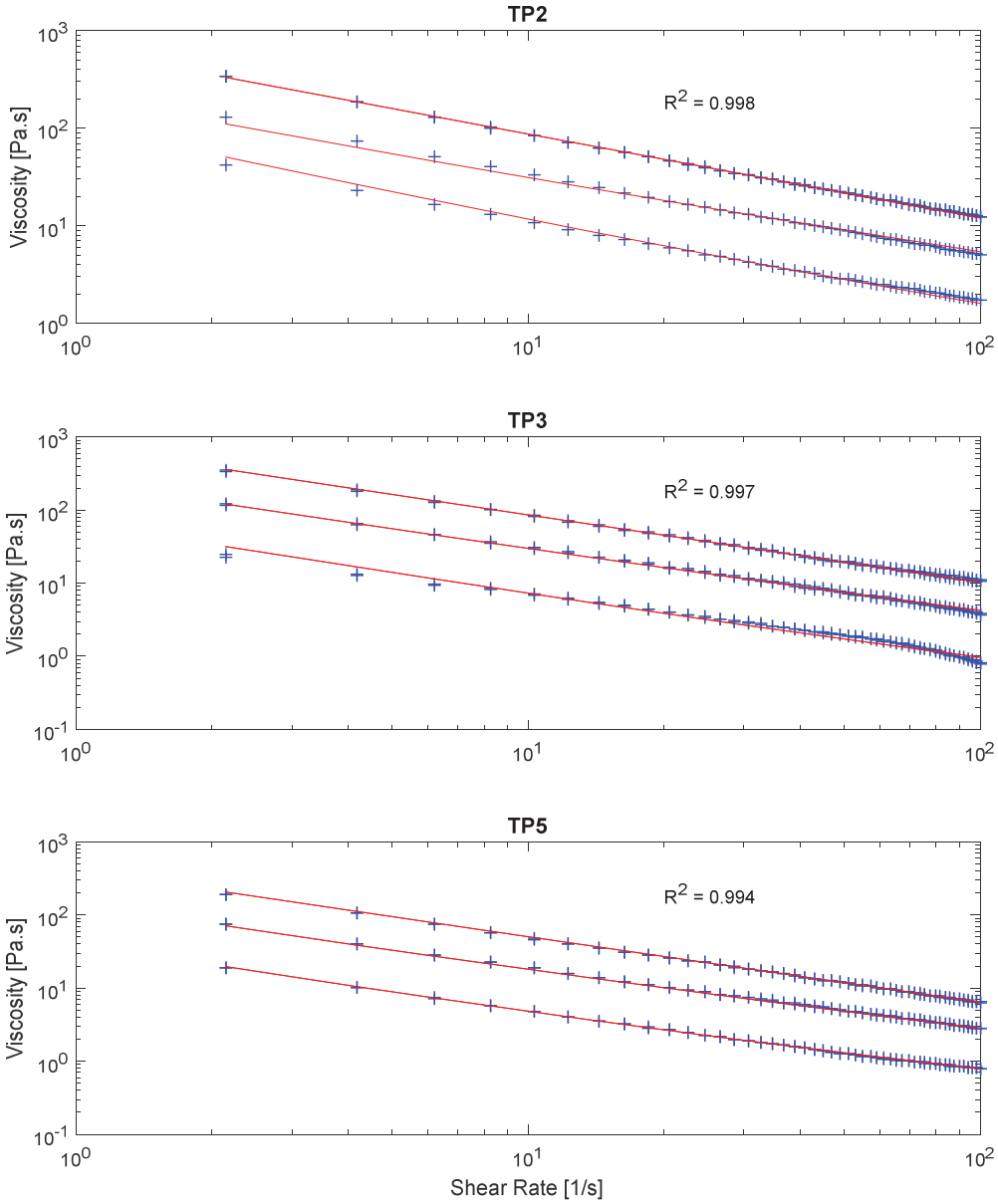

Figure 5.17 - Model predictions for TP2, TP3 and TP5 when all parameters were paste specific.

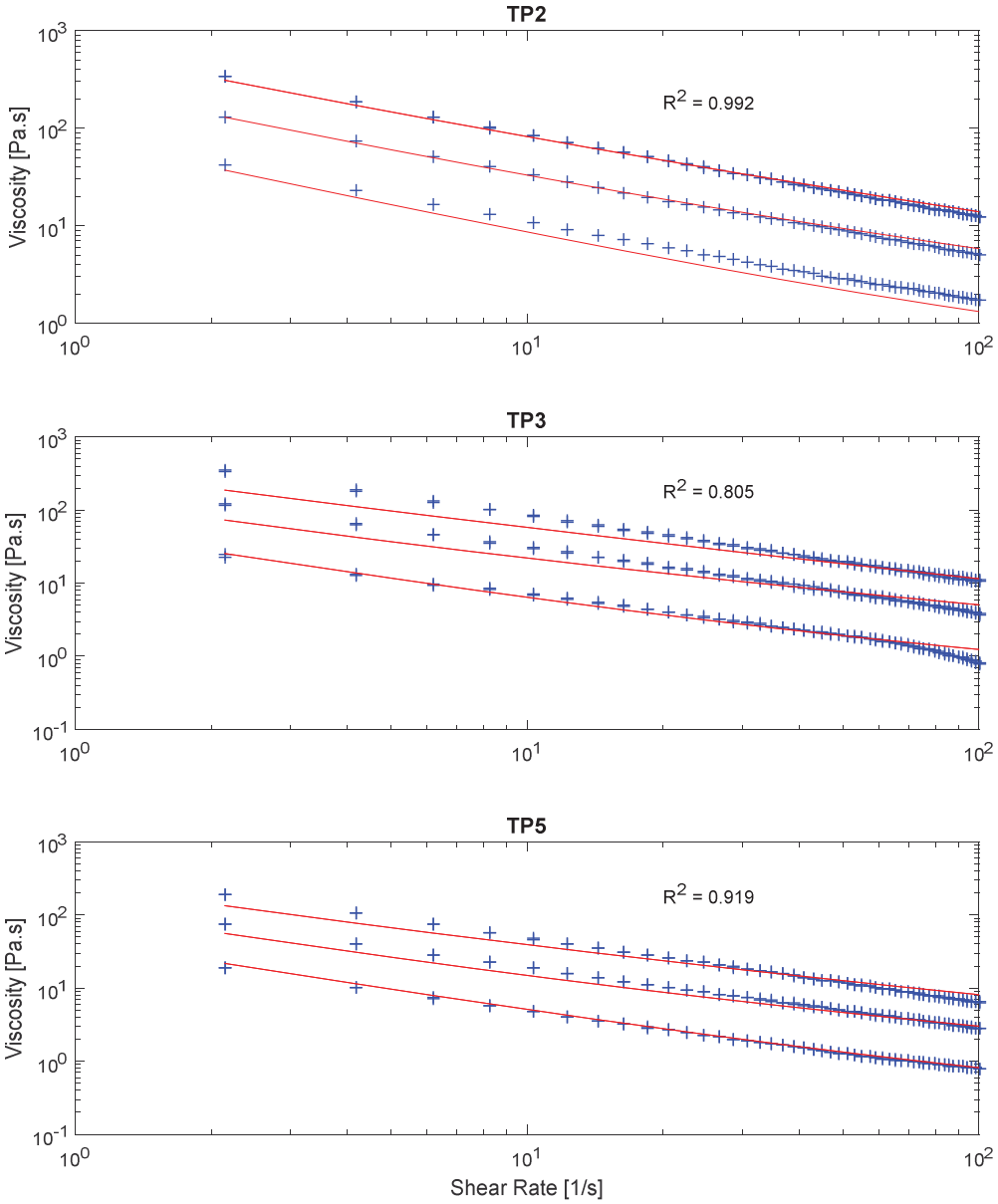

Figure 5.18 - Model predictions for TP2, TP3 and TP5 when only σ_{ob} was paste specific.

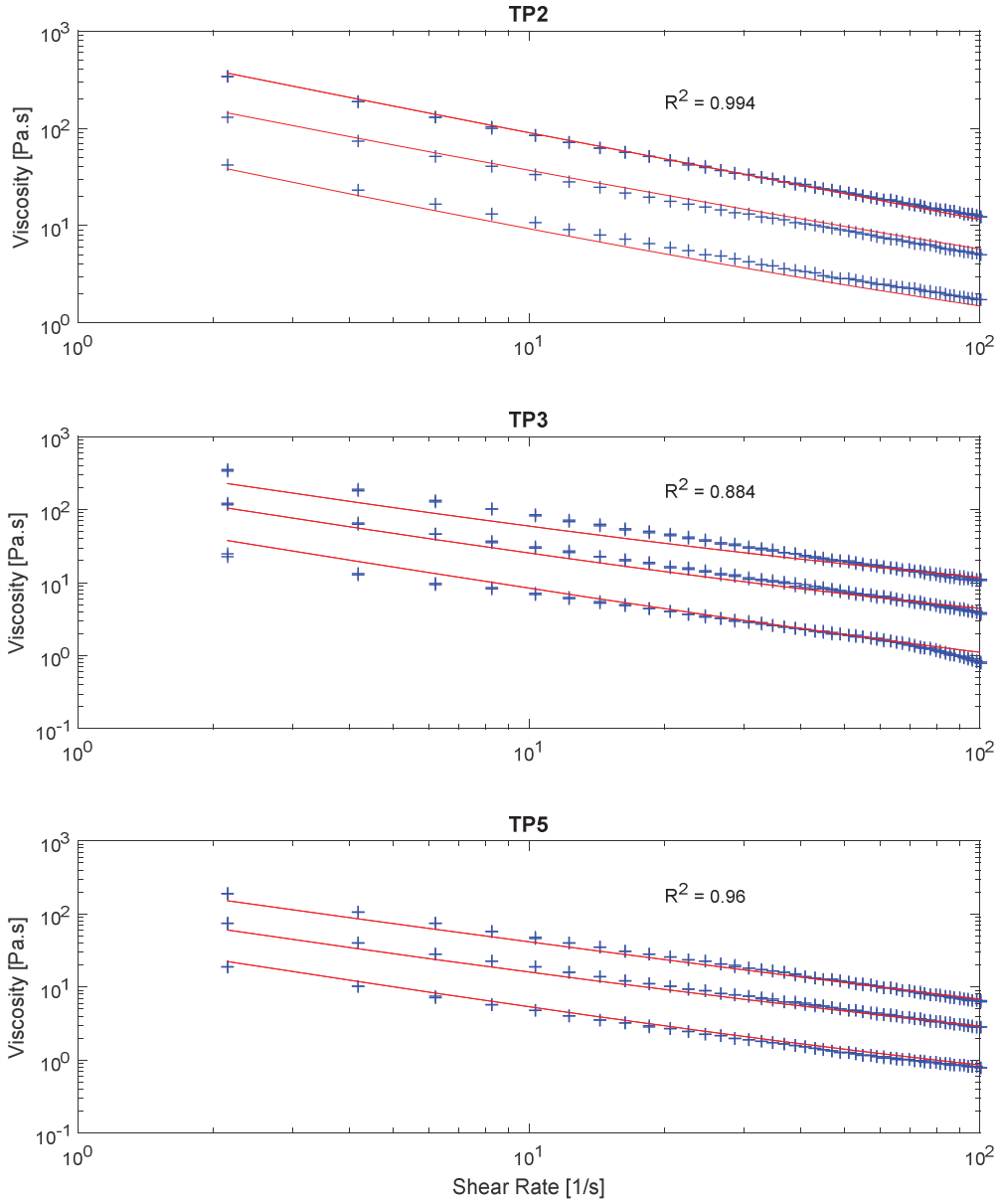

Figure 5.19 - Model predictions for TP2, TP3 and TP5 when σ_{ob} and n_{slope} were paste specific.

5.9 Conclusions

In summary, these results indicate that much of the variations in flow behaviour of different tomato pastes can be explained by the variations in the insoluble and soluble components (%WIS and °Brix). Further, the effect of %WIS on the flow behaviour of tomato concentrate is stronger than °Brix.

Based on trends in experimental data collected for pastes with a wide range of soluble and insoluble solids content, two mathematical models were developed; one based on exponential relationships and the other with power relationships describing the effect of WIS content on Herschel Bulkley model parameters.

This model was fitted to the base experimental data collected using two different tomato paste samples and it was found that the power model predicted the experimental data the best. Furthermore, only one paste specific parameter (σ_{ob}) (+ 4 other common fitted parameters) was needed to predict the whole data set.

When applied to pastes (and their dilutions) formed by blending TP1 and TP4 together, the same model with only one paste specific parameter could also fit the experimental data well. When applied to three other pastes (and their dilutions), the one paste specific parameter model could predict the general trends but better predictions could be made if a second parameter (n_{slope}) could be different for different pastes.

Conclusions and Recommendations

This work found that much of the variation in flow properties of tomato concentrates can be explained by appropriate characterisation of the %WIS and °Brix levels in the paste. The %WIS fraction in tomato paste can be calculated using the measured total solids and °Brix levels in the paste. However, the °Brix level needs to be adjusted to account for differences between the refractive index of serum vs sucrose to obtain actual soluble solids content and thus give accurate %WIS concentration.

Serum contributes to the flow behaviour of tomato paste due to the presence of soluble solids in the serum. In particular, it was found that primarily sugars cause this effect, potentially by enhancing the pectin-pectin interactions in the WIS components of the paste. Since the contribution of soluble pectin to the rheology of tomato paste was not determined in this study, it is of interest to evaluate whether soluble pectin contributes to the flow behaviour, since in the present work sugars seem to play the dominant effect to the flow behaviour of the paste. In this work it was found that there were measurable differences in serum viscosity between pastes, however good overall model predictions could be achieved without considering the serum phase beyond the soluble solids concentration.

The Herschel-Bulkley model was found to be the most appropriate model to describe the flow behaviour of tomato paste. Herschel Bulkley parameters could then be linked to the %WIS and °Brix levels in the paste. For some pastes the model could be fitted with just one paste specific parameter plus four other generally fitted constants (which apply to any paste). When applied to other pastes however, at least one of the other parameters was also required to be paste specific. These parameters relate the yield stress and the flow behaviour index to %WIS. Because these two parameters need to be fitted for individual pastes, it is thought that they are influenced by the particle size and shape and/or their composition of the WIS fraction. For example elongated particles will orientate within a flow field with varying shear rates, thereby influencing the flow behaviour index.

Future work could investigate the microstructure of the paste through microscopy to evaluate the differences in the particle size and shape of the water insoluble solid components between each paste. The differences in the particle size distribution of each paste could be investigated using different techniques such wet sieving, light microscopy and laser light diffraction. Furthermore, the physicochemical properties of water insoluble solid could be determined as well; to evaluate the difference in the properties of insoluble pectin, since molecular weight and degree of methylesterification (DM) of pectin has been reported to contribute to the flow behaviour of tomato concentrate. This information is important to further expand on this theory. If links can be made between particle size, shape and composition of the WIS fraction, paste manufacturing processes could be optimised to provide targeted rheological performance from processing tomatoes.

There is potential to fit the two key paste specific parameters for a paste from a single flow curve, with the shear rate ($\dot{\gamma}$) dependency being used to fit the parameter describing how %WIS affects the

flow behaviour index (n) and the magnitude of the viscosity (η) at any shear rate used to fit the parameter describing how yield stress (σ_0) is affected by %WIS. This could provide a clear and industry implementable method to characterise tomato paste batches. Such a characterisation method would be useful for predicting flow behaviour under different processing conditions and how dilution during product formulation will affect viscosity. Future work should be carried out to extend this work to those aims.

REFERENCES

Al-Wandawi, H., Abdul-Rahman, M., & Al-Shaikhly, K. (1985). Tomato processing wastes as essential raw material source. *Journal of Agricultural and Food Chemistry*, *33*(5), 804-807.

Augusto, P. E. D., Falguera, V., Cristianini, M., & Ibarz, A. (2012). Rheological behavior of tomato juice: Steady-state shear and time-dependent modeling. *Food and Bioprocess Technology*, *5*(5), 1715-1723.

Barnes, H. A. & Carnali, J. O. (1990). The vane-in-cup as a novel rheometer geometry for shear thinning and thixotropic materials. *Journal of Rheology*, *34*(6), 841-866.

Barnes, H. A. & Nguyen, Q. D. (2001). Rotating vane rheometry—a review. *Journal of non-Newtonion Fluid Mechanics*, *98*(1), 1-14.

Barnes, H. A. (1995). A review of the slip (wall depletion) of polymer solutions, emulsions and particle suspensions in viscometers: Its cause, character, and cure. *Journal of Non-Newtonion Fluid Mechanics*, *56*(3), 221-251.

Barnes, H. A. (1999). The yield stress—a review or 'παντα ρει'—everything flows?. *Journal of Non-NewtonionFluid Mechanics*, *81*(1-2), 133-178.

Barrett, D. M., Garcia, E., & Wayne, J. E. (1998). Textural modification of processing tomatoes. *Critical Reviews in Food Science and Nutrition*, *38*(3), 173-258.

Bayod, E., Mansson, P., Innings, F., Bergenstahl, B., & Tornberg, E. (2007). Low shear rheology of concentrated tomato products. Effect of Particle Size and Time. *Food Biophysics*, *2*(4), 146-157.

Benitez, E. I., Genovese, D. B., & Lozano, J. E. (2009). Effect of typical sugars on the viscosity and colloidal stability of apple juice. *Food Hydrocolloids*, *23*(2), 519-525.

Beresovsky, N., Kopelman, I. J., & Mizrahi, S. (1995). The role of pulp interparticle interaction in determining tomato juice viscosity. *Journal of Food Processing and Preservation*, *19*(2), 133-146.

Bourne, M. C. (2002). *Food texture and viscosity: Concept and measurement* (2nd ed.). San Diego, California; London: Academic Press.

Brecht, P. E., Keng, L., Bisogni, C. M., & Munger, H. M. (1976). Effect of fruit portion, stage of ripeness and growth habit on chemical composition of fresh tomatoes. *Journal of Food Science*, *41*(4), 945-948.

Brown, H. E. & Stein, E. R. (1977). Studies on the alcohol-insoluble solids of Chico III and Homestead-24 tomatoes. *Journal of Agricultural and Food Chemistry*, *25*(4), 790-793.

Brummell, D. A. & Labavitch, J. M. (1997). Effect of antisense suppression of edopolygalacturonase activity on polyuronide molecular weight in ripening tomato fruit and in fruit homogenates. *Plant Physiology*, *115*(2), 717-725.

Brummell, D. A., (2006). Cell wall disassembly in ripening fruit. *Functional Plant Biology*, *33*(2), 103-119.

Brummell, D. A., Harpster, M. H., Civello, P. M., Palys, J. M., Bennett, A. B., & Dunsmuir, P. (1999). Modification of expansin protein abundance in tomato fruit alters softening and cell wall polymer metabolism during ripening. *The Plant Cell*, *11*(11), 2203-2216.

Brummell, D. A.,& Harpster, M. H. (2001). Cell wall metabolismin fruit softening and quality and its manipulation in transgenic plants. *Plant Molecular Biology*, *47*(1-2), 311-340.

Campbell, C. F. (2004). *Optimisation of tomato paste production, storage and use*. (Unpbublished master's thesis). Massey University, Palmerston North, New Zealand.

Carrington, S. & Langride, J. (2005). *Viscometer or rheometer? Making the decision*. Retrieved from http://www.iesmat.com/iesmat/upload/file/Malvern/Productos-MAL/REO-Viscometer%20or%20Rheometer.%20Making%20the%20decision.pdf

Chhabra, R. P. & Richardson, J. F. (2008). *Non-Newtonion flow and applied rheology: Engineering applications* (2nd ed.). Amsterdam; Oxford: Butterworth-Heinemann.

Christiaens, S., Van Buggenhout, S., Houben, K., Chaula, D., Van Loey, A. M., & Hendrickx, M. E. (2012). Unravelling process-induced pectin changes in the tomato cell wall: An integrated approach. *Food Chemistry*, *132*(3), 1534-1543.

Correia, L. R. & Mittal, G. S. (1999). Food rheological studies using coaxial rotational and capillary extrusion rheometers. *International Journal of Food Properties*, *2*(2), 139-150.

Cosgrove, D. J. (2005). Growth of plant cell wall. *Nature Reviews Molecular Cell Biology*, *6*(11), 850-861.

Davies, J. N., Hobson, G. E., & McGlasson, W. B. (1981). The constituents of tomato fruit — the influence of environment, nutrition, and genotype. *C R C Critical Reviews in Food Science and Nutrition*, *15*(3), 205-280.

Den Ouden, F. W. C. & Van Vliet, T. (2002). Effect of concentration on the rheology and serum separation of tomato suspension. *Journal of Texture Studies*, *33*(2), 91-104.

Eriksson, E. M., Bovy, A., Manning, K., Harrison, L., Andrews, J., De Silva, J., . . ., & Seymour, G. B. (2004). Effect of the c*olorless non-ripening* mutation on cell wall biochemistry and gene expression during tomato fruit development and ripening. *Plant Physiology*, *136*(4), 4184-4197.

Fito, P. J., Clemente, G., & Sanz, F. J. (1983). Rheological behaviour of tomato concentrate (hot break and cold break). *Journal of Food Engineering*, *2*(1), 51-62.

Frenkel, C., Peters, J. S., Tieman, D. M., Tiznado, M. E., & Handa, A. K. (1998). Pectin methylesterase regulates methanol and ethanol accumulation in ripening tomato (*Lycopersicon esculentum*) fruit. *The Journal of Biological Chemistry*, *273*(8), 4293-4295.

Garcia, E. & Barrett, D. M. (2006). Evaluation of processing tomatoes from two consecutive growing seasons: Quality attributes, peelability and yield. *Journal of Food Processing and Preservation*, *30*(1), 20-36.

Goodman, C. L., Fawcett, S., & Barringer, S. A. (2002). Flavor, viscosity, and color analyses of hot and cold break tomato juices. *Journal of Food Science*, *67*(1), 404-408.

Goose, P. G. & Binsted, R. (1973). *Tomato paste and other tomato products* (2nd ed.). London: Food Trade Press.

Gould, W. A. (1992). *Tomato production, processing, & technology* (3rd ed.). Baltimore, MD.: CTI Publications.

Gross, K. C. & Wallner, S. J. (1979). Degradation of cell wall polysaccharides during tomato fruit ripening. *Plant Physiology*, *63*(1), 117-120.

Handa, A. K., Tieman, D. M., Mishra, K. K., Thakur, B. R., & Singh, R. K. (1996). Role of pectin methylesterase in tomato fruit ripening and quality attributes of processed tomato juice. *Progress in Biotechnology*, *14*, 355-368.

Harper, J. C. & ElSahrigi, A. F. (1965). Viscometric behavior of tomato concentrates. *Journal of Food Science*, *30*(3), 470-476.

Hayes, W. A., Smith, P. G., & Morris, A. E. (1998). The production and quality of tomato concentrates. *Critical Reviews in Food Science and Nutrition*, *38*(7), 557-564.

Holdsworth, S. D. (1971). Applicability of rheological models to the interpretation of flow and processing behaviour of fluid food products. *Journal of Texture Studies*, *2*(4), 393-418.

Houben, K., Jolie, R. P., Fraeye, I., Van Loey, A. M., & Hendrickx, M. E. (2011). Comparative study of the cell wall composition of broccoli, carrot, and tomato: Structural characterization of the extractable pectins and hemicelluloses. *Carbohydrate Research*, *346*(9), 1105-1111.

Huber, D. J. & O'Donoghue E. M. (1993). Polyuronides in avocado (*Persea american*a) and tomato (*Lycopersicon esculentum*) fruits exhibit markedly different patterns of molecular weight downshifts during ripening. *Plant Physiology*, *102*(2), 473-480.

Koch, J. L. & Nevins, D. J. (1989). Tomato fruit cell wall: I. Use of purified tomato polygalacturonase and pectinmethylesterase to identify developmental changes in pectins. *Plant physiology*, *91*(3), 816-822.

Kramer, A. & Szczesniak, A. S. (1973). *Texture measurement of foods: Psychophysical fundamentals, sensory, mechanical, and chemical procedures, and their interrelationship*. Dordrecht; Boston: D. Reidel Publishing Company.

Lopez-Sanchez, P., Chapara, V., Schumm, S., & Farr, R. (2012). Shear elastic deformation and particle packing in plant cell dispersions. *Food Biophysics*, *7*(1), 1-14.

Lopez-Sanchez, P., Nijsse, J., Blonk H. C., Bialek, L., Schumm, S., & Langton, M. (2011). Effect of mechanical and thermal treatments on the microstructure and rheological properties

of carrot, broccoli and tomato dispersions. *Journal of the Science of Food and Agriculture*, *91*(2), 207-217.

Luh, B. S., Sarhan, M. A., & Wang, Z. (1984). Pectins and fibers in processing tomatoes. *Food Technology in Australia*, *36*(2), 70-73.

Markovic, K., Vahcic, N., Kovacevic Ganic, K., & Banovic, M. (2007). Aroma volatiles of tomatoes and tomato products evaluated by solid-phase microextraction. *Flavour and Fragrance Journal*, *22*(5), 395-400.

Marsh, G. L., Buhlert, J. E., Leonard, S. J. (1980). Effect of composition upon Bostwick consistency of tomato concentrate. *Journal of Food Science*, *45*(3), 703-706.

Miedes, E. & Lorences, E. P. (2009). Xyloglucan endotransglucosylase/hydrolases (XTHs) during tomato fruit growth and ripening. *Journal of Plant Physiology*, *166*(5), 489-498.

Moelants, K. R. N., Cardinaels, R., De Greef, K., Daels, E., Van Buggenhout, S., Van Loey, A. M., . . ., & Hendrickx, M. E. (2014a). Effect of calcium ions and pH on the structure and rheology of carrot-derived suspensions. *Food Hydrocolloids*, *36*(1), 382-391.

Moelants, K. R. N., Cardinaels, R., Jolie, R. P., Verrijssen, T. A. J., Van Buggenhout, S., Van Loey, A. M., . . ., & Hendrickx, M. E. (2014b). Rheology of concentrated tomato-derived suspensions: Effects of particle characteristics. *Food and Bioprocess Technology*, *7*(1), 248-264.

Moelants, K. R. N., Cardinaels, R., Van Buggenhout, S., Van Loey, A. M., Moldenaers, P., & Hendrickx, M. E. (2014c). A review on the relationships between processing, food Structure, and rheological Properties of plant-tissue-based food suspensions. *Comprehensive Reviews in Food Science and Food Safety*, *13*(3), 241-260.

Moelants, K. R. N., Jolie, R. P., Palmers, S. K. J., Cardinaels, R., Christiaens, S., Van Buggenhout, S., . . ., & Hendrickx, M. E. (2013).The effects of process-induced pectin changes on the viscosity of carrot and tomato sera. *Food and Bioprocess Technology*, *6*(10), 2870-2883.

Moresi, M. & Liverrotti, C. (1982). Economic study of tomato paste production. *International Journal of Food Science & Technology*, *17*(2), 177-192.

Moshrefi, M., & Luh, B. S., (1984). Purification and characterization of two tomato polygalacturonase isoenzymes. *Journal of Food Biochemistry*, *8*(1), 39-54.

Noomhorm, A. & Tansakul, A. (1992). Effect of pulp-finisher operation on quality of tomato juice and tomato puree. *Journal of Food Process Engineering*, *15*(4), 229-239.

Oakenfull, D. & Scott, A. (1984). Hydrophobic interaction in the gelation of high methoxyl pectins. *Journal of Food Science*, *49*(4), 1093-1098.

Petro-Turza, M. (1986). Flavour of tomato and tomato products. *Food Reviews International*, *2*(3), 309-351.

Pressey, R. (1983). β-Galactosidases in ripening tomatoes. *Plant Physiology*, *71*(1), 132-135.

Rao, M. A. & Cooley, H. J. (1983). Applicability of flow models with yield for tomato concentrates. *Journal of Food Process Engineering*, *6*(3), 159-173.

Rao, M. A. & Cooley, H. J. (1992). Rheological behavior of tomato pastes in steady and dynamic shear. *Journal of Texture Studies*, *23*(4), 415-425.

Rao, M. A. (2007). *Rheology of Fluid and Semisolid Foods Principles and Applications* (2nd ed.). New York: Springer.

Rao, M. A., Bourne, M. C., & Cooley, H. J. (1981). Flow properties of tomato concentrates. *Journal of Texture Studies*, *12*(4), 521-538.

Ridley, B. L., O'Neill M. A., & Mohnen, D. (2001). Pectins: Structure, biosynthesis, and oligogalacturonide-related signaling. *Phytochemistry*, *57*(6), 929-967.

Rodrigo, D., Cortes, C., Clynen, E., Schoofs, L., Van Loey, A., & Hendrickx, M. E. (2006). Thermal and high-pressure stability of purified polygalacturonase and pectinmethylesterase from four different tomato processing varieties. *Food Research International*, *39*(4), 440-448.

Servais, C., Jones, R., & Roberts, I. (2002). The influence of particle size distribution on the processing of food. *Journal of Food Engineering*, *51*(3), 201-208.

Sharma, S. K., LeMaguer, M., Liptay, A., & Poysa, V. (1996). Effect of composition on the rheological properties of tomato thin pulp. *Food Research International*, *29*(2), 175-179.

Sharma, S. K., Liptay, A., & LeMaguer, M. (1997). Molecular characterization, physicochemical and functional properties of tomato fruit pectin. *Food Research International*, *30*(7), 543-547.

Sherkat, F. & Luh, B. S. (1977). Effect of break temperature on quality of paste, reconstituted juice, and sauce made from M-32 tomatoes. *Canadian Institute of Food Science and Technology Journal*. *10*(2). 92-96.

Shi, J. & LeMaguer, M. (2000). Lycopene in tomatoes: Chemical and physical properties affected by food processing. *Critical Reviews in Food Science and Nutrition*, *40*(1), 1-42.

Sila D. N., Van Buggenhout, S., Duvetter, T., Fraeye, I., De Roeck, A., Van Loey, A., & Hendrickx, M. E. (2009). Pectins in processed fruit and vegetables: Part II-structure function relationship. *Comprehensive Reviews in Food Science and Food Safety*, *8*(2), 86-104.

Smith, D. L., Abbott, J. A., & Gross, K. C. (2002). Down-regulation of tomato β-Galactosidases 4 result in decreased fruit softening. *Plant Physiology*, *129*(4), 1755-1762.

Srichantra, A. (2002). *Modelling of the break process to improve tomato paste production quality*. (Unpbublished master's thesis). Massey University, Palmerston North, New Zealand.

Takada, N. & Nelson, P. E. (1983). A new consistency method for tomato products: The precipitate weight ratio. *Journal of Food Science*, *48*(5), 1460-1462.

Tanglertpaibul, T. & Rao, M. A. (1987a). Rheological properties of tomato concentrates as affected by particle size and methods of concentration. *Journal of Food Science*, *52*(1), 141-145.

Tanglertpaibul, T. & Rao, M. A. (1987b). Flow properties of tomato concentrates: Effect of serum viscosity and pulp content. *Journal of Food Science*, *52*(2), 318-321.

Thakur, B. R., Singh, R. K., & Handa, A. K. (1995). Effect of homogenization pressure on consistency of tomato juice. *Journal of Food Quality*, *18*(5), 389-396.

Thakur, B. R., Singh, R. K., Handa, A. K., & Rao, M. A. (1997). Chemistry and uses of pectin – a review. *Critical Reviews in Food Science and Nutrition*, *37*(1), 47-73.

Thakur, B. R., Singh, R. K., Tieman, D. M., & Handa, A. K. (1996). Tomato product quality from transgenic fruits with reduced pectin methylesterase. *Journal of Food Science*, *61*(1), 85-87.

Van Buren, J. P. (1991). Function of Pectin in Plant Tissue Structure and Firmness. In R. H. Walter (Eds.), *The chemistry and technology of pectin* (pp. 1-22). San Diego: Academic Press.

Vercet, A., Sanchez, C., Burgos, J., Montanes, L., & Buesa, P. L. (2002). The effects of manothermosonication on tomato pectic enzymes and tomato paste rheological properties. *Journal of Food Engineering*. *53*(3), 273-278.

Voragen, A. G. J., Coenen, G., Verhoef, R. P., & Schols, H. A. (2009). Pectin, a versatile polysaccharide present in plant cell walls. *Structural Chemistry*, *20*(2), 263-275.

Walkinshaw, M. D. & Arnott, S. (1981). Conformations and interactions of pectins: II. Models for junction zones in pectinic acid and calcium pectate gels. *Journal of Molecular Biology*, *153*(4), 1075-1085.

Whittenberger, R. T. & Nutting, G. C. (1958). High viscosity of cell wall suspensions prepared from tomato juice. *Food Technology, 12*, 420-424.

Winsor, G. W., Davies, J. N., & Massey, D. M. (1962). Composition of tomato fruit. III. - Juices from whole fruit and locules at different stages of ripeness. *Journal of the Science of Food and Agriculture*, *13*(2), 108-115.

Wu, J., Gamage, T. V., Vilkhu, K. S., Simons, L. K., & Mawson, R. (2008). Effect of thermosonication on quality improvement of tomato juice. *Innovative Food Science & Emerging Technologies*. *9*(2), 186-195.

Xu, S, Shoemaker, C. F., & Luh, B. S. (1986). Effect of break temperature on rheological properties and microstructure of tomato juices and pastes. *Journal of Food Science*, *51*(2), 399-402.

Yoo, B. & Rao, M. A. (1994). Effect of unimodal particle size and pulp content on rheological properties of tomato puree. *Journal of Texture Studies*, *25*(4), 421-436.

Yoo, B. & Rao, M. A. (1995). Yield stress and relative viscosity of tomato concentrates: Effect of total solids and finisher screen size. *Journal of Food Science*, *60*(4), 777-779.

York, W. S., Kumar Kolli, V. S., Orlando, R., Albersheim, P., & Darvill, A. G. (1996). The structures of arabinoxyloglucans produced by solanaceous plants. *Carbohydrate Research*, *285*, 99-128.